Effects of α7 nicotinic receptors on NMDA-mediated excitotoxicity in organotypic hippocampal slice cultures

A Thesis

Submitted to the Graduate Faculty

in Partial Fulfilment of the Requirements of the Degree of

MASTER OF SCIENCE

Department of Biomedical Sciences

Faculty of Veterinary Medicine

University of Prince Edward Island

Denise Happ

Charlottetown, P.E.I.

August, 2016

THESIS/DISSERTATION NON-EXCLUSIVE LICENSE

Family Name: Happ	Given Name, Middle Name (if applicable): Denise Fabienne
Full Name of University: University of Prince Edward Island	
Faculty, Department, School: Department of Biomedical Sciences	
Degree for which thesis/dissertation was presented: Master of Sciences	Date Degree Awarded August 16, 2016:
Thesis/dissertation Title: Effects of α7 nicotinic receptors on NMDA-mediated excitotoxicity in organotypic hippocampal slice cultures	

In consideration of my University making my thesis/dissertation available to interested persons, I, Denise Happ, hereby grant a non-exclusive, for the full term of copyright protection, license to my University, University of Prince Edward Island:

(a) to archive, preserve, produce, reproduce, publish, communicate, convert into any format, and to make available in print or online by telecommunication to the public for non-commercial purposes;
(b) to sub-license to Library and Archives Canada any of the acts mentioned in paragraph (a).

I undertake to submit my thesis/dissertation, through my University, to Library and Archives Canada. Any abstract submitted with the thesis/dissertation will be considered to form part of the thesis/dissertation.

I represent that my thesis/dissertation is my original work, does not infringe any rights of others, including privacy rights, and that I have the right to make the grant conferred by this non-exclusive license.

If third party copyrighted material was included in my thesis/dissertation for which, under the terms of the *Copyright Act*, written permission from the copyright owners is required I have obtained such permission from the copyright owners to do the acts mentioned in paragraph (a) above for the full term of copyright protection

I retain copyright ownership and moral rights in my thesis/dissertation, and may deal with the copyright in my thesis/dissertation, in any way consistent with rights granted by me to my University in this non-exclusive license.

I further promise to inform any person to whom I may hereafter assign or license my copyright in my thesis/dissertation of the rights granted by me to my University in this non-exclusive license.

Signature	**Date**

University of Prince Edward Island

Faculty of Veterinary Medicine

Charlottetown

CERTIFICATION OF THESIS WORK

We, the undersigned, certify that Denise F. Happ, B.Sc. (Hochschule Furtwangen University, Germany), candidate for the degree of Master of Science has presented her thesis with the following title:

Effects of α7 nicotinic receptors on NMDA-mediated excitotoxicity in organotypic hippocampal slice cultures

that the thesis is acceptable in form and content, and that a satisfactory knowledge of the field covered by the thesis was demonstrated by the candidate through an oral examination held on _____ .

Examiners' Names Examiners' Signatures

Dr. Robert Gilmour

Dr. Rebecca Reed-Jones

Dr. Sandra McConkey

Dr. Daphne Gill

Dr. Andrew Tasker

Date

ABSTRACT

Glutamate, the main excitatory neurotransmitter in the mammalian brain, plays an important role during brain development and physiological functioning throughout life by activation of ionotropic NMDA receptors. However, glutamate is also involved in a pathological process called excitotoxicity, whereby elevated release of glutamate over-activates synaptic and extrasynaptic NMDA receptors leading to rapid neuronal cell death. This excitotoxic mechanism is largely responsible for cell death in many neuropathological diseases, including stroke.

Recent literature has suggested an interaction between NMDA receptors and nicotinergic signaling via the α7 nicotinic acetylcholine receptors (α7 nAChRs). The potential role of α7 nAChRs in mediating glutamate toxicity, however, is somewhat controversial with reports of α7 nAChRs being both neuroprotective and neurotoxic in certain systems. The purpose of this thesis was to investigate the effects of co-activation of α7 nAChRs on NMDA-mediated excitotoxicity *in vitro* using organotypic hippocampal slice cultures (OHSCs).

In order to compare the effects of different treatments on cell viability of OHSCs, a standardized method to objectively quantify cell death using the fluorescent dye propidium iodide (PI), a common marker for membrane integrity and cell injury, was developed. Hippocampal subfields were separated sing simple landmarks and PI intensity was quantified by densitometry in 10 template-oriented counting fields.

OHSCs were prepared from postnatal day 5-6 Sprague-Dawley rats according to the membrane interface method and maintained for 13 days. After confirming viability using

PI, slices were exposed for 4 hours to varying concentrations of NMDA and PI uptake was quantified after 24 hours in fresh media. Exposure to increasing concentrations of NMDA resulted in a dose-dependent increase in PI fluorescence intensity, an effect found in all hippocampal subfields analysed (dentate gyrus, CA1, and CA3). Furthermore, comparison of PI uptake in the three subfields showed a region-specific vulnerability of the hippocampus to NMDA-mediated cytotoxicity, with the CA1 region being the most sensitive.

To characterize the contribution of α7 nAChRs in NMDA-mediated excitotoxicity, OHSCs were exposed to a combination of NMDA and the specific α7 nAChR agonist choline and the allosteric potentiating ligand galantamine. Results revealed that co-activation of α7 nAChRs does not significantly alter NMDA-induced excitotoxic cell damage in OHSCs as measured by PI uptake. Activation of α7 nAChRs in the absence of NMDA, however, significantly increased cell death in some hippocampal regions, suggesting a possible neurotoxic effect that would require further investigation.

ACKNOWLEDGMENTS

I would like to thank the members of my supervisory committee, Dr. Collins Kamunde, Dr. Sunny Hartwig, Dr. Tracy Doucette and Dr. Daphne Gill, for their many comments and helpful suggestions.

I would like to extend special thanks to my supervisor, Dr. Andy Tasker, whose expertise, guidance, and encouragement made this work possible. Thank you for all of your help throughout the years.

I also thank Debra MacDonald for the technical training, assistance and support. Thank you to all of the current and past students in the lab for their assistance with this project in and outside of the lab.

I would like to acknowledge and thank the Department of Biomedical Sciences, Innovation PEI Graduate Student Award, and the Dr. Regis Duffy Graduate Science Scholarship for personal funding as well as AVC Internal Research Fund and the Lundbeckfonden for providing funding for the research.

Finally, thank you to my family and friends for their support and encouragement over the years.

TABLE OF CONTENTS

LIST OF FIGURES

LIST OF TABLES

ABBREVIATIONS

Aβ	β-amyloid
ACh	acetylcholine
AChE	acetylcholinesterase
AD	Alzheimer's disease
Akt	protein kinase B
AMPA	a-amino-3-hydroxy-5-methyl-4-isoxazolepropionic acid
ANOVA	analysis of variance
APL	allosteric potentiating ligand
ATP	adenosine triphosphate
BBB	blood brain barrier
BCL-2	B-cell lymphoma 2
BDNF	brain-derived neurotrophic factor
CA	cornu ammonis
CaMKIV	calmodulin kinase IV
CRE	cyclic adenosine monophosphate response element
CREB	CRE binding protein
CNS	central nervous system
DAPI	4', 6-diamidino-2-phenylindole
DG	dentate gyrus
DIV	day *in vitro*
DMXB-A	3-[(2,4-dimethoxy) benzylidene]anabaseine
DNA	deoxyribonucleic acid
DOM	domoic acid
ERK	extracellular signal-regulated kinase

FJC	Fluoro-Jade C
GABA	gamma-aminobutyric acid
GFAP	glial fibrillary acidic protein
GLAST	glutamate aspartate transporter
GLT-1	glutamate transporter 1
Glu	glutamate
GluR	glutamate receptor
GPCR	G-protein coupled receptor
HEK-293	human embryonic kidney-293 cell line
iGluR	ionotropic glutamate receptor
JAK2	januse kinase 2
LDH	lactate dehydrogenase
LTP	long-term potentiation
MEM	minimum essential media
mGluR	metabotropic glutamate receptor
nAChR	nicotinic acetylcholine receptor
NMDA	N-methyl-D-aspartate
NMDAR	NMDA receptor
NO	nitric oxide
NOS	nitric oxide synthase
OHSC	organotypic hippocampal slice culture
PBS	phosphate buffered saline
PI	propidium iodide
PI3K	phosphatidylinositol 3-kinase
PND	postnatal day

PSD95	postsynaptic density protein-95
SEM	standard error of the mean
WST-1	water soluble tetrazolium-1

CHAPTER 1:

GENERAL INTRODUCTION

1.1 STROKE

Stroke is one of the main causes of death and disability, affecting approximately 800,000 people each year in the United States alone (Mozaffarian *et al*, 2016). Furthermore, the majority of survivors are left with disabilities, including motor disabilities as well as cognitive deficits and depressive symptoms (Adamson *et al*, 2004; Go *et al*, 2013). The impact of stroke extends far beyond the individual into the wider public and economy: direct and indirect costs associated with hospitalization and rehabilitation amount to approximately $33 billion in the United States alone (in 2011 to 2012) (Mozaffarian *et al*, 2016).

Stroke is a diverse neurological condition broadly categorized as either ischemic or hemorrhagic. Ischemic strokes result from occlusion of a cerebral artery by a thrombus or embolus, causing a lack of oxygen and glucose, which eventually leads to cell injury or cell death within the affected brain region. In contrast, rupture of an artery within the brain is the underlying cause of hemorrhagic strokes. About 85-90% of all strokes diagnosed are ischemic (Go *et al*, 2013). Because of its high prevalence, the work in this thesis will focus on ischemic strokes.

1.2 THE PATHOLOGY OF ISCHEMIA

When blood supply to a brain region is interrupted, a complex series of cellular events is triggered that leads to the degeneration of brain tissue. These pathological events are often referred to as an ischemic cascade (Lee *et al*, 2000) (see Figure 1-1 for an overview). While the initial insult can rapidly lead to brain damage in areas that

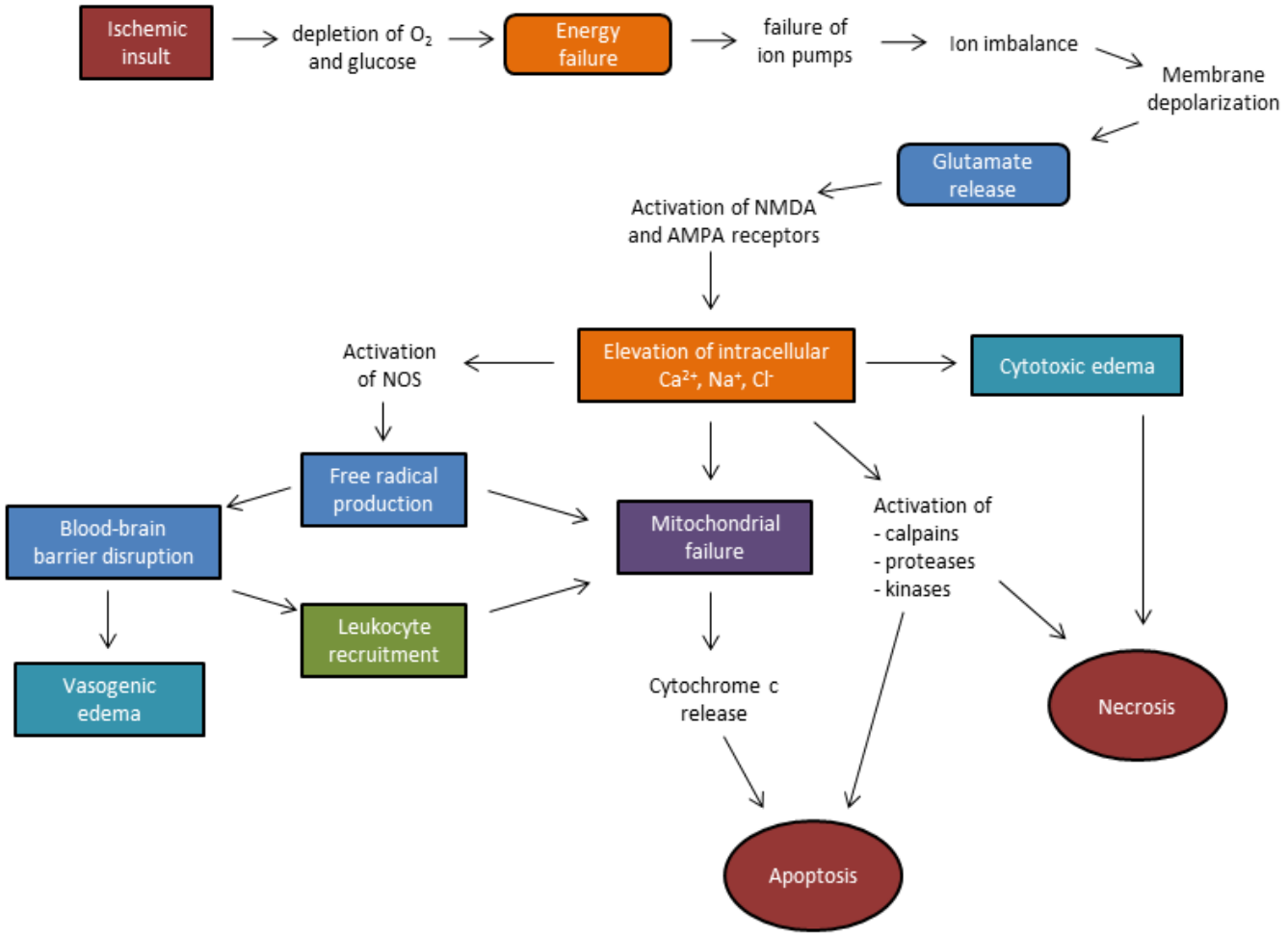

Figure 1-1: Overview of the pathological events in the ischemic cascade. Following an ischemic insult, loss of oxygen and glucose cause energy loss and downstream effects such as excitotoxicity, free radical production and blood-brain barrier disruption, that can result in apoptosis or necrosis. Figure created by Denise Happ, based on information from several publications cited in section 1.2.

are severely affected, ischemic brain injury to less affected cells may occur hours or even days later (Durukan and Tatlisumak, 2007). The fundamental mechanisms of the ischemic cascade have been identified, but the exact sequence of events is difficult to determine as many events of the ischemic cascade demonstrate overlapping features and are indistinguishably connected (Neumar, 2000).

Ischemic core and penumbra

Depending on the severity and length of the reduction in blood flow, the affected brain tissue can be divided into two regions: the ischemic core and the surrounding ischemic penumbra. The core of the infarct is characterized by complete lack of blood flow resulting in irreversible cell death within minutes. In contrast, the ischemic penumbra experiences less severe ischemic damage due to the presence of collateral blood vessels that continue to supply the area. Although the moderate reduction in blood flow can cause further damage, cells in the penumbra can maintain structural integrity, membrane potential and ion gradients temporarily. Thus, the disruption of cellular homeostasis is less severe and leads to the development of a region with reversible damage. The penumbra can be salvaged provided blood flow is restored in time, but the tissue can also progress to irreversible damage (Hertz, 2008). Following stroke, neuronal cell death can be caused by necrotic or apoptotic mechanisms, depending on the intensity of the stimulus. Acute, permanent vascular occlusion results in necrotic cell deaths, which predominantly characterizes neuronal cells within the ischemic core. In contrast, cells undergo a delayed type of cell death called apoptosis subsequent to milder injury, particularly within the penumbra (Bonfoco *et al,* 1995; Neumar, 2000).

Energy depletion and failure of ion pumps

The brain is dependent on a steady supply of oxygen and glucose from the blood to produce adenosine triphosphate (ATP) and thereby maintain energy-dependent physiological function. As a result of diminished blood flow, depletion of oxygen and glucose causes a subsequent decrease in ATP that leads to the dysfunction of ATP-dependent ion pumps that maintain the neuronal resting potential, such as Na^+/K^+-ATPase and Ca^{2+}-ATPase, as well as the reversal of Na^+/Ca^{2+} transporter. Failure of these ion pumps results in elevated concentrations of intracellular sodium, calcium and chloride as well as high extracellular levels of potassium, leading to the loss of neuronal membrane potential and depolarization of neurons and glial cells (Lipton, 1999).

Due to this anoxic depolarization, excessive amounts of neurotransmitters, particularly glutamate (Glu), are released into the extracellular environment, promoting further advancement of injury cascades and initiating Glu-mediated excitotoxic cell death (Lee *et al*, 2000).

Glutamate-mediated excitotoxicity

Under physiological conditions, extracellular Glu is maintained at low levels by presynaptic and astrocytic reuptake mechanisms. Following ischemic stroke, these sequestering systems are impaired causing accumulation of Glu in the extracellular space (Takahashi *et al*, 1997). The excessive levels of Glu over-activate various types of glutamate receptors (GluRs), especially the ionotropic *N*-methyl-D-aspartate (NMDA) receptor (NMDAR), which leads to an overflow of Ca^{2+} into the cell. Stimulation of

GluRs also promotes the influx of sodium and chloride, with water following passively, causing swelling in the neuronal cell body and dendrites (Lee *et al*, 2000).

Calcium overload is generally thought to be a key factor in excitotoxicity-mediated cell death (Arundine and Tymianski, 2003; Doyle *et al*, 2008; Hazell, 2007; Szydlowska and Tymianski, 2010). In addition to calcium influx from the extracellular compartment, Ca^{2+} may also be released from intracellular stores, such as the endoplasmic reticulum (Paschen and Doutheil, 1999; Pisani *et al*, 2000) or mitochondria (Szydlowska and Tymianski, 2010; Webster, 2012). An increase in Ca^{2+} concentrations can initiate the activation of several enzymes, including calpains and other proteases, lipases, phosphatases, nitric oxide (NO) synthase (NOS), and endonucleases (Szydlowska and Tymianski, 2010; Xing *et al*, 2012). The consequences of changed activity of these enzymes include overproduction of free radicals, lipid peroxidation, irreversible mitochondrial damage, and ultimately induction of necrotic and apoptotic cell death (Durukan and Tatlisumak, 2007).

Mitochondrial damage

Mitochondria play an important role in cellular energy production, physiological calcium homeostasis and generation of oxygen radicals (Norenberg and Rao, 2007). Upon excitotoxicity-mediated calcium inflow, mitochondria can take up Ca^{2+} in an effort to recover the intracellular concentration. However, mitochondrial calcium overload can cause the production of reactive oxygen species such as superoxide and reduced ATP synthesis. In addition, the mitochondria undergo a phenomenon called “mitochondrial permeability transition”, resulting from the formation and opening of a permeability

transition pore in the inner membrane of the mitochondria. The increased permeability of the mitochondrial membrane promotes mitochondrial swelling and the release of apoptotic mediators, such as cytochrome c and apoptosis inducing factor (Dirnagl, 2012; Norenberg and Rao, 2007; Starkov *et al*, 2004).

Oxidative Stress

During ischemic injury, endogenous defences against reactive oxygen species, such as glutathione and superoxide dismutase, may be impaired as a result of decreased energy production (Hazell, 2007). Damaging free radicals, including superoxide, hydroxyl radical, and NO, can be produced by mitochondria and NMDA receptor-mediated activation of NOS. Additionally, overproduction of free radicals can follow reperfusion, as the reoxygenation provides a substrate for numerous enzymatic oxidation reactions (Sugawara *et al*, 2004). Free radicals, such as NO and superoxide, can damage endothelial cells through activation of matrix metalloproteinases and thereby disrupt the blood brain barrier (BBB). Increased BBB permeability contributes further to ischemic injury and cell death by allowing the influx of inflammatory cells and toxins (Chen *et al*, 2011; Doyle *et al*, 2008). Additionally, elevated influx of Na^+ and Cl^- due to altered BBB permeability can cause passive influx of water, leading to edema (Dirnagl *et al*, 1999; Gotoh *et al*, 1985).

1.3 GLUTAMATE AND GLUTAMATE RECEPTORS IN THE BRAIN

The amino acid Glu is the main excitatory neurotransmitter in the mammalian central nervous system (CNS). Due to the ubiquitous distribution of glutamatergic synapses, Glu

is critically involved in physiological functioning including brain development, plasticity, and memory processes (Meldrum, 2000). High concentrations of Glu, however, can have detrimental effects on neurons and cause neuronal cell death by excitotoxicity. It has been suggested that excitotoxicity is an extension of physiological function, and that excessive activation of GluRs results in neuronal damage (Sattler and Tymianski, 2001). This pathological process has been implicated in a variety of neuropathological diseases, including stroke and traumatic brain injury (Arundine and Tymianski, 2003; Kalia *et al*, 2008), as well as in neurodegenerative diseases, such as Alzheimer's disease (AD) (Miguel-Hidalgo *et al*, 2002), Parkinson's disease (Armentero *et al*, 2006), and Huntington's disease (Ferrante *et al*, 1993).

The balance of glutamatergic activity is important for normal functioning of the brain. The extracellular Glu concentration is normally kept low by Na^+-dependent Glu transporters, such as the glutamate aspartate transporter (GLAST) and glutamate transporter 1 (GLT-1) (Robinson and Jackson, 2016). GLAST and GLT-1 are preferentially expressed on astrocytes, providing this cell type with an enormous capacity for Glu uptake. Once inside the astrocytes, Glu can be oxidatively metabolized or transformed into glutamine, which is released and subsequently taken up by neurons to use as a Glu precursor (Schousboe and Waagepetersen, 2005).

The excitatory responses of Glu are mediated by two receptor families: metabotropic glutamate receptors (mGluRs) and ionotropic glutamate receptors (iGluRs). Metabotropic glutamate receptors are ligand-gated G-protein coupled receptors (GPCRs) that can alter the activity of iGluRs and coupled channels via second messenger cascades (Boldyrev, 2000). The mGluR family consists of eight different receptor types, which can

be subdivided into groups 1-3 depending on receptor structure and physiological activity (Hermans and Challiss, 2001). Metabotropic GluRs are expressed by neurons and glia in the CNS and are typically located near the synaptic cleft, where they can modulate the effect of Glu on postsynaptic receptors and the release of Glu and other neurotransmitters (Julio-Pieper *et al*, 2011).

The ionotropic receptor family is divided into NMDA, α-amino-3-hydroxy-5-methyl-4-isoxazolepropionic acid (AMPA), and 2-carboxy-3-carboxymethyl-4-isopropenylpyrrolidine (kainate) receptor subfamilies, each of which are named after their prototypical agonists. All iGluRs are typically made up of four subunits that form the ion channel pore allowing cation influx upon Glu binding (Traynelis *et al*, 2010). Over the years, almost every type of GluR has been implicated in excitotoxic cell death, but NMDAR activation is thought to be the primary cause of Glu-mediated excitotoxicity due to its abundant expression and high calcium permeability (Mehta *et al*, 2013).

1.3.1 The NMDA receptor

NMDA receptors are heterotetramers that are formed by combination of the receptor subunits NR1, NR2 and NR3. For the assembly of a functional NMDA receptor, two NR1 subunits appear to be obligatory and can be combined with either two NR2 subunits or, less commonly, a combination of NR2 and NR3 subunits (Traynelis *et al*, 2010). Through alternative splicing eight different NR1 isoforms can be generated. There are four different NR2 subunits (NR2A-D) encoded by four genes, with the NR2A and NR2B being the predominant NR2 subunits in the hippocampus. The NR3 family contains two members (NR3A-B) encoded by two genes (Paoletti, 2011). Consequently, a multitude of possible combinations of subunits are possible allowing for NMDA

receptor assemblies with distinct patterns of expression and functional properties (Paoletti and Neyton, 2007). This functional diversity is reflected in differences in channel conductance, gating properties, regional expression profiles, pharmacological properties and downstream signaling mechanisms. For example, NMDARs containing NR2A or NR2B subunits show a higher conductance and higher sensitivity to the Mg^{2+} block compared to receptors containing NR2C and NR2D subunits (Paoletti, 2011).

NMDA receptors are generally expressed throughout the brain, but the expression of distinct subunits is differentially regulated depending on the developmental stage and brain area. Monyer *et al* (1994) showed that the NR1 subunit is expressed at high levels in the majority of neurons throughout development. Early in development expression of the NR2B subunit predominates, but then decreases over time, whereas NR2A is absent at first and increases with maturation in the hippocampus and cortex. Although evidence suggests this is a general trend, the expression of subunits may vary within different brain regions (Cull-Candy *et al,* 2001; Gladding and Raymond, 2011; Yamakura and Shimoji, 1999). Additionally, there may also be variations in the NR2 subunit composition depending on the cellular location of the NMDA receptor (Cull-Candy *et al*, 2001). With regards to the subcellular location, NMDARs are typically found at postsynaptic sites, but presynaptic NMDARs have also been described (Corlew *et al*, 2008).

Compared to other iGluRs, the classical NMDARs (i.e. NMDARs lacking NR3 subunits) have several unique characteristics. First, the activation of NMDARs requires simultaneous binding of Glu and its co-agonist glycine. The NR2 subunit contains the binding site for Glu, whereas the glycine binding site can be found on the NR1 subunit (Kalia *et al,* 2008). Moreover, the receptor channel is blocked by extracellular Mg^{2+} at

resting potential. The Mg^{2+} block is removed by membrane depolarization resulting in a voltage-dependence. In addition to Na^{+} and K^{+}, the NMDAR channel is also highly permeable to Ca^{2+} and displays slower activation and deactivation kinetics compared to AMPA and kainate receptors. Finally, the activity of the classical NMDAR can be modulated by extracellular compounds, which are usually small molecules or ions such as Zn^{2+} and H^{+} (Paoletti, 2011).

1.4 NMDA RECEPTOR-MEDIATED NEURONAL SURVIVAL AND ISCHEMIC INJURY

NMDA receptor signaling plays a dual role in the physiology and pathophysiology of the CNS. While physiological function of NMDARs mediated by Ca^{2+} entry is important during brain development and throughout life, intense or chronic activation of NMDARs under pathological conditions can lead to cell death via excitotoxic mechanisms. The term excitotoxicity was coined by Olney, who showed that this specific neurotoxic mechanism was not limited to retinal neurons (Olney, 1969). Subsequent experiments suggested the involvement of calcium as a key element of Glu-mediated toxicity (Choi, 1985; Simon *et al*, 1984) and NMDA receptors as the primary source of toxic Ca^{2+} entry (Rothman and Olney, 1987; Tymianski *et al*, 1993a).

In the last 30 years, excitotoxicity linked to NMDA receptors has been implicated as the underlying cause in many neuropathological diseases due to acute excitotoxic insults during stroke (Margaill *et al*, 1996) or traumatic brain injury (Biegon *et al*, 2004; Faden

et al, 1989). In stroke specifically, Glu excitotoxicity mediated by NMDA receptors seems to be the main pathway to neuronal cell death (Zhou and Sheng, 2013).

The mechanism of NMDAR-mediated excitotoxicity is thought to be linked to excessive Ca^{2+} entry. Because of its potentially devastating consequences, intracellular calcium levels are usually highly regulated via sequestration and extrusion, for example via the plasma membrane Na^{+}/Ca^{2+} exchanger. Under ischemic conditions, however, these regulatory sodium-calcium-transporters may be dysfunctional, leading to the deregulation of calcium homeostasis (Bano *et al*, 2005)

Antagonists of NMDARs have been shown to protect against excitotoxic cell death in ischemic models *in vivo* (Margaill *et al*, 1996; Yu *et al*, 2015) and *in vitro* (Garcia de Arriba *et al*, 2006), but many experimental NMDAR antagonists are ineffective or produce unacceptable side effects in clinical studies (Ikonomidou and Turski, 2002; Minnerup *et al*, 2012; Sacco *et al*, 2001). For this reason, research has since focused on the dual actions of NMDA receptors and specific downstream signaling pathways, as these receptors seem to be able to promote neuronal health as well as cause neuronal death (Hardingham *et al*, 2002; Liu *et al*, 2007; Papadia and Hardingham, 2007). Using this approach, a neuroprotective agent for stroke called NA-1 has shown promising results in several animal models (Cook *et al*, 2012; Sun *et al*, 2008) as well as in a phase 2 clinical trial (Hill *et al*, 2012) and is currently undergoing phase III clinical trials. NA-1 inhibits the interaction between NMDA receptors and the postsynaptic density protein-95 (PSD95), dissociating the receptors from neurotoxic downstream signaling pathways without affecting necessary synaptic activity (Aarts *et al*, 2002).

Various theories to explain these seemingly contradictory actions of NMDARs have been brought forward, the most prominent being the degree of Ca^{2+} entry, the role of receptor location and the subunit composition (see Table 1-1 for an overview of the different theories). Early research identified the amount of calcium entering through NMDA receptors as a determining factor for the dual role of NMDARs. While excess NMDA receptor activity leads to neuronal death due to excessive Ca^{2+} influx, too little activation of NMDARs can also be detrimental. Therefore, moderate stimulation of NMDA receptors seems to be key for neuronal survival (Lipton and Nakanishi, 1999).

More recent studies have offered an alternative theory that suggests different roles for synaptic versus extrasynaptic NMDARs. As mentioned above, NMDARs can be localized at synaptic, extrasynaptic, and perisynaptic sites. During early development of hippocampal neurons, extrasynaptic NMDARs make up the largest part of the NMDAR population. The ratio of extrasynaptic to synaptic NMDARs decreases over time, but a significant number of NMDARs stay at extrasynaptic locations throughout life (Cottrell *et al*, 2000; Petralia *et al*, 2010). Experiments conducted by Hardingham *et al* (2002) in hippocampal neurons revealed synaptic NMDARs are neuroprotective, whereas extrasynaptic NMDARs seem to be associated with cell death pathways. Moreover, the distinct receptor groups may be linked to different signaling pathways depending on their subcellular location (Hardingham *et al*, 2002; Ivanov *et al*, 2006), resulting in either cell survival or cell death. Therefore, excitotoxicity may not be the consequence of a general calcium overload, but rather calcium entry through a distinct subgroup of NMDARs may

Table 1-1: Overview of theories to explain opposing roles of NMDA receptor activation

Theory	Details	References
Calcium hypothesis	Excessive intracellular Ca^{2+} levels initiates cell death signaling mechanisms	Choi, 1985, 1987
Source specificity of Ca^{2+}	Main determinant of Ca^{2+} toxicity is not the degree of Ca^{2+} loading, but the entry route	Sattler *et al*, 1998; Tymianski *et al*, 1993
NMDA receptor location	Synaptic NMDA receptors promote neuronal survival, while extrasynaptic NMDARs mediate excitotoxicity	Hardingham and Bading, 2010
NMDA receptor composition	Differential roles for NR2A- and NR2B-containing NMDA receptors, with NR2A mediating neuronal survival and NR2B inducing excitotoxicity	Liu *et al*, 2007

cause neuronal cell death (Hardingham and Bading, 2010). In contrast, work by Sattler *et al* (2000) in cortical cell cultures provided evidence that NMDA receptors located at synapses as well as outside of synapses have the ability to mediate excitotoxicity *in vitro*. The authors proposed that the mechanism of receptor stimulation controls the fate of the neurons, not their receptor location.

Some literature suggests that the subunit composition of NMDARs, rather than subcellular receptor localization, confers the seemingly opposing effects of NMDAR activation. Special attention has been paid to NR2A and NR2B subunits, as they exhibit distinct properties. For example, NR2A-containing receptor channels exhibit a higher open probability than NR2B-containing receptors, whereas NR1/NR2B receptors contribute more to calcium influx than NR1/NR2A (Erreger *et al*, 2005). Additional differences in receptor characteristics include deactivation times (Vicini *et al*, 1998), varying affinity to Glu (Sanz-Clemente *et al*, 2013), and differential roles in long-term potentiation (LTP) (Massey *et al*, 2004). With regards to excitotoxicity, work by Liu *et al* (2007) provided evidence for the importance of subunit composition, irrespective of receptor localization. Using both *in vitro* and *in vivo* models, synaptic and extrasynaptic NR2A-containing NMDARs showed a neuroprotective effect, whereas activation of either synaptic or extrasynaptic NR2B-containing receptors resulted in excitotoxicity. For example, blockade of NR2B-containing receptors with a subunit specific antagonist prevented neuronal cell death following NMDA application *in vitro*, whereas inhibition of NR2A-containing receptors increased NMDA-induced cell death (Liu *et al*, 2007). The authors suggest that different NMDAR subunits may be connected to distinct downstream signaling mechanisms causing these opposing effects.

While the molecular basis for excitotoxicity has not yet been fully defined, it seems likely that several factors – receptor location (synaptic vs extrasynaptic), subunit composition (NR2A vs NR2B) as well as the amount of Ca^{2+} entering the cell – are involved in the excitotoxic effects of NMDAR over-activation (Stanika *et al*, 2010). However, it appears that neuronal survival mediated by NMDA receptors is generally associated with protein kinase B (Akt) and cyclic adenosine monophosphate response element (CRE) binding protein (CREB)-mediated signaling (Hardingham *et al*, 2002; Jantas *et al*, 2009; Wang *et al*, 2012), whereas neuronal death is linked to the NOS and calpain pathway, among others (Lai *et al*, 2014; Wei *et al*, 2012; Zhou *et al*, 2008).

Physiological patterns of NMDAR stimulation are required to ensure neuronal survival, whereas inhibition of NMDAR activity can cause neuronal death (Brenneman *et al*, 1990). Several downstream signaling pathways have been linked to NMDA receptor-dependent survival (see Figure 1-2 for an overview). One route to neuronal survival is based on the induction of survival genes. Activation of NMDARs allows calcium to enter the cell, which can subsequently be transported to the cell soma and invade the nucleus. Nuclear Ca^{2+} can then activate the transcription factor CREB via the calmodulin kinase IV (CaMKIV) or the extracellular signal-regulated kinase (ERK) pathway. CREB in turn upregulates many pro-survival genes including brain-derived neurotrophic factor (BDNF), but can also inhibit the expression of death-signaling genes (Lai *et al*, 2014). Additional pro-survival genes, such as TNF-α and Calbindin, can be turned on by NMDAR-induced activation of NFκB (Hardingham and Bading, 2003).

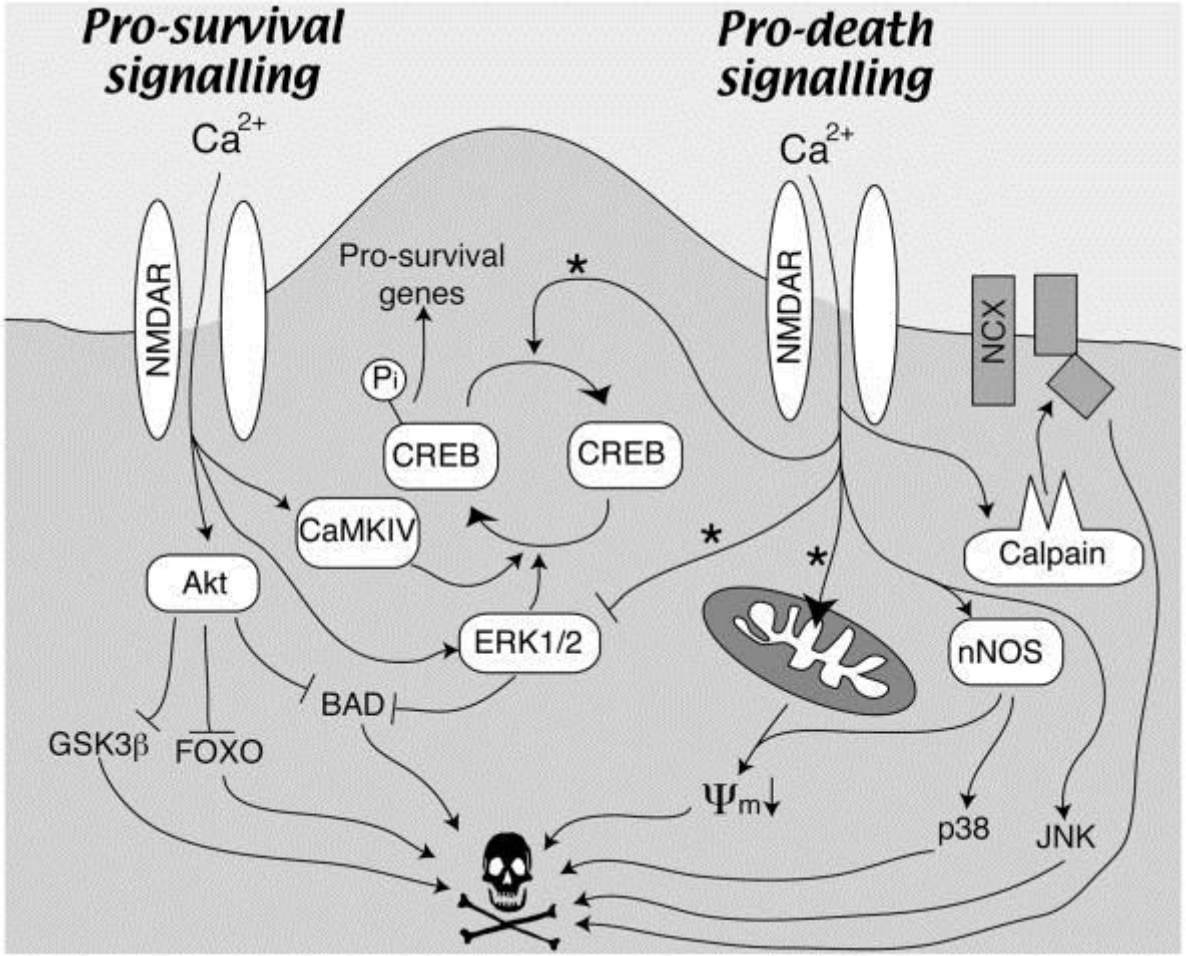

Figure 1-2: General overview of pro-survival and pro-death signalling pathways associated with NMDA receptors. The pathways marked with a * are favoured by extrasynaptic NMDAR activation (Papadia and Hardingham, 2007), reprinted with permission from SAGE Publications, Inc. Journals.

Another important element for neuronal survival is the activation of the protein kinase Akt as a result of stimulation of phosphatidylinositol 3-kinase (PI3K) or activation of the calcium-calmodulin dependent protein kinase kinase. Akt in turn promotes neuronal survival through inhibition of several death-signaling proteins, including glycogen synthase kinase-3, the B-cell lymphoma 2 (BCL-2) family member BCL-2-associated death promotor and the forkhead transcription factor (Lai *et al*, 2014). Another mechanism through which physiological NMDAR activity can ensure neuronal survival is by enhancing protection against oxidative stress (Papadia *et al*, 2008).

Pathological stimulation of NMDA receptors, resulting in disruption of intracellular calcium homeostasis, can cause neuronal death via apoptosis or necrosis depending on the intensity of the insult (see Figure 1-2 for an overview). Antagonism of NMDAR-mediated survival pathways, such as dephosphorylation and therefore inactivation of CREB as well as ERK activity is an important mechanism in cell death (Hardingham and Bading, 2010). For example, excitotoxicity can recruit the death-associated protein kinase 1, which can not only augment the activity of the NMDAR, but also inhibit the pro-survival signaling mediated by ERK (Lai *et al*, 2014). Furthermore, the NR2 subunit has been shown to interact with PSD95. Through interaction with neuronal NOS, PSD95 can couple NMDAR activity to NO toxicity (Aarts *et al*, 2002; Sattler *et al*, 1999). NO can trigger lipid peroxidation and deoxyribonucleic acid (DNA) damage as well as inhibit pro-survival mechanisms (Lai *et al*, 2014; Sattler and Tymianski, 2001). Other important pathways involved in neuronal death include activation of the calpain signaling cascade, which causes the cleavage of essential cellular proteins, and stimulation of members of

the mitogen-activated protein kinase family, stress-signaling proteins such as p38 and c-Jun N-terminal kinase that regulate pro-death signaling genes (Lai *et al*, 2014).

1.5 ACETYLCHOLINE AND ACETYLCHOLINE RECEPTORS

Acetylcholine (ACh) is an endogenous neurotransmitter, located in both the central nervous system and the peripheral nervous system. While ACh acts as a fast-acting neurotransmitter at neuromuscular junctions in the peripheral nervous system, it seems to function mainly as a neuromodulator in the brain. In addition to engaging in classical synaptic transmission between presynaptic and postsynaptic neurons, acetylcholine can also influence neuronal excitability in the CNS, modulate presynaptic neurotransmitter release, and coordinate the firing of groups of neurons (Picciotto *et al*, 2012).

Acetylcholine is formed by the enzyme choline acetyltransferase from acetyl coenzyme A and choline. The postsynaptic action of ACh is terminated by the hydrolytic enzyme acetylcholinesterase (AChE), which hydrolyzes acetylcholine into acetate and choline resulting in the rapid decrease of ACh concentrations in the extrasynaptic compartment. Choline is normally taken up by high affinity Na^+-choline transporters present in most cholinergic nerve terminals (Colović *et al*, 2013), however, some ACh receptors can be activated by choline alone (Alkondon *et al*, 1997b).

As a neuromodulator, ACh plays an important role in brain development, learning, memory, and attention, regulating neuronal excitability via two main receptor classes, the ligand-gated nicotinic ACh receptor (nAChR) channels or G protein-coupled muscarinic ACh receptors (Dani and Bertrand, 2007). The two receptor types are named after their

sensitivity to the plant molecules nicotine and muscarine, respectively (Albuquerque *et al*, 2009). Dysfunction of the cholinergic system has been implicated in neuronal degeneration and cognitive deficits in diseases such as AD, schizophrenia, and Parkinson's disease (Hurst *et al*, 2013; Resende and Adhikari, 2009).

1.5.1 Nicotinic acetylcholine receptors

Nicotinic receptors are ligand-gated ion channels and occur as homomeric or heteromeric assemblies of five transmembrane subunits. A variety of distinct nAChR subunits (α1-10, β1-4, γ, δ, ε) have been identified so far (Pohanka, 2012). The α8 subunit, however, has not yet been found in mammalian tissue (Dani and Bertrand, 2007). Different combinations of these subunits are possible, leading to a wide variety of possible nicotinic receptor subtypes displaying distinct pharmacological properties and functions.

Neuronal nicotinic receptors typically consist of a combination of α and β subunits or of α subunits only (α7 or α9). While the α7 subunit seems to predominantly form homopentameric receptors, some evidence suggests that other subunits, such as β2, can combine with the α7 to form a heteromeric receptor (Murray *et al*, 2012). The most common nAChR subtypes in the mammalian brain are receptors containing α4β2 or homomeric α7 subtypes (Pohanka, 2012). The α7 receptor is expressed at high levels in the hippocampus, hypothalamus, amygdala, cerebral cortex, and olfactory areas (Séguéla *et al*, 1993).

While nicotinic receptors can be found at postsynaptic sites in the CNS (Alkondon *et al*, 1998; Roerig *et al*, 1997), most nAChRs seem to be presynaptic (Gray *et al*, 1996;

McGehee *et al*, 1995) consistent with their role as neuromodulators. Some nAChRs are also found at the surface of cell bodies and axons (Arroyo-Jimenez *et al*, 1999; Hill *et al*, 1993; Kawai *et al*, 2007). The ligand binding site is located between α subunits and select non-α subunits or at the interface of two α subunits as is the case for the homomeric α7 nAChR. Once the ligand binds to the binding site, the nicotinic receptor undergoes a sequence of conformational changes from a resting to an activated state leading to the opening of the ion channel pore. Because the activated state of the receptor is unstable, further conformational changes occur and lead to a non-conducting desensitized state (Papke, 2014). Many channels will initially open with high probability upon agonist binding. However, desensitized channels will begin to accumulate and remain in the desensitized state, decreasing the probability of further opening of channels with agonist binding until levels of ligand occupancy are decreased by diffusion or metabolism of the transmitter (Papke, 2014). When open, the nicotinic receptor channel allows the influx of sodium and potassium, and depending on the subunit composition it can also be permeable to Ca^{2+} (Dani and Bertrand, 2007).

The subunit composition of nicotinic receptors, which is highly variable due to a wide range of possible combinations, determines the electrophysiological and pharmacological characteristics, and thus the receptor's role in the CNS. Nicotinic acetylcholine receptors have the ability to modulate the release of other neurotransmitters, including Glu and gamma-aminobutyric acid (GABA), as well as to directly depolarise postsynaptic neurons (Albuquerque *et al*, 2009). Hence, nAChRs can have a wide range of functions. As the α7 nAChR is central to this thesis, its

physiological function and involvement in neuropathological diseases will be discussed in more detail.

1.5.2 The α7 nicotinic acetylcholine receptor

Among the different nicotinic acetylcholine receptors, the α7 nAChR in particular is implicated in cognitive functions of the CNS and thought to have important clinical implications for diseases such as AD and schizophrenia (Conejero-Goldberg *et al*, 2008). The α7 subunit is one of the most prevalent nicotinic receptor subunits in the CNS and is thought to be expressed mainly as a homomeric receptor. However, they have also been shown to form functional receptors with other subunits (Anand *et al*, 1993; Liu *et al*, 2009; Mowrey *et al*, 2013; Murray *et al*, 2012). In the hippocampus, nAChRs can be found at particularly high levels, with the α4β2 and the α7 receptors representing the most common nicotinic receptors in this area (Adams *et al*, 2002; Fabian-Fine *et al*, 2001; Séguéla *et al*, 1993). Furthermore, functional α7 nAChRs are expressed throughout hippocampal subregions such as the dentate gyrus (DG), CA1, and CA3 (Adams *et al*, 2002; Fabian-Fine *et al*, 2001; Sudweeks and Yakel, 2000). Ultrastructural studies of the rat hippocampus provided evidence that α7 nAChRs are present at both presynaptic and postsynaptic sites (Fabian-Fine *et al*, 2001). Additionally, non-neuronal cells may also express α7 nAChRs. For example, Shen and Yakel (2012) have shown that α7 nAChRs can be localized on astrocytes in acute hippocampal slices.

In comparison with other nicotinic receptors, the α7 nAChR has unique pharmacological properties. For example, it is not only permeable to sodium, but also shows a high calcium permeability (Bertrand *et al*, 1993; Fayuk and Yakel, 2005), which suggests it may have a similar role to NMDA receptors in synaptic plasticity (Cheng and

Yakel, 2015). Other characteristics include short channel open times, fast desensitization kinetics and low affinity for ACh (Mike *et al*, 2000). The α7 nAChR is activated by ACh and selectively by its metabolite choline (Alkondon *et al*, 1997b).

The α7 nAChR can also influence intracellular calcium levels, either directly through voltage activated channels via activation of ERK1/2 (Dajas-Bailador *et al*, 2002a) or indirectly from intracellular sources following nicotinic ryanodine receptor channel activation (Dajas-Bailador *et al*, 2002b). The α7 nAChR-mediated rise in Ca^{2+} levels can induce neurotransmitter release (Koukouli and Maskos, 2015), including Glu (Aramakis and Metherate, 1998) and GABA (Guo *et al*, 1998).

Drugs that potentiate central cholinergic transmission are currently the main treatment strategy for symptoms of diseases characterized by cognitive impairment, including AD and schizophrenia. Many studies provide evidence for the involvement of α7 nAChRs in cognitive functions of the CNS. Several selective α7 nAChR agonists have been shown to improve attention, learning, and memory in both animals and humans (Cincotta *et al*, 2008; Thomsen *et al*, 2010). Furthermore, inhibition of α7 nAChR-mediated signaling using antagonists such as methyllycaconitine may impair working memory function but not reference memory function in rats (Levin *et al*, 2002), suggesting that α7 nAChRs may preferentially impact particular forms of memory over others.

With regards to clinical importance, altered expression and activity of α7 nAChRs appears to be involved in cognitive deficits characterized in patients with schizophrenia (Adler *et al*, 1998; Freedman *et al*, 1995), Alzheimer's disease (Burghaus *et al*, 2000;

Hellström-Lindahl *et al*, 1999; Yu *et al*, 2005), and Parkinson's disease (Banerjee *et al*, 2000). For example, Olincy *et al* (2006) conducted a proof-of-concept trial of 3-[(2,4-dimethoxy) benzylidene]anabaseine (DMXB-A), a partial α7 nAChR agonist, in schizophrenia patients. Administration of DMXB-A was able to improve cognitive functions such as attention and memory, as measured by a specific test battery for the assessment of neuropsychological status. The cognitive improvement abilities of α7 nAChRs have also been demonstrated in animal models of AD (Medeiros *et al*, 2014; Prickaerts *et al*, 2012). Given this promising data from preclinical models, several compounds that enhance α7 nAChR activation are currently undergoing clinical trials for the treatment of AD and schizophrenia (Wallace and Porter, 2011).

An alternative approach to increase α7 nAChR function is to sensitize these receptors to activation by the endogenous agonist ACh using allosteric potentiating ligands (APLs) such as galantamine (Santos *et al*, 2002). Because of its distinct desensitization kinetics and low sensitivity to ACh, the α7 nAChR is a perfect candidate for allosteric modulation (Dani and Bertrand, 2007; Williams *et al*, 2011). Galantamine is currently available for treatment of mild to moderate cognitive impairments in AD due to its actions as an inhibitor of AChE (Deardorff *et al*, 2015). At lower concentrations, however, galantamine can also act as an α7 nAChR APL (Maelicke and Albuquerque, 1996; Pereira *et al*, 2002; Samochocki *et al*, 2003; Storch *et al*, 1995). Using a mouse model of AD, Bhattacharya *et al* (2014) have demonstrated improvement of cognitive and behavioural symptoms following galantamine administration as well as potential disease-modifying and neuroprotective properties of galantamine. For example, galantamine

treatment was able to decrease the density of amyloid beta (Aβ) placques in the hippocampus of affected mice.

However, α7 nAChRs also have neurotoxic properties. One of the hallmark signs of AD is the accumulation of the abnormally folded protein Aβ, particularly the 42-amino-acid form $A\beta_{1-42}$. These Aβ oligomers are thought to impair neuronal function and cognition (Danysz and Parsons, 2012). The α7 nAChR can bind directly to Aβ (Wang *et al*, 2000a, 2000b), which may contribute to cell death in the pathogenesis of AD (Conejero-Goldberg *et al*, 2008).

Additionally, α7 nAChRs can be linked to neurotoxicity in the absence of other disease mechanisms. For example, stimulation of α7 nAChRs in PC12 cells, a rat cell line derived from a neuroendocrine tumor of the adrenal medulla, has been shown to induce neuronal survival as well as neuronal death depending on the degree of activation through activation of different intracellular transduction processes (Li *et al*, 1999).

1.6 INTERACTION BETWEEN NMDA RECEPTORS AND A7 NICOTINIC RECEPTORS

NMDA receptors and α7 nicotinic acetylcholine receptors are ligand-gated ion channels permeable to calcium and other ions. Both receptor types are expressed in the hippocampus. Physiologically, they are thought to be involved in cognitive processes, such as synaptic plasticity, learning and memory. However, both nicotinic receptor-mediated mechanisms and NMDAR dysfunction have been implicated in various neuropathological diseases.

The properties and function of NMDARs and α7 nAChRs are dependent on subunit composition. Additionally, receptor phosphorylation, interaction with intracellular proteins, and interaction with GPCRs can influence the activity of these ligand-gated ion channels (Li *et al*, 2014). For example, protein kinase C-mediated phosphorylation can regulate NMDAR function (Chen and Huang, 1992; Wang *et al*, 2014), whereas dephosphorylation of α7 nAChRs by tyrosine kinases appears to enhance receptor activity and expression (Cho *et al*, 2005; Wiesner and Fuhrer, 2006)

Recent experiments have provided evidence that different types of ion channel receptors can also directly interact with each other, possibly affecting receptor function. In a co-immunoprecipitation experiment, Li *et al* (2012) identified the presence of a complex between NMDARs, in particular the NR2A subunit, and α7 nAChRs in rat hippocampal tissue *in vivo*. Functional implications of disruption of the α7 nAChRs-NMDAR interaction using a specifically engineered protein peptide included reduced ERK activity and changes in behavior related to nicotine dependence. A follow-up study addressed questions about the functional effects of this receptor interaction. NMDAR-dependent miniature excitatory postsynaptic currents were enhanced by exposure to choline, a selective α7 receptor agonist. This effect was abolished by administration of the aforementioned interfering peptide, demonstrating that the α7 nAChR-NR2A interaction is essential for modulation of NMDAR function. In the same study, behavioural tests in mice indicated an important role of this complex in non-spatial learning and memory (Li *et al*, 2013).

A functional interaction between α7 nAChRs and NMDARs in physiological and pathophysiological events has been reported in previous publications. For example,

presynaptic stimulation of α7 nAChRs is known to facilitate glutamatergic transmission (Girod *et al*, 2000). Furthermore, α7 nicotinic receptors can influence presynaptic NMDAR expression (Lin *et al*, 2010). Zappettini *et al* (2014) not only provided immunocytochemical evidence for the co-localization of α7 nAChRs and NMDARs in the nucleus accumbens of rats, but also showed that choline-induced stimulation of α7 nicotinic receptors potentiates the function of NR2A-containing NMDA receptors.

With regards to NMDA-induced excitotoxicity, activation of α7 nAChR has been shown to have neuroprotective properties in acute hippocampal slices (Ferchmin *et al*, 2003), in neocortical cultures, and in rat models of focal ischemia (Shimohama *et al*, 1998). Some evidence exists to support the neuroprotective effect of choline pre-treatment 72 h prior to NMDA administration in organotypic hippocampal slice cultures (Mulholland *et al*, 2004). On the other hand, over-activation of this receptor subtype has been suggested to be neurotoxic. For example, exposure to high doses of the partial nicotinic agonists DMXB have been shown to induce cell death via α7 nicotinic receptors (Li *et al*, 1999). Additionally, α7 nAChRs were implicated in neurotoxic effects in a human neuroblastoma cell line (Guerra-Álvarez *et al*, 2015) and in a model of glutamatergic injury (Laudenbach *et al*, 2002).

1.7 ORGANOTYPIC HIPPOCAMPAL SLICE CULTURES

In vitro cell cultures are an important addition to *in vivo* animal models of stroke, as they allow for high throughput screening and study of molecular signaling pathways in a tightly regulated environment, while also reducing the number of animals used. Primary

dissociated cell cultures of neurons or other brain cell types are a commonly used tool in research, but have the disadvantage that many characteristics of the *in vivo* situation, such as connections to other cells and cell types, are not replicated. In contrast, organotypic brain slice cultures preserve the structural and cellular organization of the tissue and uphold synaptic connections from the original tissue (Cho *et al*, 2007). Easy experimental access and the possibility for exact regulation of the extracellular environment are additional advantages. These make organotypic brain slice cultures a viable alternative to the intact animal, combining the complexity of the *in vivo* context with the ability to regulate the extracellular environment.

Brain slice cultures have been successfully prepared from a wide range of brain regions, including hippocampus (Wang and Andreasson, 2010), cortex (Kang and Morrison, 2015), cerebellum (Campeau *et al*, 2013), striatum (Jäderstad *et al*, 2010), and spinal cord (Mazzone *et al*, 2013). More recently, organotypic slice co-culture systems have been developed, which allow for the evaluation of inter-neuronal responses and functional relationships across brain regions (Guthrie *et al*, 2005). Especially organotypic hippocampal slice cultures (OHSCs) have been used extensively to study the development and functional role of the hippocampal formation (Gambrill and Barria, 2011) as well as neuronal damage (Butler *et al*, 2010) and neuroprotection (Ring *et al*, 2010).

1.7.1 Hippocampus

The hippocampus, a small sea-horse-shaped structure located in both hemispheres under the cerebral cortex, is an important part of the limbic system. It can be divided into two main parts: the DG and the hippocampus proper. The latter is also referred to as

Ammon's horn, or *cornu ammonis* (CA), and consists of four different subfields designated CA1-4. There are other areas that are not considered a part of the hippocampus, but are closely associated with it, including the subiculum and the entorhinal cortex. Therefore, these regions are often combined under the term hippocampal formation (Parkin, 1996).

Hippocampal neurons are interconnected by projections of excitatory neurons. Receiving input from the entorhinal cortex via the performant path, the DG sends excitatory axons, also called mossy fibers, to the CA3 region. Cells from CA3 then project further to the CA1 neurons via the Schaffer collaterals (Andersen *et al*, 1971). Functionally, the hippocampus is known to be involved in cognitive functions, such as learning and memory processes (Shapiro and Eichenbaum, 1999). The concept of LTP, which describes the strengthening of synapses caused by repeated patterns of synaptic activity, has been extensively studied in this brain structure. As a form of synaptic plasticity, LTP is believed to be one of the primary cellular mechanisms underlying learning and memory (Baudry *et al*, 2015).

Glutamate receptors, particularly NMDA receptors, are thought to be involved in learning and memory processes (Bliss and Lomo, 1973). The importance of NMDA receptors in learning and synaptic plasticity is supported by experiments studying the effect of a NMDAR antagonist on behavioral effects of rats in certain learning tasks. Administration of the selective NMDA receptor antagonist 2-amino-5-phosphono-pentanoic acid caused impairment of spatial learning as well as a total block of hippocampal LTP *in vivo* (Morris, 1989). NMDARs are expressed at high levels in the rat

hippocampus (Monaghan and Cotman, 1985; Moriyoshi *et al*, 1991), which also makes it an interesting region to study mechanisms of excitotoxicity.

With importance to this thesis, the α7 nicotinic acetylcholine receptor is also highly expressed in the rat hippocampus (Adams *et al*, 2002; Séguéla *et al*, 1993), suggesting a potential involvement in regulating synaptic transmission, plasticity, and neurodegeneration (Fabian-Fine *et al*, 2001). For example, stimulation of α7 nAChRs has been shown to enhance LTP (Fujii *et al*, 1999; Hunter *et al*, 1994). This effect is possibly because of increased presynaptic release of Glu and postsynaptic depolarization, both of which can be mediated by the α7 nAChR (Cheng and Yakel, 2015; Ge and Dani, 2005). Furthermore, the presence of a complex between NMDA receptors and α7 nAChRs has initially been described in rat hippocampal tissue (Li *et al*, 2012, 2013). Therefore, the hippocampus is an appropriate region of the brain to investigate the potential interaction of NMDA receptors and α7 nAChRs with regards to excitotoxicity in organotypic slice cultures.

1.7.2 Methodological aspects for the use of organotypic hippocampal slice cultures

Several techniques have been developed over the years to prepare and maintain organotypic slices of brain tissue in long-term culture. The two predominant procedures are the roller tube technique and the membrane interface method. In organotypic cultures prepared by using a roller tube as described by Gähwiler (1981), brain tissue is attached to glass coverslips, embedded in plasma clots or collagen matrix and incubated in slowly rotating culture tubes. A very unique characteristic of these roller-tube cultures is the monolayer aspect, as the slice cultures flatten considerably after 2-3 weeks *in vitro* to approximately 50 µm, thus facilitating experiments where optimal optical conditions are

necessary (Gähwiler *et al*, 1997). However, the thinning of the tissue may generate large experimental variability, as overall health of the slice and diffusion distances are linked to slice thickness (Guy *et al*, 2011). The difficulty of the roller tube preparation method is an additional disadvantage (Cho *et al*, 2007).

First described by Stoppini *et al* (1991), the membrane interface method has further increased the use of organotypic slice cultures due to the easier preparation procedure compared to the roller tube technique (Lossi *et al*, 2009). In membrane cultures, tissue slices are placed onto a semiporous membrane at the interface between humidified air and culture medium on the underside of the membrane. In contrast to roller-tube cultures, slice cultures grown by the interface method usually remain a few cell layers thick and flatten from an initial 400 µm to approximately 100-150 µm (Stoppini *et al*, 1991). Brain slices prepared by either technique preserve many essential characteristics of the original tissue, including proper morpho-anatomical organisation, structural integrity, neuronal connectivity, and glial-neuronal interactions, and can be maintained in culture for fairly long periods of time (Bahr *et al*, 1995; Gähwiler *et al*, 1997). However, most recent experimental studies use adaptations of the membrane interface method.

Organotypic slice cultures are typically prepared from brains of animals at the early postnatal stage (postnatal day [PND] 0 to 12). At this age, the brain tissue has matured enough to establish cytoarchitectonic fundamentals and basic synaptic connections. Additionally, slice cultures prepared from postnatal brain tissue appear to be more resistant to mechanical trauma during the culturing procedure and exhibit a high degree of plasticity. In comparison to the embryonic stage, the larger size of postnatal brains also facilitates the culture preparation (Cho *et al*, 2007). More recently, efforts to use

adolescent or adult animals have been made, but the viability of these slices seems to decrease with age, making long-term culture difficult (Humpel, 2015a).

Using OHSCs, it is also possible to reduce the number of experimental animals needed. Typically, about 20-25 slices can be obtained from a single donor animal. Multiple data points can be generated from cultures derived from each individual animal, thereby sparing a significant number of live animals.

It is important to note the limitations of *in vitro* preparations including ways they deviate from *in vivo* conditions. For example, the CA1 region in organotypic hippocampal slices exhibits a more complex pattern of dendritic branching than observed *in vivo*. Additionally, *in vitro* preparations exhibit a significant increase in the frequency of glutamatergic miniature synaptic currents, suggesting that there are an increased number of total synapses *in vitro*. However, during subsequent stages of culture, maturation and development in the *in vitro* conditions almost entirely match development observed *in vivo* (De Simoni *et al*, 2003).

Collectively, OHSCs offer a highly effective compromise between complex *in vivo* models and monolayers *in vitro* cultures. As they preserve many of the *in vivo* characteristics and permit the precise control of the extracellular environment, organotypic hippocampal slice cultures represent an important tool for the study of neurophysiological and pathophysiological questions.

1.7.3 Rationale to use organotypic hippocampal slice cultures as an *in vitro* model of excitotoxicity

Organotypic hippocampal slice cultures have not only been commonly used to investigate physiological functions of the hippocampus, but also to study mechanisms of neuronal death underlying diseases, including stroke, epilepsy, or Alzheimer's disease. Oxygen-glucose deprivation and administration of excitotoxins (Ahlgren *et al*, 2011; Bruno *et al*, 1994; Wise-Faberowski *et al*, 2009a) are the two most common models of ischemia and stroke in organotypic slice cultures. While administration of excitotoxins such as Glu or NMDA only models one aspect of the ischemic cascade, it permits the investigation of the involvement of specific GluRs (Noraberg *et al*, 2005).

In addition to preserving the cytoarchitecture of the tissue, organotypic hippocampal slice cultures have been shown to stably express NMDA receptors and other GluRs in long-term culture conditions despite an initial small decrease in expression after tissue cutting (Bahr *et al*, 1995). Furthermore, the expression of various NMDAR subunits in OHSCs is comparable to expression levels *in vivo*, and NMDARs expressed in cultures are functional and can induce excitotoxic cell death (Ahlgren *et al*, 2011).

The hippocampus also expresses α7 nAChRs at high levels (Adams *et al*, 2002; Fabian-Fine *et al*, 2001). Importantly, expression of α7 nAChRs is maintained in OHSCs (Mielke and Mealing, 2009). Therefore, OHSCs present a valuable *in vitro* model for the investigation of the potential interaction between α7 nAChRs and NMDARs after excitotoxic insult.

1.8 EXPERIMENTAL RATIONALE, HYPOTHESIS AND STUDY OBJECTIVES

While physiological activation of NMDA receptors is necessary for neuronal survival, over-activation of NMDA receptors by excess levels of glutamate leads to rapid neuronal cell death by excitotoxicity. This process is believed to be the underlying cause of neurodegeneration following stroke. Recent literature has suggested a possible interaction between NMDARs and α7 nAChRs, but the exact role of α7 nAChRs in mediating excitotoxicity is still unclear with reports of nAChRs being both neurotoxic and neuroprotective in certain systems. The aim of this thesis was to investigate the possible interaction between NMDARs and α7 nAChRs *in vitro* using organotypic hippocampal slice cultures.

The hypothesis for this thesis is that co-activation of α7 nicotinic acetylcholine receptors alters NMDA-induced neurotoxicity in organotypic hippocampal slice cultures.

Using OHSCs, the primary objectives for research outlined within this thesis were twofold:

1) To develop a method to objectively quantify cell death in organotypic hippocampal slice cultures using propidium iodide (PI) exclusion
2) To establish a dose-response curve for NMDA toxicity
3) To determine the effects of co-activation of α7 nicotinic acetylcholine receptors on NMDA-mediated excitotoxicity

CHAPTER 2:

DEVELOPMENT OF A METHOD TO OBJECTIVELY QUANTIFY CELL DEATH IN ORGANOTYPIC HIPPOCAMPAL SLICE CULTURES USING PROPIDIUM IODIDE

A modified version of this chapter is published as: **Happ,D.F., Tasker, R.A., A method for objectively quantifying propidium iodide exclusion in organotypic hippocampal slice cultures. Journal of Neuroscience Methods 269 (2016) 1-5**

SUMMARY

Organotypic hippocampal slice cultures retain the normal hippocampal cytoarchitecture, function, and cellular diversity observed *in vivo*, and therefore present an attractive *in vitro* model to investigate physiological functions of the hippocampus as well as mechanisms of neuronal death. OHSCs have been increasingly used to study mechanisms of neurotoxicity underlying neuropathological diseases such as stroke by either oxygen-glucose deprivation or exposure to excitotoxins such as NMDA. The fluorescent dye propidium iodide is a commonly used marker for membrane integrity and cell injury. However, no standardized format for quantifying PI uptake in OHSCs exists. In the study presented in this chapter, organotypic hippocampal slice cultures were prepared from 5-6 day old rats according to the interface method and maintained for 13 days. After confirming viability, slices were exposed for 4 hours to varying concentrations of NMDA and re-evaluated by PI exclusion after 24 hours in fresh media. To quantify PI uptake, subfields were separated using simple landmarks and densitometric quantification of PI fluorescence intensity in 10 template-oriented counting fields. This protocol describes a simple method to objectively quantify cell death in OHSCs. The method provides a standardized format, is applicable to cultures of differing shapes and sizes, and permits comparisons between hippocampal subfields. This method was therefore deemed to be appropriate to use for studying the effects of receptor interaction in the following chapters of this thesis.

2.1 INTRODUCTION

During an ischemic stroke, a complex series of multiple cellular events is triggered (see Chapter 1, Section 1.4). The current hypothesis is that lack of blood flow restricting oxygen and glucose exchange leads to depletion of energy, which impairs cellular ion pumps, resulting in cell depolarization. As voltage-dependent calcium channels become activated, excitatory neurotransmitters such as Glu are released into the extracellular space and accumulate due to failure of energy-dependent reuptake mechanisms (Dirnagl and Endres, 2014).

Glu is the main excitatory neurotransmitter in the mammalian CNS. Through activation of ionotropic receptors and a family of G-protein coupled metabotropic receptors, Glu is involved in numerous processes during brain development as well as physiological function throughout life. Despite its critical role in normal brain development and function, over-activation of the Glu system can lead to rapid cell death in the CNS by a process called excitotoxicity (Meldrum, 2000).

During an ischemic attack, the excessive extracellular levels of Glu can over-stimulate NMDA and AMPA receptors resulting in a massive influx of divalent cations, especially Ca^{2+}. Due to their high Ca^{2+} permeability, NMDARs contribute greatly to the intracellular calcium overload, which may subsequently activate signaling cascades causing neuronal cell death. NMDAR-mediated calcium influx is associated with cytotoxicity in many pathological states, including brain ischemia, traumatic brain injury, and multiple neurological diseases such as AD, Parkinson's Disease, and amyotrophic lateral sclerosis (Dong *et al*, 2009; Szydlowska and Tymianski, 2010).

Many clinical trials investigating the neuroprotective potential of drugs, such as NMDAR inhibitors, have been unsuccessful, arguably due to lack of sufficient pre-clinical data (Ginsberg, 2008). The traditional approach to pre-clinical characterisation of potential drugs – extensive *in vivo* testing in animal models – has some significant drawbacks, including lengthy animal surgery to model the neuropathology of stroke, and laborious monitoring of physiological parameters following *in vivo* manipulation (Cho *et al*, 2007). The use of *in vitro* cell culture preparations, such as organotypic slice cultures, may present an alternative to *in vivo* models for the study of pathological mechanisms underlying neurodegenerative diseases (Humpel, 2015b).

Organotypic hippocampal slice cultures have become a valuable *in vitro* preparation to study a wide range of CNS functions including mechanisms of neurotoxicity. This is mainly because they offer unique advantages over other *in vitro* models such as primary dissociated cultures. OHSCs can be maintained *in vitro* for several weeks and, importantly, the slice cultures replicate many aspects of the *in vivo* context as they largely preserve the normal cytoarchitecture of the hippocampus and maintain intact neuronal activities (Cho *et al*, 2007). Furthermore, this system provides good pharmacological accessibility and allows for exact control of the extracellular environment, which simplifies the scientific correlation between molecular changes and neuropathological outcomes (Bernaudin *et al*, 1998). Therefore, OHSCs present an attractive and more easily manipulated alternative to studying the hippocampus *in vivo*.

Organotypic slice cultures have been successfully established from a variety of CNS regions, including cerebral cortex, striatum, and cerebellum. The hippocampus is of particular interest as this region of the brain is known to be susceptible to Glu-mediated

signaling and excitotoxicity. Due to extensive multidisciplinary research, this area of the brain is also the best characterized in slice cultures (Lossi *et al*, 2009). Slice cultures prepared from the hippocampus not only retain the hippocampal architecture, but they also preserve the intrinsic connectivity between the hippocampal regions DG, CA3, and CA1 (Gutiérrez and Heinemann, 1999). Additionally, Gerace *et al (*2012) have shown that the distribution of Glu receptors is very similar to that observed *in situ*.

With relevance to this thesis, OHSCs have been used increasingly for the investigation of mechanisms of neuronal damage underlying neuropathological diseases such as stroke. To mimic the events after an ischemic-hypoxic insult, OHSCs are commonly subjected to either oxygen glucose deprivation or exposure to excitotoxins such as NMDA. In this way, slice cultures are oftentimes used for screening of therapeutic molecules or novel genes (Abdel-Hamid and Tymianski, 1997; Kleczkowska *et al*, 2015).

There are numerous methods to study cell death in OHSCs. These techniques include fluorescent staining (e.g. PI, Hoechst 33342, Fluoro-Jade), enzymatic assays (e.g. measuring the amount of lactate dehydrogenase (LDH) released into the media from damaged cells), and ultrastructural analysis. The cell impermeable dye PI is one of the most commonly used measures of neuronal death. Compared to healthy neurons, damaged or dead cells have compromised membrane integrity, allowing otherwise membrane-impermeable molecules to pass through. The polar compound PI readily enters neurons with damaged membranes and, once inside, binds to nucleic acids. It intercalates with DNA with a stoichiometry of one dye molecule per 4-5 base pairs with little sequence preference, rendering the dye to fluoresce brightly red (Cho *et al*, 2007;

Hezel *et al*, 2012; Noraberg *et al*, 1999). PI is considered to be non-toxic to neurons, and its uncomplicated application makes it a popular method to assess neuronal cell death.

Although PI incorporation has been commonly employed as a marker for membrane integrity and cell viability in OHSCs and other *in vivo* preparations for decades, there is considerable variability in the methods used to measure and quantify PI. In older studies, PI uptake was frequently assessed qualitatively or semi-quantitatively using nominal scales (e.g. 0-4) to score toxicity of compounds (Liu *et al*, 2003; Simantov *et al*, 1999). Another technique to quantify PI labeling in OHSCs was to transform images after thresholding analysis to binary displays. This way, PI-positive cells were presented as white pixels over black background pixels, and cell death could be assessed by counting pixels (Kasof *et al*, 1995). Similar measures based on binary images of PI fluorescence intensity are occasionally still used today (Katayama *et al*, 2012). With the advancement of microscopes and imaging software, cell counting can also be performed without the transformation into binary images (Radley *et al*, 2012; Wise-Faberowski *et al*, 2009b).

With the advance of computer imaging software, the most commonly used measure to objectively assess PI uptake is based on the quantitative densitometric analysis. However, a review of the current literature reveals a lack of consistency in the reported methods. Some authors suggest measuring gray-level intensity (Laake *et al*, 1999) as opposed to measuring fluorescence intensity directly. Cell damage can be calculated as the percentage of the total area labeled PI-positive (Kreutz *et al*, 2011) or as the percentage of the regional area in which PI fluorescence was detected using defined regions of interest within hippocampal subregions (Graulich *et al*, 2002). Furthermore, PI uptake has also been reported as the percentage of fluorescence intensity of control

groups (Butler *et al*, 2013; Gregersen *et al*, 2013; Lutz *et al*, 2015; Smith *et al*, 2010) or, more commonly, as the percentage of maximal fluorescence intensity. Various methods have been described to acquire terminal images representing maximal PI fluorescence intensity and therefore 100% cell death, including superfusion with 100 µM NMDA for 1 hour (Kim *et al*, 2015; Kleczkowska *et al*, 2015; Xu *et al*, 2003), exposure to 50 mM Glu for 1 h (Noraberg *et al*, 1999), and low-temperature exposure (4°C) for 24 hours (Allard *et al*, 2015). However, the induction of maximal cell death for each slice has the disadvantage that treated slice cultures cannot be used for other subsequent procedures, such as protein isolation or immunohistochemical staining, after the insult.

The specific objective of this study was to develop a simple and reproducible method to objectively quantify cell death in OHSC using PI exclusion with a standardized format. To demonstrate the utility of the method we used exposure to varying concentrations of the excitotoxin NMDA.

2.2 METHODS

2.2.1 Experimental animals

Offspring born in-house from untimed pregnant Sprague-Dawley rats (Charles River, Quebec, Canada) were used to prepare the organotypic hippocampal slice cultures. After arrival at the facility, dams were housed individually with *ad libitum* access to water and Purina Rodent Chow. The housing facility was maintained at approximately 22°C under a 12 h light-dark cycle (lights on at 06:00, off at 18:00). The day of parturition was designated as PND0. Animals were left undisturbed until the day of culturing on PND5/6.

Studies were carried out under approval from the University of Prince Edward Island Animal Care Committee, and were in accordance with the Canadian Council on Animal Care guidelines.

2.2.2 Preparation and maintenance of organotypic hippocampal slice cultures

The slice cultures were prepared according to the interface method of Stoppini *et al* (1991) with minor modifications. On PND5/6, rat pups were quickly decapitated, and the brain was removed and hippocampus dissected under aseptic conditions. The two hippocampi were dissected consecutively and stored temporarily in ice cold dissection medium containing 1% penicillin/streptomycin-solution (Gibco, NY, USA), 25 mM HEPES (pH 7.2-7.5, Fisher Scientific, NJ, USA) and 10 mM Tris (pH 7.2-7.3; Fisher Scientific) in Minimum Essential Media (MEM; Gibco, USA). The dissected hippocampi were straightened and transversely sliced throughout the entire length into 400 µm sections using a mechanical tissue chopper (Stoelting, IL, USA). The slices were immediately transferred into ice cold dissection medium. Slices were then separated by gently pipetting the tissue up and down using a plastic transfer pipette. Under a light microscope, slices with intact hippocampal morphology were placed onto 0.4 µm porous Millipore inserts (Millipore, MA, USA). Any excess medium from the top of the insert was suctioned off. Membrane inserts containing three slices each were transferred to individual 35 mm cell culture dishes (Fisher Scientific) filled with 1 ml of serum-based medium containing 50% MEM, 25% Hank's balanced salt solution (Gibco), 12 mM HEPES, 25% heat-inactivated horse serum (Gibco), and 1% penicillin-streptomycin solution. Slice cultures were incubated in a humidified chamber at 37ºC in 5% CO_2 for 13 days to allow for good adherence to the membrane and the loss of any dead or damaged

cells on the surface of the slices. The media was changed the day after preparing cultures and then every three days.

2.2.3 Assessing viability using propidium iodide

At 13 days *in vitro* (DIV13) and before any experiments, OHSCs were exposed to PI (5 µg/ml; Sigma-Aldrich, MO, USA) for 30 minutes to assess cell culture viability. Using a Fluoroarc exciter lamp with a Zeiss Axioplan2 microscope equipped with a standard rhodamine filter, PI uptake was recorded with an AxioCam HR digital camera (Carl Zeiss Canada Ltd, ON, Canada) at this and subsequent stages. All images were taken with a 5× objective. The camera was connected to a computer loaded with the Axiovision Software as provided by the manufacturer. To ensure consistency and proper comparability of experimental results, the same exposure settings were used during all experiments (see Table 2-1). Slice cultures displaying distinct PI fluorescence were excluded from further experiments. PI-negative slices, however, were exposed to the indicated treatment conditions.

Table 2-1: Fluorescence microscope settings for propidium iodide imaging

Exposure time	22.1 ms / 104%
Brightness	-0.5
Contrast	1.00
Slope	1.07
Color offset	0.00
Saturation	1.0

2.2.4 Drug application

Healthy OHSCs, as determined by PI uptake (see above), were exposed to different concentrations of NMDA (Sigma-Aldrich) (1 µM, 10 µM, 50 µM, 100 µM, 500 µM and

1 mM) in 0.9% saline, or to 0.9% saline alone as control for 4 hours. Slice cultures were then transferred to fresh culture medium for 24 hours. After this 24 hour period, PI uptake was measured again to determine the effects of drug exposure on cell viability. Additionally, light microscope pictures of each slice were taken to facilitate identification of hippocampal structures. Negative control slices were exposed to the same amount of saline. To serve as positive controls, OHSCs were exposed to ice cold 70% ethanol for 24 hours at -20°C. A minimum of 6 slices were analysed and averaged per treatment condition with rat pup as the unit of variance.

2.2.5 Image analysis and quantification of PI fluorescence

The digital pictures of propidium iodide uptake taken by the fluorescence microscope (1300×1030 pixels) were analyzed by densitometry with the public domain Java image processing program ImageJ® inspired by NIH Image (National Institute of Health, MD, USA) for the Macintosh.

Because of the irregularly shaped and sized slice cultures, a standardized method of quantifying PI uptake was needed to be able to consistently compare cell viability. For this reason, a standard template of 9 movable, circular regions of interest, with three in each of the hippocampal regions (DG, CA3 and CA1), was developed (see Figure 2-1). Within the ImageJ software, the circles were specified as 80×80 pixels. Using conventional landmarks, the hippocampal subfields were identified. To facilitate optical separation of the hippocampal regions, a straight line was drawn connecting the two arms of the DG and extending through the *cornu ammonis* area. In order to standardize the placing of the measuring fields, the first circle was placed at the midpoint of each region, with the other two circles placed equally distant from the midpoint and the boundaries.

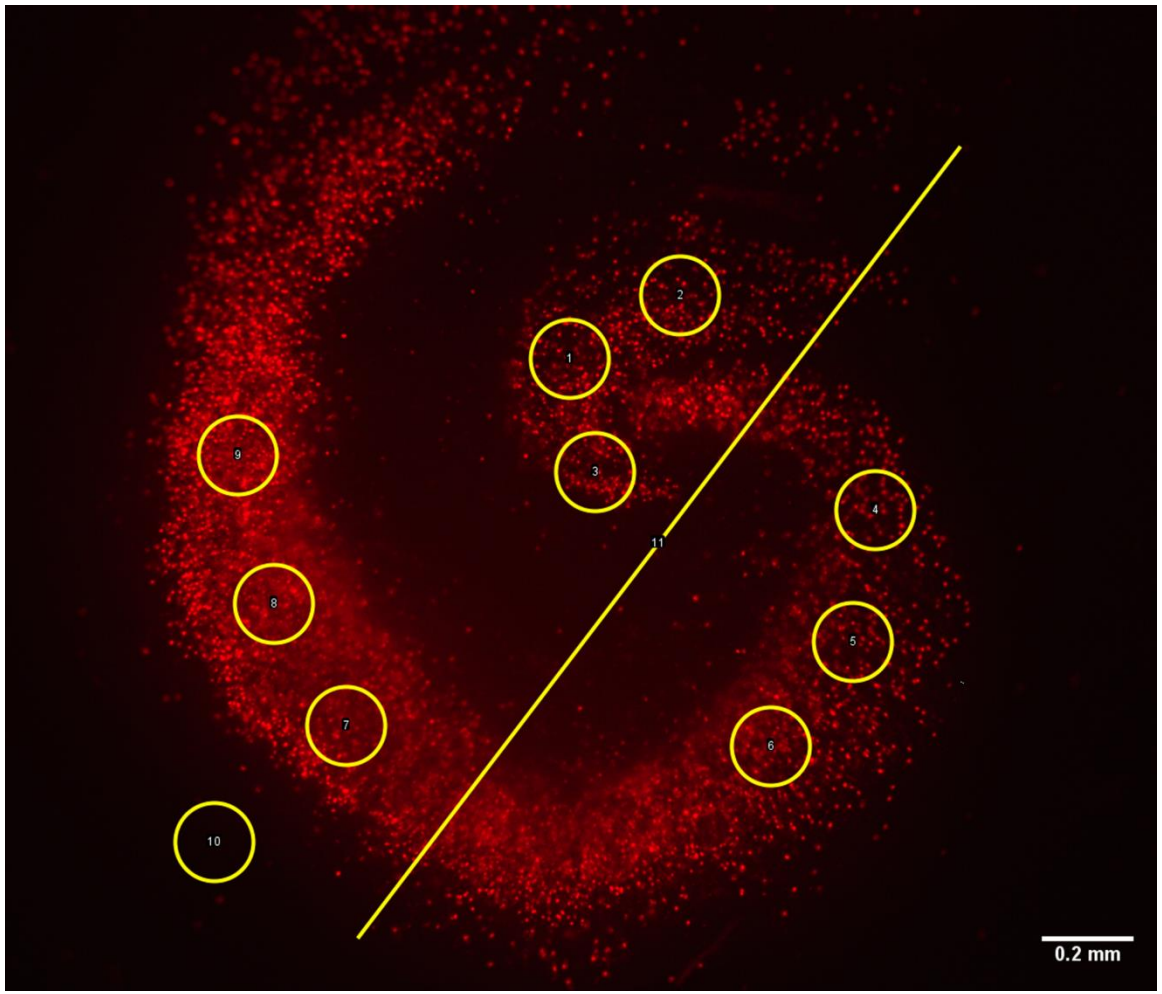

Figure 2-1: Standard template for quantification of propidium iodide. Representative illustration shows placement of measurement windows in the hippocampal areas (dentate gyrus, CA3 and CA1) of propidium iodide-stained organotypic hippocampal slice cultures.

Additionally, a tenth circle was placed adjacent to the slice culture to allow for subtraction of any background noise. The raw integrated density, the sum of the pixel values, was calculated for every circle of each slice.

The PI uptake recorded after low temperature exposure to 70% ethanol represented maximum cell death. In this way, the PI uptake induced by NMDA exposure could be expressed as the percentage of the maximal PI uptake.

2.2.6 Data analysis

All densitometric data were expressed as mean ± standard error of the mean (SEM). The dose-response-curve for NMDA-induced excitotoxicity was created with 5-12 slices from 5-7 different preparations (n=5-7). Statistical significance was assessed in SPSS Statistics Version 23 (IBM Corporation, NY, USA).

A one-way analysis of variance (ANOVA) followed by a Games-Howell procedure was conducted to determine the effect of increasing NMDA concentrations on the combined cell death for the whole slice culture. Two-way mixed factorial ANOVA was used to compare PI uptake among the different hippocampal regions DG, CA1, and CA3. Post-hoc tests were performed with the Games-Howell procedure. Subsequently, effects of drug exposure on cell viability were analyzed for each hippocampal region separately using one-way ANOVA followed by the Games-Howell procedure. Differences were considered significant at $p<0.05$.

2.3 RESULTS

2.3.1 Dose dependent excitotoxic effects of NMDA

Hippocampal structure in all organotypic slice cultures included in the analysis was well preserved and PI uptake was very low before agonist exposure. Normality of the data was confirmed (p=0.200) using the Kolmogorov-Smirnov test. Levene's test of equality of error variances was significant ($F_{6,35}$=4.56, p=0.002) Therefore, Welch's F ratio was used to determine the significance of the ANOVA and the Games-Howell procedure was selected to investigate between-group differences.

Cell death varied significantly in slice cultures exposed to different concentrations of NMDA based on ANOVA ($F_{6,35}$= 7.1746, p<0.0005). In control cultures treated with saline, cell death occurred spontaneously on a small scale with a basal PI uptake of 4.28% ± 0.38 (n=5). As shown in Figure 2-2, slice cultures treated with NMDA (1-1000 µM) for 4 hours revealed a dose-dependent increase in PI uptake when data from all hippocampal subfields as recorded 24 hours later were combined. Addition of 1 µM NMDA to the culture medium resulted in a significant increase in the level of PI incorporation compared to the control group (8.26% ± 0.44, n=6, p=0.001). PI uptake further progressed with increasing concentrations of NMDA (26.81% ± 2.89, n=7, p=0.002; 37.18% ± 6.14, n=6, p=0.024; 38.54% ± 5.06, n=6, p=0.009; 31.26% ± 3.85, n=6, p=0.007; 47.42% ± 2.82, n=6, p<0.0005 for 10, 50, 100, 500 and 1000 µM NMDA, respectively). The levels of PI fluorescence intensity after exposure to 10, 50, 100, 500 and 1000 µM NMDA were also significantly different from slice cultures treated with 1 µM NMDA. Furthermore, PI uptake was significantly increased in slices exposed to 1000 µM NMDA compared to OHSC exposed to 10 µM NMDA (p=0.005). However, there

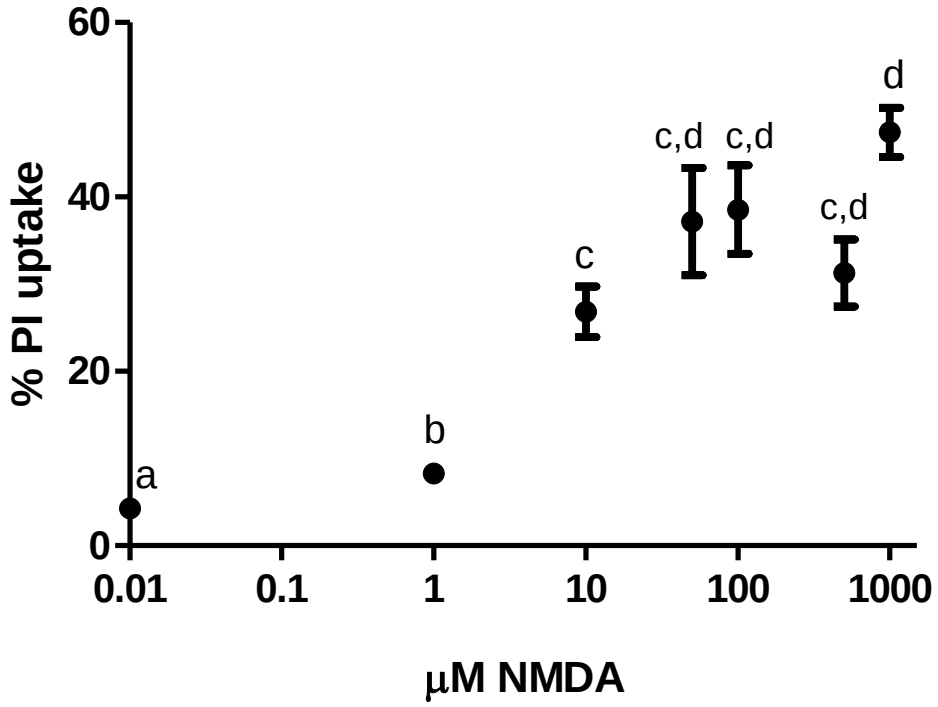

Figure 2-2: Dose-response relationship between increasing concentrations of NMDA and propidium iodide (PI) uptake measured for the entire hippocampal slice culture. Maximal cell death (100%) was measured in OHSCs exposed to 70% ethanol for 24 h at -20°C. Data are shown as means ± SEM, with n = 5–7, Different letters indicate significant differences between groups (p<0.05) using one-way ANOVA with Games-Howell procedure. The value of 0.01 µM NMDA represents saline as a control.

was no significant difference between cell death in slice cultures exposed to 50, 100, 500 or 1000 μM NMDA.

2.3.2 Differential susceptibility of hippocampal subfields to NMDA

The hippocampus has been shown to exhibit region-specific vulnerability to various types of insults (Kosuge *et al*, 2008; Stanika *et al*, 2010). In order to determine whether there was an interaction between NMDA concentration and hippocampal region, the data were analyzed using a one-way ANOVA with repeated measures design (with the hippocampal regions DG, CA3, and CA1 as within-subject factors). Figure 2-3 shows the dose-response relationship for NMDA in the three hippocampal subfields, DG, CA1, and CA3. Mauchly's test of sphericity was significant ($p<0.0005$) and therefore the Greenhouse-Geisser correction was used to assess the F-value. A significant difference between hippocampal regions was found ($F_{1.33,45.61}=136.54$, $p<0.0005$). Pairwise comparisons using Bonferroni adjustment revealed that each hippocampal region was significantly different from each other ($p\leq0.001$). Therefore, the hippocampal subfields were subsequently analyzed separately using one-way ANOVA (Welch's F-value) followed by Games-Howell procedure as Levene's test for homogeneity of variance was significant for all three regions (DG: $p=0.021$; CA1: $p<0.0005$; CA3: $p=0.002$). The general trends observed in the combined values are reflected in the individual regions. A significant effect of NMDA concentration was found in all three regions (DG: $F_{6,35}=44.206$, $p<0.0005$; CA3: $F_{6,35}=42.955$, $p<0.0005$; CA1: $F_{6,35}=52.466$, $p<0.0005$). However, higher values of PI uptake were generally observed in the CA1 region compared to CA3 and DG (see Table 2-2 for a summary of all the values).

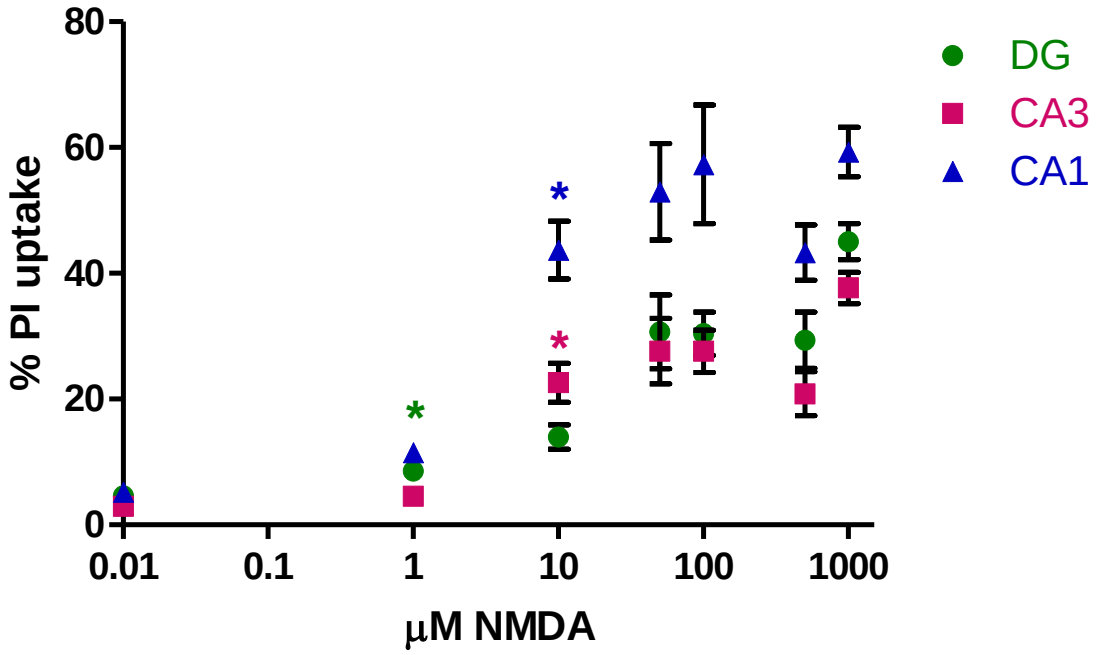

Figure 2-3: Dose–response relationship between increasing concentrations of NMDA and cellular propidium iodide (PI) uptake, measured for the hippocampal subregions separately. The maximal PI uptake after 24 h low-temperature exposure to 70% ethanol was set to 100%. Data are shown as means ± SEM, with n = 5–7. The value of 0.01 µM NMDA represents saline as a control. Using a one-way ANOVA with repeated measures design, a significant difference between hippocampal regions was found ($F_{1.33,45.61}$=136.54, p<0.0005). * indicates the first concentration to be significantly different (p<0.05) from saline treated control cultures in the respective region, with following asterisks omitted for clarity.

Table 2-2: Propidium iodide uptake in the dentate gyrus (DG) and CA3 and CA1 hippocampal regions in organotypic slice cultures treated with increasing concentrations of NMDA or saline as negative control for 4 hours, as recorded after 24 h in fresh media. Data expressed as percentage of positive control exposed to 70% ethanol at low temperature for 24 h (mean ± SEM). a indicates significance (p<0.05) from saline, b from 1 µM NMDA, c from 10 µM NMDA and d from 500 µM NMDA in the respective region.

	CA1	CA3	DG
Saline	5.21 ± 0.58	2.98 ± 0.36	4.62 ± 0.38
1 µM NMDA	$11.51 \pm 1.47_{a}$	4.59 ± 0.20	$8.60 \pm 0.61_{a}$
10 µM NMDA	$43.70 \pm 4.60_{a,b}$	$22.61 \pm 3.08_{a,b}$	13.98 ± 1.94
50 µM NMDA	$52.99 \pm 7.66_{a,b}$	$27.60 \pm 5.20_{a,b}$	$30.69 \pm 5.87_{a}$
100 µM NMDA	$57.33 \pm 9.45_{a,b}$	$27.62 \pm 3.36_{a,b}$	$30.40 \pm 3.41_{a,b,c}$
500 µM NMDA	$43.29 \pm 4.39_{a,b}$	$20.86 \pm 3.49_{a,b}$	$29.37 \pm 4.44_{a,b}$
1000 µM NMDA	$59.30 \pm 3.91_{a,b}$	$37.68 \pm 2.5_{a,b,c,d}$	$45.03 \pm 2.85_{a,b,c}$

In the DG, a basal PI uptake of 4.62% ± 0.38 (n=5) was observed in the saline-treated cultures. Figure 2-3 shows the increase in PI uptake for slice cultures treated with NMDA (1-1000 µM). Addition of 1 µM NMDA to the culture medium resulted in a significant increase in the level of PI incorporation compared to the control group (8.59% ± 0.61, n=6, p=0.006). Increasing concentrations of NMDA induced significantly higher levels of PI incorporation (13.98% ± 1.94, n=7, p=0.024; 30.69% ± 5.87, n=6, p=0.051; 30.40% ± 3.41, n=6, p=0.005; 29.37% ± 4.44, n=6, p=0.020; 45.03% ± 2.85, n=6, p<0.0005 for 10, 50, 100, 500 and 1000 µM NMDA, respectively).

There was no significant difference in PI uptake between control OHSCs (2.98% ± 0.36, n=5) and slices treated with 1 µM NMDA (4.59% ± 0.20, n=6, p=0.061) in the CA3 region. However, addition of higher concentrations of NMDA revealed significant differences in PI uptake (22.61% ± 3.08, n=7, p=0.006; 27.60% ± 5.20, n=6, p=0.040; 27.62% ± 3.36, n=6, p=0.006; 20.86% ± 3.49, n=6, p=0.029; for 10, 50, 100 and 500, respectively), but did not exceed 37.68% ± 2.50 after exposure to 1000 µM NMDA (n=6, p<0.0005). PI uptake in the CA3 region generally seems to be lower when compared to the DG.

The highest PI uptake of 59.30% ± 3.91 was recorded in the CA1 region after treatment with 1000 µM NMDA (n=6, p<0.0005 from control). Slice cultures treated with saline (5.21% ± 0.58, n=5) or 1 µM NMDA (11.51% ± 1.47, n=6, p=0.054) did not exhibit significant differences in PI uptake. However, levels of PI uptake differed significantly in slice cultures treated with higher doses of NMDA (43.70% ± 4.60, n=7, p=0.024; 52.99% ± 7.66, n=6, p=0.051; 57.33% ± 9.45, n=6, p=0.005; 43.29% ± 4.39,

n=6, *p*=0.020; for 10, 50, 100 and 500 µM NMDA, respectively) compared to control slices.

2.4 DISCUSSION

Many neuropathological and neurodegenerative diseases, including stroke, traumatic brain injury and AD, are associated with neuronal cell death as a result of Glu -mediated excitotoxicity. Elevations of extracellular Glu over-activate ionotropic NMDA receptors leading to massive calcium influx, mitochondrial dysfunction, and the formation of reactive oxygen species, which contribute to the ongoing cell death (Durukan and Tatlisumak, 2007). Organotypic hippocampal slice cultures are a valuable alternative to *in vivo* models to investigate the toxic effects of excessive Glu levels in the brain (Ring *et al*, 2010). One way to evaluate the outcome of neurotoxicity is to expose slice cultures to excitotoxins such as NMDA. The fluorescent dye PI can only enter damaged or dead cells due to their comprised membrane integrity and is therefore a frequently used marker of cell injury. Various protocols to assess PI uptake have been reported in the literature (Butler *et al*, 2013; Katayama *et al*, 2012; Wise-Faberowski *et al*, 2009b), but there is a substantial inconsistency in the methods used.

Therefore, the aim of this study was to develop a method to objectively quantify PI uptake in OHSCs that is simple, reproducible, and provides a standardized means of measuring cell death in hippocampal subfields. Slice cultures were exposed to varying concentrations of NMDA to illustrate the value of the devised method.

The principal findings of this study were two-fold. First, exposure to increasing concentrations of NMDA produced a dose-dependent increase in PI fluorescence intensity and therefore cell death in OHSCs. This effect was found in all hippocampal subfields. Second, comparison of PI uptake in the three subfields CA1, CA3, and DG showed a region-specific vulnerability of the hippocampus to NMDA-mediated cell death, with the CA1 area being the most sensitive. Both of these findings are consistent with previously published results (Ikegaya and Matsuki, 2002; Kristensen *et al*, 2001).

The hippocampus is one of the regions in the brain most vulnerable to ischemia, and the selective susceptibility of the hippocampal subfields to certain insults is a common theme in the literature. First described in histological studies of epileptic brains by Sommer (1880), the characteristic vulnerability of certain areas of the hippocampus to injury has since been observed clinically (Bartsch *et al*, 2015; Hatanpaa *et al*, 2014) and has also been replicated in experimental animal models, including gerbils (Bonnekoh *et al*, 1990), rats (Jarrard and Meldrum, 1993), cats (Schmidt-Kastner *et al*, 1990), and monkeys (Lavenex *et al*, 2011), *in vivo* and *in vitro* (Kosuge *et al*, 2008; Stanika *et al*, 2010). Together, all these studies have shown that the CA1 subfield of the hippocampus seems to be the most susceptible region to ischemic insults, whereas the DG and CA3 area appear to be more resistant. However, there may be differences in the distinct pattern of vulnerability depending on the neurotoxin used, as Ikegaya and Matsuki (2002) showed the selective vulnerability of CA1 neurons to NMDA, CA3 neurons to kainic acid, and DG region to colchicine.

Although the ischemic cascade causing neuronal cell death has been delineated, the mechanisms underlying this distinctive pattern of susceptibility to injury are not well

understood. The two main hypotheses trying to explain regional differences in vulnerability, originally developed by Spielmeyer (1927) and Vogt and Vogt (1937), propose either variations in hippocampal vasculature or intrinsic differences in physiological and biochemical properties of neurons respectively as primary causes. Because experiments performed in hippocampal slice cultures, which are separated from blood supply, still showed patterns of selective vulnerability, the concept of intrinsic differences prevails (Bernaudin *et al*, 1998; Newell *et al*, 1990).

Glu-mediated excitotoxicity is an important part of the ischemic cascade, and therefore the specific expression pattern of Glu type receptors has been of immense interest. Coultrap *et al* (2005) showed that expression of the NMDA receptor subunits NR1 and NR2B differs among the hippocampal regions. For example, there is a greater expression of NR2B in the CA1 versus the CA3 or DG. This may have important functional implications, as various NMDAR characteristics such as channel opening, Ca^{2+} entry and agonist affinities are dependent on the subunit composition (Burnashev *et al*, 1995; Chen *et al*, 1999; Laube *et al*, 1997) (see Section 1.4). Experiments conducted by Butler *et al* (2010) confirmed the greater density of the NR1 and NR2B subunit in CA1 relative to DG and CA3. Using an *in vitro* oxygen-glucose deprivation model, this ischemic insult has been shown to modulate NMDA responses in CA1 and CA3 neurons via a tyrosine kinase phosphorylation, which may underlie the differential susceptibility of CA1 compared to CA3 (Gee *et al*, 2006).

Additional factors may be involved in the selective vulnerability of hippocampal neurons, including differences in endoplasmic reticulum stress-induced neurotoxicity (Kosuge *et al*, 2008), in neuronal NOS expression (Black *et al*, 1995) and calcium-

mediated mitochondrial dysfunction (Friberg *et al*, 1999; Stanika *et al*, 2010). Besides neuron-neuron interactions, connections between neurons and glia cells may also be implicated (Bernaudin *et al*, 1998). Due to their Glu reuptake mechanisms, astrocytes have the ability to regulate extracellular levels of Glu. Hence, the role of astrocytes with regards to the characteristic susceptibility of CA1 neurons has also been studied. After transient forebrain ischemia in rats, the loss of Glu uptake activity of astrocytes in the CA1 region, which is in part due to mitochondrial dysfunction and oxidative damage in CA1 astrocytes, can contribute to the selective vulnerability of CA1 neurons (Ouyang *et al*, 2007). Furthermore, astrocytes from adult monkey hippocampal tissue exhibit lower astrocytic coverage of excitatory synapses as well as lower expression level of genes linked to Glu uptake and metabolism or glycolysis in CA1 versus CA3, causing the CA1 region to be more vulnerable to ischemic insults (Lavenex *et al*, 2011).

Although densitometric analysis of PI fluorescence intensity is currently the most commonly used method to evaluate cell death in organotypic hippocampal slice cultures, various measures have been developed, including the enzymatic MTT assay (Wise-Faberowski *et al*, 2009b), or counterstaining methods to compute a ratio of the number of dead vs live cells. Radley *et al* (2012), for example, used Hoechst labeling, which stains cell nuclei, to acquire the total number of cells and then calculated the percentage of cell death as cells stained with PI divided by the total amount. Double-labeling with PI and fluorescein diacetate, as a measure of enzyme activity, is another commonly used counterstaining method (Sato and Matsuki, 2002). There has been an ongoing debate in the literature whether this approach gives a more accurate depiction of cell death – compared to only counting dead cells in the culture – as it may take differences in cell

density in OHSCs into account. However, measurement of cell death by PI uptake was shown to agree with manual cell counting of live vs dead cells (Newell *et al*, 1995). Additionally, the value of PI fluorescence intensity seems to correlate with other markers of neuronal loss, including LDH efflux, Nissl cell staining, and Fluoro-Jade staining (Noraberg *et al*, 1999). Furthermore, Abdel-Hamid and Tymianski (1997) showed that mean PI fluorescence intensity is linearly related to the number of pyknotic nuclei, a histological indicator for cell degeneration, in organotypic hippocampal slice cultures. PI uptake is therefore a viable measure of neurotoxicity in organotypic slice cultures (Cho *et al*, 2007; Noraberg *et al*, 1999).

PI fluorescence intensity is often reported as the percentage of maximum PI uptake or cell death in order to compare different treatment conditions to each other. Among other methods, a terminal image representing maximal PI uptake and thus maximum cell death can be acquired by exposure of the same slice culture to high concentrations of Glu or other excitotoxins such as NMDA (Kleczkowska *et al*, 2015; Noraberg *et al*, 1999), low temperature exposure for 24 hours (Abdel-Hamid and Tymianski, 1997; Allard *et al*, 2015), or exposure to Triton X-100 (Sato and Matsuki, 2002). This way, PI uptake in OHSCs after exposure to a specific treatment can be expressed as a relative percentage of the maximal possible fluorescence intensity. However, the induction of maximal cell death has the disadvantage that treated slice cultures cannot be used for subsequent procedures after the insult, such as protein isolation or immunohistochemical staining. The protocol defined in this chapter offers the advantage that mean maximal PI uptake can be determined using only a subset of the cultures. The percent maximal uptake for cultures in the varying treatment groups can then be calculated subsequently without the

induction of maximal cell death. This way PI uptake can still be assessed objectively on a continuous scale with minimal variability. Additionally, it allows for the possibility to use the same slice culture not only to assess the effects of a specific treatment on cell viability, but also on protein or gene expression using techniques such as protein isolation, western blotting, and immunohistochemical staining. Consequently, multiple data points can be generated from slice cultures derived from each individual animal, which can reduce the number of animals used to obtain comprehensive information.

A potential issue to note in this study is the entry mechanism of PI. As mentioned above, PI can enter cells that have a damaged or leaky cell membrane. Therefore, PI fluorescence has not only been correlated with other markers of neuronal cell loss, but it is also an indicator of membrane integrity. It is possible that some neurons have a damaged cell membrane and die later than 24 hours after the switch to fresh media, whereas other neurons may recover and survive after initial uptake of PI (Mayer *et al*, 2002). However, previous literature has shown that PI uptake correlates well with a variety of different markers of cell death in organotypic hippocampal slice cultures (Noraberg *et al*, 1999). Furthermore, a study by Sato and Matsuki (2002) demonstrated the selective vulnerability of the hippocampus even when cell density was accounted for by double labelling with PI and fluorescein diacetate (Sato and Matsuki, 2002). Studies by Tymianski *et al* (1993a, 1993b) also suggest that NMDA and other agonists of NMDA receptors cause rapidly occurring neuronal degeneration that can be complete within hours. Therefore it is likely that the results reflect actual cell death.

The method described in this thesis also offers the possibility to cater to differing dimensions of individual slices. Due to inherent differences in hippocampal form and

because organotypic hippocampal slice cultures are growing *in vitro* without any constraint from surrounding brain areas, the size and shape of the cultures varies even between replicates. Standardized landmarks facilitate the separation of the slice culture into the three hippocampal subfields, given that the arms of the DG are visible. Additionally, the location of regions of interest can be adjusted in order to accommodate different shapes of OHSCs. Owing to the fact that regional indicators are necessary, the use of this method is limited to the analysis of cell death in organotypic cultures and is not applicable to dissociated cell cultures.

Using this method, a dose-dependent increase in PI uptake was observed after exposure to increasing concentrations of NMDA. Interestingly, administration of doses as high as 1 mM NMDA did not exceed 50% and 60% of maximal PI uptake, when measured for the entire hippocampal slice culture and for the CA1 region, respectively. This is in contrast to other authors who report a PI uptake of 75-100% after exposure to similar or lower concentrations of NMDA (Kristensen *et al*, 2001; Ring *et al*, 2010; Sakaguchi *et al*, 1997). However, only about 30% cell death in CA1 after exposure to 1 mM NMDA was reported in a recent study by Kleczkowska *et al* (2015). The authors also claim that frequently used concentrations of NMDA (100 µM) did not induce damage in organotypic hippocampal slice cultures. This discrepancy in PI uptake following exposure to NMDA may be due to variations in experimental procedures, such as distinctions in culture medium, exposure timing, or conceivably the method of standardizing cell death. Kristensen *et al* (2001), for example, exposed OHSCs to 50 mM Glu to acquire maximal PI fluorescence intensity, whereas maximal PI uptake was assessed after 24 hour low-temperature exposure to 70% ethanol in this study or after

treatment with supramaximal concentrations of NMDA in the study conducted by Kleczkowska *et al* (2015). The potential reason for this is unclear, but a possible explanation for this discrepancy is the composition of OHSCs and a potential implication of glial cell death in the measurement of maximal PI uptake. Organotypic slice cultures are not only made up of neuronal cells, but also glial cells. In comparison to neurons, glial cells generally are more resistant to ischemic insults (Goldberg and Choi, 1993). However, they are susceptible to cell injury mediated by exposure to ethanol or extremely high doses of NMDA (Holownia *et al*, 1997). Hence, depending on the method to induce maximal cell death, the measure of maximal PI uptake is based on the death of neurons alone versus the death of neurons and glial cells combined. In the current study, about 50% PI uptake was measured after treatment with 1 mM NMDA. This value most likely indicates 100% neuronal damage, as exposure to this concentration of NMDA presumably does not affect or only minimally affects the population of glial cells (compare Appendix D). A similar conclusion was drawn by Abdel-Hamid and Tymianski (1997). In their experiments, 60 minutes of oxygen-glucose deprivation result in almost complete degeneration of neurons in OHSCs as confirmed by histology, which accounted for about 40% of maximal PI fluorescence achieved by exposure to NMDA and kainic acid followed by low-temperature exposure for 24 h.

To further explore the potential implication of glial cell death in the maximal PI uptake, double-label immunohistochemistry with the neuronal marker NeuN and glial fibrillary acidic protein (GFAP) was performed on untreated OHSCs fixed in formalin and stored in ethylene glycol at -20°C (see Appendix D). The results indicate that the ratio of neuronal to glial cells is about 50/50. This ratio, however, seems to vary between

hippocampal subfields. It is possible that the differences in glial cell numbers may contribute to regional differences, but further in-depth studies are needed to confirm this hypothesis.

CHAPTER 3:

EVALUATION OF INTERACTION OF NMDA RECEPTORS AND A7 NICOTINIC ACETYLCHOLINE RECEPTORS

SUMMARY

Physiological activation of ionotropic NMDA receptors by glutamate plays an important role during brain development and physiological functioning throughout life. However, excess levels of Glu can over-activate synaptic and extrasynaptic NMDA receptors leading to rapid neuronal cell death by a process called excitotoxicity. This pathological mechanism is largely responsible for cell death in many neuropathological diseases, including stroke. Many recent publications have indicated a possible interaction between NMDA receptors and nicotinergic signaling via alpha7 nicotinic acetylcholine receptors (α7 nAChRs). The potential role of nAChRs in mediating Glu toxicity, however, is somewhat controversial with reports of nAChRs being both neuroprotective and neurotoxic in certain systems. To investigate the possible interaction between NMDA receptors and α7 nAChRs *in vitro*, organotypic hippocampal slice cultures were prepared from 5-6 day old Sprague-Dawley rats and maintained for 13 days on semiporous membrane inserts at 37°C. The contribution of α7 nAChRs in NMDA-mediated excitotoxicity was characterized by administering NMDA in combination with the specific α7 nAChR agonist choline and the APL galantamine. The results obtained show that co-activation of α7 nAChRs does not significantly alter NMDA-induced excitotoxic cell damage in OHSCs. However, activation of α7 nicotinic receptors alone significantly increased cell death in some hippocampal regions as measured by PI uptake, suggesting a possible neurotoxic effect that would require further investigation.

3.1 INTRODUCTION

Stroke is one of the most frequent causes of death, disability, and economic expense worldwide. The majority of stroke cases are ischemic strokes, caused by the interruption of blood flow to the brain (Go *et al*, 2013). The only currently approved drug treatment for ischemic strokes is the use of thrombolytic drugs, such as tissue plasminogen activator (tPA). These drugs aim to dissolve the blood clot to remove the blockage and therefore restore cerebral blood flow. The time window for treatment with tPA is 4.5 h after the onset of stroke symptoms (del Zoppo *et al*, 2009). Due to its narrow therapeutic window and numerous contraindications, only about 5% of patients receive intravenous thrombolysis within the appropriate time window (Balami *et al*, 2013; Moretti *et al*, 2015; Pandya *et al*, 2011).

Many different approaches to find new treatment strategies for ischemic strokes have been made over the years, but they have been ultimately unsuccessful. For example, preclinical trials testing NMDA receptor antagonists, anti-inflammatory agents, and antioxidants were quite promising, but failed in clinical testing (O'Collins *et al*, 2006). A better understanding of excitotoxicity in ischemic stroke and the underlying pathological mechanisms as well as validation of novel potential neuroprotective agents in appropriate models are necessary to address the lack of effective treatments for ischemic stroke.

The loss of blood supply in the brain causes cell death by initiating the ischemic cascade. These pathophysiological events occur within minutes of the vascular occlusion. The order of these events is difficult to determine, as many events demonstrate overlapping features. Although the initial insult can lead to brain damage very rapidly, ischemic brain injury may last hours or even days (Durukan and Tatlisumak, 2007).

Diminished blood flow leads to the depletion of oxygen and glucose in ischemic brain tissue. Energy failure causes dysfunction of ATP-dependent ion pumps and subsequent ionic imbalance in the ischemic brain tissue, including elevation of intracellular sodium, calcium, and chloride as well as elevated levels of extracellular potassium (Durukan and Tatlisumak, 2007). Consequently, the neuronal membrane potential is lost resulting in the depolarization of neuronal and glial cells, resulting in the release of large amounts of Glu into the extracellular space. These excess levels over-activate GluRs, particularly NMDA receptors, leading to further increases of intracellular concentrations of Ca^{2+}, Na^{+}, and Cl^{-} (Durukan and Tatlisumak, 2007).

High intracellular Ca^{2+} levels are not only due to influx from extracellular sources, but calcium can also be released from intracellular storage, including endoplasmic reticulum (Pisani *et al*, 2000) or mitochondria (Webster, 2012). Calcium can trigger pathophysiological events by activating various Ca^{2+}-dependent enzymes, such as protein kinase C, phospholipases, calpains and other proteases, cyclooxygenase, NOS, and endonucleases (Szydlowska and Tymianski, 2010; Xing *et al*, 2012). Furthermore, Ca^{2+}-mediated mitochondrial damage may trigger release of apoptotic and inflammatory mediators as well as free radical production (Turner *et al*, 2013).

Several studies have demonstrated the importance of calcium in mediating the toxic effects of brain ischemia. Although the exact mechanisms remain controversial, it is commonly accepted that calcium overload through distinct entry routes can trigger specific second messenger pathways that initiate cell death mechanisms. More specifically, calcium entry via voltage-gated Ca^{2+} channels is not associated with

ischemic damage, whereas nearly all members of the GluR family have been implicated in excitotoxicity (Szydlowska and Tymianski, 2010).

The ionotropic NMDAR is of particular interest with regards to calcium toxicity and brain ischemia, as these receptors are highly permeable to Ca^{2+}. NMDA receptors are voltage-dependent ion channels comprised of four subunits, which are a combination of NR1, NR2, and NR3 subunits. Most NMDA receptors in the mammalian CNS are assembled from two NR1 and two NR2 subunits (Traynelis *et al*, 2010). A unique characteristic of these classical NMDARs is the requirement for simultaneous binding of Glu and glycine to open the channel. Additionally, the channel pore is blocked by Mg^{2+} at resting potential. Upon depolarization of the membrane, the Mg^{2+} block is removed and monovalent cations as well as divalent cations, especially Ca^{2+}, can enter the cell (Kalia *et al*, 2008).

NMDARs are widely distributed in the brain and are typically localized at postsynaptic sites. Because of the important role of NMDARs in synaptic transmission, neuronal maturation, and synaptic plasticity, the dysfunction of NMDAR-mediated signaling is thought to contribute to the pathophysiology of various neurological conditions, including stroke (Margaill *et al*, 1996) and AD (Danysz and Parsons, 2012). Distinct intracellular signaling mechanisms have been linked to both NMDAR-dependent neuronal survival and neuronal death. For example, NMDARs can promote neuronal survival by induction of pro-survival genes, such as BDNF (Soriano *et al*, 2006), or enhancing protection against oxidative stress (Papadia *et al*, 2008). In contrast, neuronal death can be induced by NMDAR-mediated inactivation of CREB, an important part of the pro-survival pathway, and activation of NOS (Hardingham *et al*, 2002). Receptor

location and subunit composition, as well as excessive NMDAR-dependent intracellular calcium levels, are implicated in regulating this dual mode of NMDA receptors (Hardingham *et al*, 2002; Liu *et al*, 2007; Stanika *et al*, 2010).

Receptor function and activity of ligand-gated ion channels including the NMDAR is regulated by receptor phosphorylation (Smart, 1997) as well as by intracellular proteins and cell surface receptors like GPCRs through direct protein-protein coupling (Kim and Sheng, 2004; Lee *et al*, 2002). While functional dimerization has generally been established between GPCRs as well as between GPCRs and ligand-gated ion channels (Bulenger *et al*, 2005; Lee *et al*, 2002), Li *et al* (2012) recently reported the formation of a protein complex between two ligand-gated ion channels – the NMDA receptor and the α7 nicotinic acetylcholine receptor – through direct protein-protein interaction. A specifically developed interfering peptide was shown to be able to disrupt the formation of this complex, which resulted in changes in intracellular signaling pathways and rat behavior.

Neuronal nicotinic acetylcholine receptors are pentameric ligand-gated ion channels made up of combinations of α and β subunits. In the mammalian brain, the majority of nicotinic receptors are assembled in either α4β2 or α7 configurations (Pohanka, 2012). Nicotinic receptors can present as homopentameric receptors, formed by five identical subunits. The α7 subunit, for example, is thought to be predominantly expressed as a homopentamer in the CNS, although co-assembly with other subunits is possible (Couturier *et al*, 1990; Murray *et al*, 2012).

Particularly high levels of the α7 nAChR can be found in the hippocampus, where functional α7 nAChRs are expressed throughout all hippocampal subregions. On a subcellular level, the majority of α7 nicotinic receptors are localized on the presynapse, but some α7 nAChRs can also be expressed at somatic, perisynaptic, or postsynaptic sites. Pharmacologically, α7 nAChR channels are unique in that they demonstrate a high permeability to Ca^{2+} - similar to NMDA receptors. Additionally, α7 nAChRs exhibit a rather low affinity for ACh, but can be activated with full efficacy by choline (Albuquerque *et al*, 2009). The endogenous choline concentration in the extracellular space is thought to be around 4 to 6 μM (Mike *et al*, 2000), while the intracellular concentrations as well as the amount of bound choline is much higher (Klein *et al*, 1998).

Activity of α7 nAChRs can also be enhanced by application of APLs such as galantamine. Although galantamine also acts as an inhibitor of AChE, it has been shown to enhance the channel opening probability of nAChRs induced by relatively low concentrations of nicotinic agonists (Samochocki *et al*, 2000; Schrattenholz *et al*, 1996). However, galantamine lacks selectivity as it displays APL action on various neuronal nAChR subtypes, including α7, α4β2, and α3β4 (Samochocki *et al*, 2003).

With regards to physiological function, α7 nAChRs have been implicated in the regulation of the release of neurotransmitters from presynaptic terminals, including GABA and Glu, in the hippocampus and in other areas of the brain (Alkondon *et al*, 1997a; Gray *et al*, 1996; Guo *et al*, 1998). Evidence further suggests the ability to modify glutamatergic transmission at postsynaptic locations (Biton *et al*, 2007; Cheng and Yakel, 2014). While calcium signaling mediated by presynaptic α7 nAChR can enhance Glu release, α7 nicotinic receptors located at the postsynapse have been suggested to initiate a

Ca^{2+} signal that can act via calmodulin to reduce the responsiveness of NMDA receptors (Fisher and Dani, 2000).

Furthermore, the direct interaction between α7 nAChR and NMDAR has recently been reported, as mentioned above (Li *et al*, 2012). Follow-up work by the same group has further supported the functional importance of α7 nAChR-NMDAR coupling. Disruption of this α7 nAChR-NMDAR interaction by a specific interfering peptide caused impairments in novel object recognition in mice, suggesting that the complex affects NMDA-mediated function and some aspects of learning and memory (Li *et al*, 2013).

Although α7 nAChRs are implicated in Glu- and NMDAR-mediated signaling, the potential role of α7 nAChRs in excitotoxic mechanisms remains controversial as there are reports supporting both a neuroprotective and a neurotoxic role of α7 nAChRs in certain systems. For example, activation of α7 nicotinic receptors has been shown to promote neuroprotection against β-amyloid cytotoxicity (Kihara *et al*, 1997), oxidative stress (Cormier *et al*, 2003), and excitotoxicity (Shimohama *et al*, 1998). In contrast, α7 nAChRs may also be involved in neurotoxicity such that over-activation of α7 nAChRs may cause toxic intracellular calcium concentrations triggering apoptotic signaling. For example, over-activation of α7 receptors has been shown to trigger cell death following application of high concentrations of a specific agonist in PC12 cells (Li *et al*, 1999). Furthermore, α7 nAChR-mediated neurotoxic effects have also been demonstrated in a murine model of glutamatergic injury (Laudenbach *et al*, 2002), and in a human neuroblastoma cell line (Guerra-Álvarez *et al*, 2015).

Given the primary role of NMDA receptor-mediated excitotoxicity in the ischemic injury process and the potential of α7 nAChRs to modulate NMDAR activity and function, it was of interest to determine whether co-activation of α7 nAChRs changes NMDA-induced neurotoxicity and could therefore be an achievable therapeutic approach for reducing brain damage following excitotoxic insults.

Organotypic hippocampal slice cultures present an attractive *in vitro* model to investigate receptor function as they not only preserve many features of *in vivo* cells, but also allow precise control of the extracellular environment as well as ease of experimental access (Humpel, 2015b). Drugs can easily be applied to mimic the excitotoxic insult and to stimulate α7 nAChRs without the pharmacokinetic restrictions of *in vivo* models. Both NMDA receptors and α7 nAChRs are expressed in organotypic hippocampal slice cultures (Ahlgren *et al*, 2011; Mielke and Mealing, 2009). Previous literature has shown that OHSCs are an appropriate model to study excitotoxicity induced by GluRs. The method of measuring PI uptake as described in Chapter 2 allows for an objective and quantitative analysis of cell death to compare the effects of drug administration on cell viability *in vitro* (Noraberg *et al*, 1999; Zimmer *et al*, 2000).

3.2 METHODS

3.2.1 Experimental animals

Offspring born in-house from untimed pregnant Sprague-Dawley rats (Charles River, Quebec, Canada) were used to prepare the organotypic hippocampal slice cultures. After arrival at the facility, dams were housed individually with *ad libitum* access to water and

Purina Rodent Chow. The housing facility was maintained at approximately 22°C under a 12 h light-dark cycle (lights on at 06:00, off at 18:00). The day of parturition was designated as PND0. Animals were left undisturbed until the day of culturing on PND5/6. Studies were carried out under approval from the University of Prince Edward Island Animal Care Committee, and were in accordance with the Canadian Council on Animal Care guidelines.

3.2.2 Preparation and maintenance of organotypic hippocampal slice cultures

Organotypic hippocampal slice cultures were prepared as described in Chapter 2 (see Section 2.2.2). Briefly, 5-6 day old rat pups were quickly decapitated. The two hippocampi were dissected under aseptic conditions and transversely sliced into 400 µm sections using a tissue chopper (Stoelting, IL, USA). Under a light microscope, slices with intact hippocampal morphology were placed onto 0.4 µm porous membrane inserts (Millipore, MA, USA). Membrane inserts with three slices each were transferred to individual 35 mm cell culture dishes (Fisher Scientific, NJ, USA) filled with 1 ml of serum-based medium containing 50% MEM (Gibco, NY, USA), 25% Hank's balanced salt solution, 25% heat-inactivated horse serum, 1% penicillin-streptomycin solution (Gibco, USA) and 12 mM HEPES (Fisher Scientific, USA). Slice cultures were incubated at 37°C in 5% CO_2 until day 13 *in vitro*.

3.2.3 Assessing viability in organotypic slice cultures

Viability of slice cultures was assessed at DIV13 using PI (Sigma-Aldrich, MO, USA) and before any experiments to ensure only live and healthy OHSCs were used. OHSCs were exposed to PI (5 µg/ml) for 30 minutes. Using a Zeiss Axioplan2

microscope, cultures were examined and OHSCs with distinct PI uptake were excluded from further experiments.

3.2.4 Drug application

Based on the results of the dose-response curve constructed from experiments in Chapter 2 (see Section 2.3), concentrations of 10 µM and 50 µM of NMDA were chosen to investigate the interaction between α7 nAChRs and NMDA receptors. Cultures were exposed to a combination of NMDA with either different concentrations of choline alone (Sigma) (10 mM and 50 mM) or together with 10 µM galantamine (Sigma), with saline used as a negative control, to compare the effect of α7 nAChR co-activation to stimulation of NMDA receptors alone. Table 3-1 summarizes all treatment conditions. Data for the exposure conditions of saline, 10 µM NMDA, and 50 µM NMDA were used from Chapter 2. As described in Chapter 2 (see Section 2.2.4), OHSCs were exposed to drugs for 4 hours and were then transferred to fresh culture medium for 24 hours. After this 24 hour period, PI uptake was measured again to determine the effects of drug exposure on cell viability. Additionally, light microscope pictures of each slice were taken to facilitate identification of hippocampal structures.

The maximum achievable PI uptake was acquired from cultures exposed to ice cold 70% ethanol for 24 hours at -20°C, which represents maximal cell death. With this method, the PI uptake induced by drug treatment could be expressed as the ratio of the maximal PI uptake. A minimum of 6 slices were analysed and averaged per treatment condition with rat pup as the unit of variance.

Table 3-1: Summary of drug treatments

Saline control groups	Lower dose NMDA	Higher dose NMDA
Saline	10 µM NMDA	50 µM NMDA
	10 µM NMDA + saline	50 µM NMDA + saline
Saline + 10 mM choline	10 µM NMDA + 10 mM choline	50 µM NMDA + 10 mM choline
Saline + saline + 10 µM galantamine	10 µM NMDA + 10 mM choline + 10 µM galantamine	50 µM NMDA + 10 mM choline + 10 µM galantamine
Saline + 50 mM choline	10 µM NMDA + 50 mM choline	50 µM NMDA +50 mM choline
	10 µM NMDA + 50 mM choline + 10 µM galantamine	50 µM NMDA + 10 mM choline + 10 µM galantamine

3.2.5 Image analysis and quantification of PI fluorescence

Images taken after a 4 hour long drug treatment and 24 hours in fresh media were analyzed by densitometry with the imaging software ImageJ® (National Institute of Health, USA). The standard template of 9 circular regions of interest as described in Section 2.2.5 of Chapter 2 was applied to the images, and PI fluorescence intensity was measured in the three hippocampal subfields, namely DG, CA1 and CA3. A tenth circle placed adjacent to the slice culture allowed for background subtraction. The raw integrated density of each slice was calculated. PI uptake induced by drug treatment was expressed as percentage of the maximal PI uptake, determined by low temperature exposure to 70% ethanol.

3.2.6 Data analysis

All densitometric data were expressed as mean ± SEM. As results of the dose-response curve revealed differences in PI uptake between cultures exposed to saline, 10 µM and 50 µM NMDA, the treatment conditions in this chapter were divided into three main groups (see Table 3-1: Summary of drug treatments) and cross comparisons between these groups were not of interest for this research. Therefore, data of these three groups were analyzed separately using a one-way ANOVA with Welch's F-value. If differences were detected, the Games-Howell post-hoc multiple comparison test was applied. The high dose NMDA group in region CA1 was analyzed using a normal one-way ANOVA, as Levene's test of homogeneity of variance for this group was not significant ($F_{5,29}$=1.273, p=0.302), followed by Tukey's post-hoc test. Statistical analyses were performed using SPSS Statistics Version 23 (IBM Corporation, NY, USA) at a level of significance of 0.05.

3.3 RESULTS

Initial experiments were performed to assess the regional and dose-dependent effects of NMDA exposure on cell damage in DIV13 cultures (see Chapter 2, Section 2.3). A significant main effect of the dose of NMDA was found as increasing concentrations of NMDA induced significant increases in PI uptake. Furthermore, a significant interaction between hippocampal region and NMDA concentration was detected, with the CA1 region being most sensitive to NMDA-induced injury. Due to this significant interaction, hippocampal subfields were subsequently analyzed separately.

Normality of the data was confirmed using the Kolmogorov-Smirnov test ($p>0.05$). In all regions, comparison of the different treatment groups (saline, lower dose NMDA and higher dose of NMDA) revealed that Levene's test of homogeneity of variances was significant ($p<0.05$). Thus, Welch's ANOVA was used to assess significance between groups (Tomarken and Serlin, 1986) followed by the Games-Howell post-hoc test. The only exception is the higher dose NMDA group in the CA1 region, where the Levene's test was not significant ($p=0.302$). For this group, differences were assessed using one-way ANOVA followed by Tukey's post-hoc test.

3.3.1 Saline control groups

Comparisons of mean percent PI uptake in OHSCs exposed to saline alone or in combination with α7 nAChR agonists revealed a number of treatment effects (see Figure 3-1 and Table 3-2).

In the DG, a significant between groups effect was found using Welch's ANOVA ($F_{3,7.98}=8.631$, $p=0.007$). OHSCs exposed to saline alone exhibited PI uptake of 4.62% ± 0.38 (n=5). Addition of saline and 10 µM galantamine to potentiate endogenously present choline resulted in a faint PI uptake as seen through the microscope, but this group was not significantly different from saline treated slice cultures (10.14% ± 2.16, $n=6$, $p=0.165$). Upon activation of α7 nicotinic receptors with choline, PI uptake and thus cell death seemed to increase. In cultures exposed to saline and low dose of choline, PI uptake was 15.03% ± 3.04 ($n=5$, $p=0.084$). Addition of 50 mM choline resulted in a significant increase compared to saline alone (16.48% ± 3.21, $n=6$, $p=0.049$). No significant differences between any other groups were found.

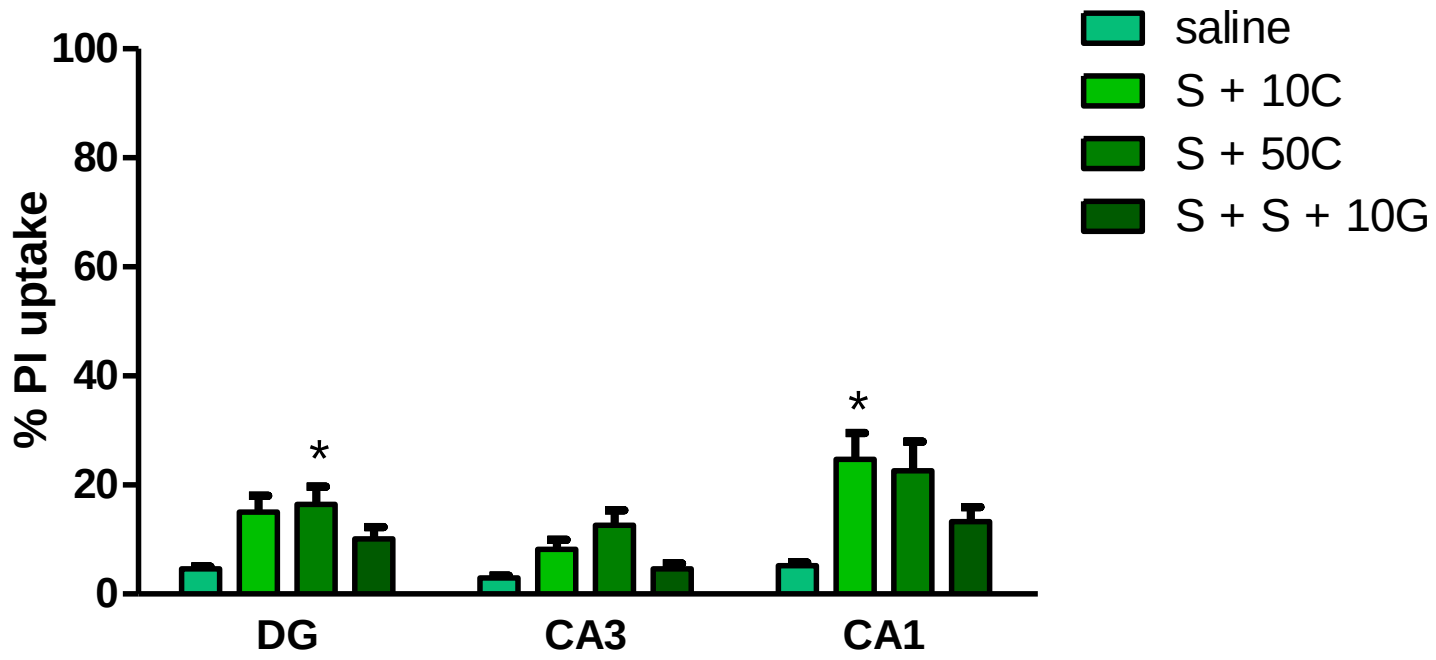

Figure 3-1: Cellular propidium iodide (PI) uptake measured in the three hippocampal regions (dentate gyrus [DG], CA1 and CA3) of organotypic hippocampal cultures after exposure to saline, saline (S) in combination with either 10 mM choline (10C) or 50 mM choline (50C) or saline, saline and 10 µM galantamine (10G). The maximal PI uptake after 24 h low-temperature exposure to 70% ethanol was set to 100%. Data are shown as means ± SEM, with n = 5–6. One way ANOVA using Welch's correction followed by Games-Howell post-hoc test revealed significant differences between the four saline control groups in all three hippocampal regions, *p<0.05 from saline.

Table 3-2: Comparison of PI uptake after exposure to saline in combination with α7 nicotinic receptor agonists in the dentate gyrus (DG), CA1 and CA3. Data are given as mean ± SEM.

	DG	CA1	CA3
saline (S)	4.62% ± 0.38	5.21% ± 0.58	2.98% ± 0.36
S + 10 mM choline (10 C)	15.03% ± 3.04	24.73% ± 4.81	8.23% ± 1.76
S + 50 mM choline (50 C)	16.48% ± 3.21	22.64% ± 5.33	12.62% ± 2.71
S + S + 10 µM galantamine (10 G)	10.14% ± 2.16	13.25% ± 2.71	4.49% ± 0.99

A similar trend was seen in the CA3 hippocampal region (compare Figure 3-1). Welch's ANOVA revealed significant differences between groups ($F_{3,8.02}$=6.233, p=0.016). No differences in PI uptake were found between cultures exposed to saline (2.98% ± 0.36, n=5), saline and galantamine (4.49% ± 0.99, n=6, p=0.519) and saline in combination with 10 mM choline (8.23% ± 1.76, n=5, p=0.124). Addition of the higher concentration of choline appeared to induce an increased PI uptake, as values of 12.62% ± 2.71 were measured approaching significance (n=6, p=0.056). The remaining comparisons revealed no significant differences.

Analysis of PI uptake in the CA1 region also showed a significant effect of treatment condition using Welch's ANOVA ($F_{3,8.02}$=9.696, p=0.005). Similarly to the DG and CA3 region, a low basal PI incorporation was detected after saline treatment (5.21% ± 0.58, n=5). Further addition of saline and 10 µM galantamine resulted in an apparent increase of PI uptake (Figure 3-1), but did not significantly differ from saline exposure alone (13.25% ± 2.71, n=6, p=0.105). A significant increase in PI uptake was measured in cultures in which α7 nicotinic receptors were stimulated with 10 mM choline (24.73% ± 4.81, n=5, p=0.049). When the choline concentration was increased to 50 mM, cell death

of 22.64% ± 5.33 was measured, which was not significantly different from cultures exposed to saline alone or cultures exposed to the lower concentration of choline (*n*=6, *p*=0.076 and *p*=0.991, respectively). No significant differences between any other groups were found.

3.3.2 Low dose of NMDA (10 µM) in combination with α7 nicotinic receptor agonist

Figure 3-2 shows the effect of stimulation of α7 nAChRs in combination with 10 µM NMDA on cell death, using PI uptake as a marker, in the three hippocampal regions DG, CA1 and CA3 of DIV13 organotypic hippocampal slice cultures. The data are summarized in Table 3-3: Comparison of PI uptake after exposure to a low dose of NMDA in combination with α7 nicotinic receptor agonists in the dentate gyrus (DG), CA1 and CA3. Data are given as mean ± SEM.

No significant effect of treatment conditions was found in the DG using Welch's ANOVA ($F_{5,13.718}$=0.707, *p*=0.628). OHSCs exposed to 10 µM NMDA showed a PI uptake of 13.98% ± 1.93 (n=7). As shown in the control groups, saline by itself did not induce PI uptake. Thus, addition of saline to NMDA did not affect the cell damage in slice cultures (15.47% ± 1.19, *n*=6). Co-activation of α7 nicotinic receptors was achieved using the specific agonist choline. Exposure of OHSCs to low dose (10 mM) of choline in combination with 10 µM NMDA resulted in PI incorporation of 21.26% ± 5.78 (*n*=6). Further potentiation of α7 nicotinic receptors using 10 µM galantamine did not change

the level of PI uptake (18.14% ± 2.48, *n*=6). A similar amount of cell death in slice cultures was measured after treatment with 10 µM NMDA in combination with a high

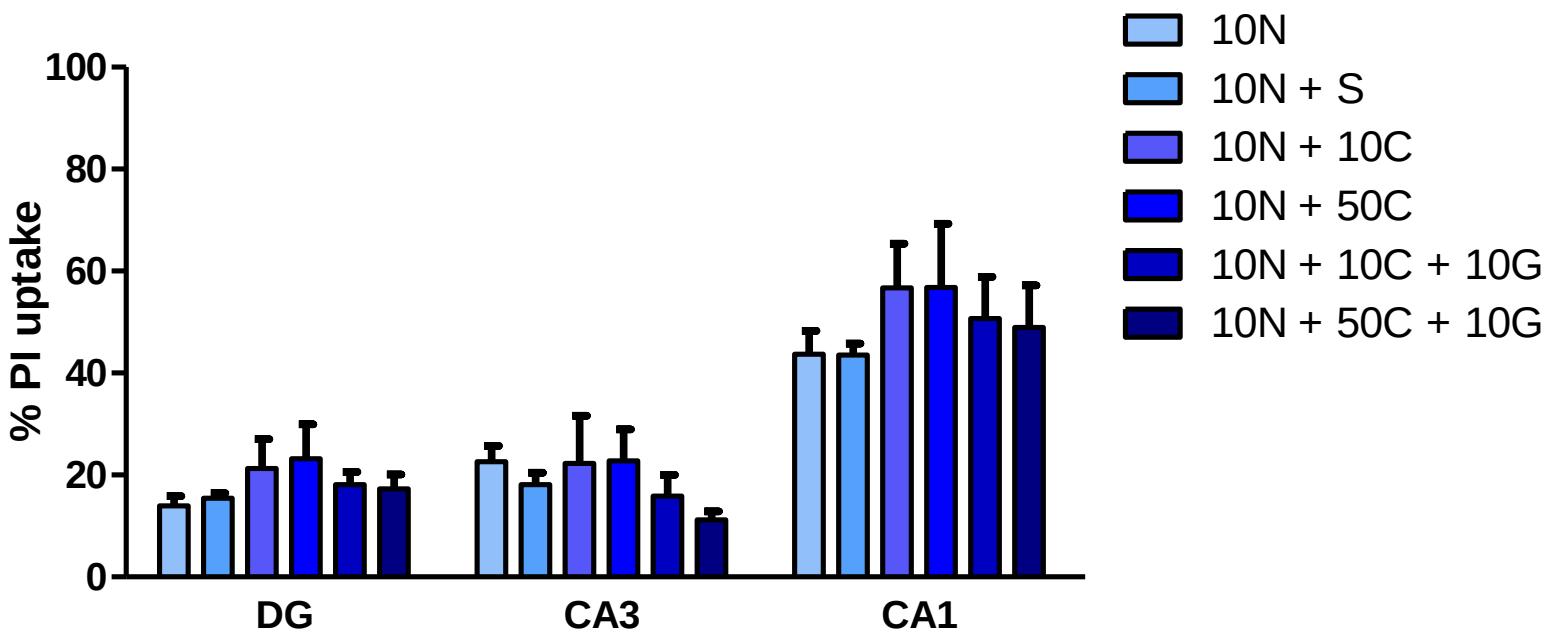

Figure 3-2: Effects of co-activation of α7 nicotinic acetylcholine receptors and NMDA receptors in organotypic hippocampal slice cultures. Histograms show quantification of cell damage using propidium iodide (PI) in the three hippocampal regions dentate gyrus (DG), CA3 and CA1 after application of 10 µM NMDA (10N) either alone or in combination with saline (S), 10 mM choline (10C), 50 mM choline (50C), 10 mM choline plus 10 µM galantamine (10G) and 50 mM choline plus 10 µM galantamine. Data are shown as means ± SEM, with n = 6–7. One way ANOVA using Welch's correction revealed no significant differences in any of the three hippocampal regions.

Table 3-3: Comparison of PI uptake after exposure to a low dose of NMDA in combination with α7 nicotinic receptor agonists in the dentate gyrus (DG), CA1 and CA3. Data are given as mean ± SEM.

	DG	CA1	CA3
10 µM NMDA (10 N)	13.96% ± 1.93	43.70% ± 4.6	22.61% ± 3.08
10 N + saline	15.47% ± 1.19	43.51% ± 2.73	18.11% ± 2.78
10 N + 10 mM choline (10 C)	21.26% ± 5.78	56.71% ± 8.66	22.32% ± 9.34
10 N + 50 mM choline (50 C)	23.22% ± 6.72	56.76% ± 12.57	22.79% ± 6.13
10 N + 10 C + 10 µM galantamine (10 G)	18.15% ± 2.48	50.67% ± 8.23	15.91% ± 4.09
10 N + 50 C + 10 G	17.26% ± 2.86	48.99% ± 8.24	11.23% ± 1.60

dose (50 mM) choline with or without 10 µM galantamine (23.22% ± 6.72 and 17.26% ± 2.86, respectively, with n=6 in both groups). Similar results were seen in the other two hippocampal regions CA1 and CA3. As in the DG, there was no main effect of treatment on cell death as measured by PI uptake using Welch's ANOVA ($F_{5,13.606}$=0.624, p=0.685 for CA1 and $F_{5,13.787}$=2.537, p=0.079 for CA3). As the CA1 has been shown to be the region most sensitive to NMDA -induced cell damage, the PI uptake was higher in this area compared to the DG and CA3. Mean PI uptake in DG, CA1 and CA3 are presented in Table 3-3 as well as in Figure 3-2 for each of the treatment groups.

3.3.3 High dose of NMDA (50 µM) in combination with α7 nicotinic receptor agonist

The effects of co-activation of α7 nAChRs on 50 µM NMDA-induced cell damage in the three hippocampal regions DG, CA1, and CA3 of DIV13 organotypic slice cultures are summarized in Figure 3-3. Similar to the results of the low dose NMDA group, analysis

with one way ANOVA using Welch's correction revealed no significant effect of treatment in the DG ($F_{5,11.734}$=2.479, p=0.093). Exposure of slice cultures to 50 µM NMDA resulted in PI uptake of 30.68% ± 5.87 (n=6). As shown in Figure 3-3, addition of saline to high dose NMDA did not affect the PI uptake in OHSCs (38.99% ± 1.17, n=6). Co-activation of α7 nicotinic receptors using low dose (10 mM) of choline in combination with 50 µM NMDA resulted in greater mean values for PI uptake compared to 50 µM NMDA and saline (55.40% ± 9.30, n=5 vs 38.99% ± 1.17, n=6). Further potentiation of α7 nicotinic receptors using 10 µM galantamine did not alter the amount of cell death (52.83% ± 6.46, n=6). Similar levels of PI uptake in OHSCs were measured after treatment with 50 µM NMDA in combination with 50 mM choline alone (56.39% ± 7.47, n=6) or with 10 µM galantamine (43.16% ± 4.69, n=6).

Comparably, no significant effect of treatment was found in the CA1 ($F_{5,29}$=1.028, p=0.420) or CA3 region ($F_{5,13.158}$=2.422, p=0.092). Again, the highest levels of PI uptake were measured in the CA1 region, providing further evidence of this region's susceptibility to NMDA-mediated excitotoxicity. Table 3-4 summarizes the mean PI uptake in DG, CA1, and CA3 for each of the treatment groups, as illustrated by Figure 3-3.

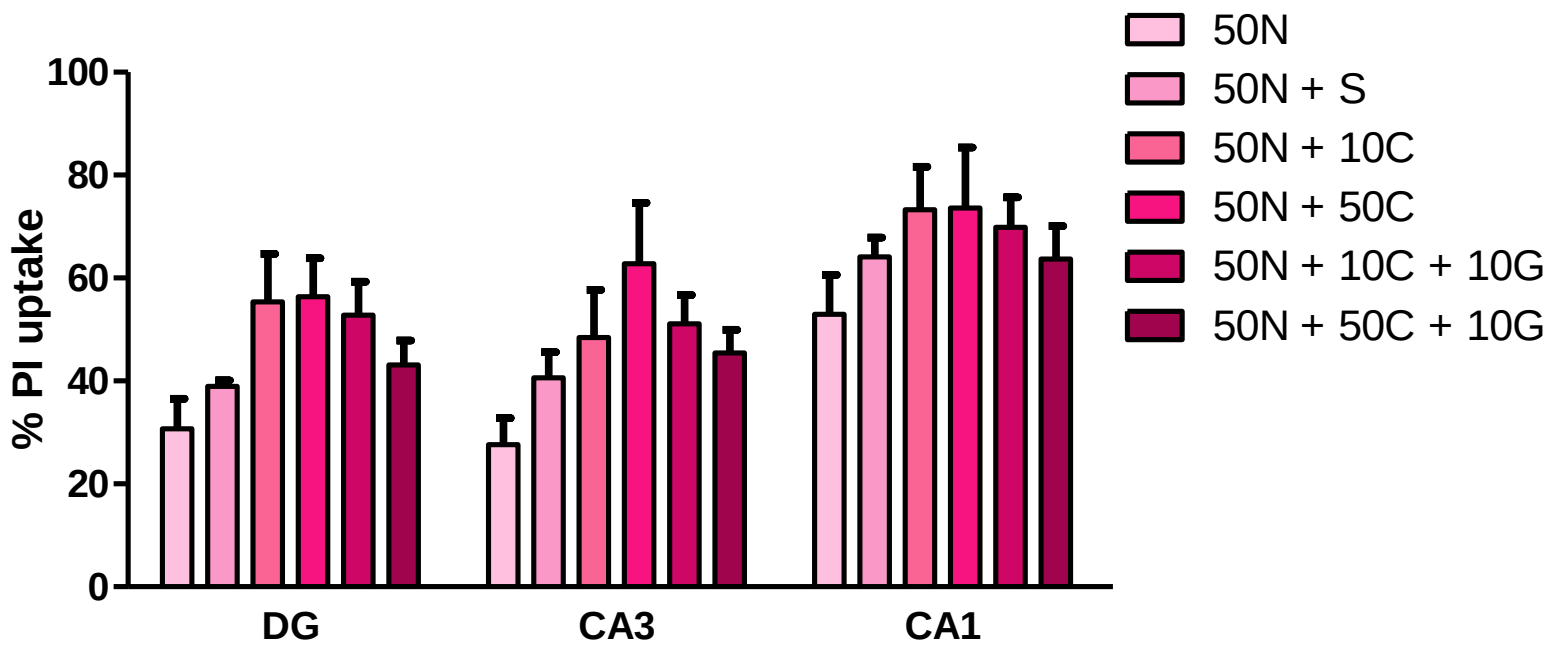

Figure 3-3: Effects of co-activation of α7 nicotinic acetylcholine receptors and NMDA receptors in organotypic hippocampal slice cultures. Histograms show quantification of cell damage using propidium iodide (PI) in the three hippocampal regions dentate gyrus (DG), CA3 and CA1 after application of 50 µM NMDA (50N) either alone or in combination with saline (S), 10 mM choline (10C), 50 mM choline (50C), 10 mM choline and 10 µM galantamine (10G) and 50 mM choline and 10 µM galantamine. Data are shown as means ± SEM, with n = 5-6. One way ANOVA using Welch's correction revealed no significant differences in any of the three hippocampal regions.

Table 3-4: Comparison of PI uptake after exposure to a high dose of NMDA in combination with α7 nicotinic receptor agonists in the dentate gyrus (DG), CA1 and CA3. Data are given as mean ± SEM.

	DG	CA1	CA3
50 µM NMDA (50 N)	30.69% ± 5.87	52.99% ± 7.66	27.60% ± 5.20
50 N + saline	38.99% ± 1.17	64.10% ± 3.76	40.59% ± 5.07
50 N + 10 mM choline (10 C)	55.40% ± 9.30	73.29% ± 8.37	49.70% ± 9.78
50 N + 50 mM choline (50 C)	56.39% ± 7.47	73.62% ± 11.77	62.81% ± 11.85
50 N + 10 C + 10 µM galantamine (10 G)	52.83% ± 6.46	69.88% ± 5.86	51.10% ± 5.65
50 N + 50 C + 10 G	43.16% ± 4.69	66.06% ± 3.15	45.45% ± 4.53

3.4 DISCUSSION

This study was designed to investigate the effects of co-activation of α7 nicotinic acetylcholine receptors on NMDA-mediated cell damage in organotypic hippocampal slice cultures. Both receptor types have been shown to be expressed in OHSCs (Bahr *et al*, 1995; Mielke and Mealing, 2009; Prendergast *et al*, 2001b). Treatment with the specific α7 nAChR agonist choline alone or in combination with galantamine, an APL of the α7 nicotinic receptor, was employed at the same time as the excitotoxic insult with NMDA to investigate this experimental aim. Using PI as a marker of cell viability, it was of interest to determine if stimulation of α7 nAChRs alters NMDA-induced neurotoxicity.

The results obtained show that administration of choline alone or in combination with the APL galantamine does not significantly change the level of NMDA-induced PI uptake. However, it is also clear that co-activation of α7 nicotinic receptors did not have a

neuroprotective effect. Rather, there seems to be a trend towards increased PI uptake and thus enhanced cell injury when α7 nAChRs and NMDARs are co-activated. Moreover, stimulation of α7 nAChRs alone, i.e. exposing OHSCs to choline in the absence of NMDA, significantly increased PI uptake in CA1 and DG as well as approached significance in CA3 when compared to saline-treated OHSCs. Exposure to galantamine alone appears to have no real effect on cell viability in OHSCs (Figure 3-1).

Although this thesis was based mainly on the interaction between NMDARs and α7 nAChRs, another role of the α7 nAChR in modulating the glutamatergic system could explain the observed results. As mentioned in section 1.5.2, the α7 nAChR can act both on presynaptic neurons and astrocytes to release Glu (Cheng and Yakel, 2014; Salamone *et al*, 2014). It is possible that this causes the increase in PI uptake seen in the saline control groups, where stimulation of α7 nAChRs with choline may induce the release of Glu resulting in activation of NMDA receptors and neurotoxicity. In OHSCs that were exposed to NMDA or DOM (see Appendix C), however, the α7 nAChR-mediated Glu release may be obscured, as this effect is small compared to the NMDA-mediated excitotoxicity. This hypothesis could be tested by administration of NMDA antagonists in the saline control groups to try and block the neurotoxic effect of choline.

To activate α7 nAChRs in this test setting, slice cultures were exposed to choline, which has been shown to be a full and selective agonist of α7-containing receptors (Alkondon *et al*, 1997b; Papke *et al*, 1996). Choline also has the ability to act as a partial agonist at α9, α4β4, α3β4 (Do *et al*, 1986; Mandelzys *et al*, 1995; Pereira *et al*, 2002; Verbitsky *et al*, 2000; Zwart and Vijverberg, 2000) and as a co-agonist with ACh at α4β2 nAChRs (Mulholland *et al*, 2004). However, Alkondon *et al* (1997a, 1997b, 1999) have

demonstrated that choline selectively activates α7 nAChRs in hippocampal neurons in either cultures or slices. Additionally, choline was administered in combination with galantamine, an APL of nicotinic receptors at low concentrations (Samochocki *et al*, 2000; Schrattenholz *et al*, 1996), to potentiate the activity of α7 nicotinic receptors in the presence of choline.

Nicotinic acetylcholine receptors, including α7 receptors, have been associated with signaling mechanisms mediating both neuroprotective and neurotoxic effects in various disease models and systems (Resende and Adhikari, 2009), although studies reporting neuroprotective actions prevail. For example, administration of nicotine can protect neurons against Aβ toxicity. This neuroprotective effect was blocked by the selective α7 nicotinic receptor antagonist α-bungarotoxin, implying an important role for α7 nAChRs in neuroprotection against Aβ cytotoxicity (Kihara *et al*, 1997). A study by Arias *et al* (2005) further confirms neuroprotective effects linked to α7 receptors afforded by nicotine as well as AChE inhibitors including galantamine. Stimulation of α7 nAChRs may also protect neurons in certain models under various other pathological conditions, including oxidative stress (Cormier *et al*, 2003), trophic factor-deprivation (Martin *et al*, 1994), and Glu-mediated excitotoxicity (Shimohama *et al*, 1998). Pre-treatment with dimethoxybenzylidene anabaseine, a α7 receptor agonist, proved to be neuroprotective against excitotoxicity in cultured neocortical neurons and against focal ischemic insults in rats. However, no neuroprotective effect was achieved when DMBX was administered concurrently with the insult (Shimohama *et al*, 1998). Similarly, preincubation with nicotine showed neuroprotective effects in acute hippocampal slices subjected to oxygen-

glucose deprivation, whereas neuroprotection did not occur in slices prepared from α7 nAChR knockout mice (Rosa *et al*, 2006).

Despite the amount of evidence suggesting a neuroprotective role, the intracellular mechanism leading to α7 nAChR-mediated neuroprotection is still unclear. Some studies point towards an involvement of the PI3K-Akt pathway in the neuroprotective actions of galantamine and nicotine (Arias *et al*, 2005), which can then trigger an increase in expression of anti-apoptotic proteins such as BCL-2 (Kihara *et al*, 2001). Another possibility is the activation of the janus kinase 2 (JAK2)/Akt signaling pathway, which can induce overexpression of the antioxidant enzyme heme oxygenase-1 (Parada *et al*, 2010).

While many studies report the neuroprotective effects of α7 nAChR-activity, some studies have linked α7 nAChRs to neurotoxicity. It has been suggested that over-activation of this receptor subtype may be neurotoxic (Li *et al*, 1999) – similar to NMDA-mediated excitotoxic effects. For example, a mutated form of this receptor that does not desensitize is associated with reduced neuronal cell viability in *C. elegans*, possibly due to calcium overload (Treinin and Chalfie, 1995). However, observations by Li *et al* (1999) indicate that normal α7 nAChRs can also induce cell death following acute application of high concentrations of nicotinic agonists *in vitro*. Furthermore, α7 receptors can induce distinct intracellular transduction processes in PC12 cells, depending on the level of activation. More specifically, the activation of protein kinase C seems to be neuroprotective, whereas cell death is dependent on tyrosine protein kinase (Li *et al*, 1999).

The results of this experiment provide further support for the potential neurotoxic effects of α7 nicotinic receptor-mediated signaling. A possible explanation for the discrepancy in the literature is that neuroprotection and neurotoxicity may depend on developmental changes in receptor expression. Laudenbach *et al* (2002) demonstrated that activation of α7 nAChRs, although protective in adult animals, induces neuronal death in a neonatal murine model of glutamatergic injury occurring between PND5 and PND10. The authors propose that this neurotoxic effect may be due to overexpression of α7 nicotinic receptors in the early postnatal stage. Supporting this notion, Broide *et al* (1996) demonstrated that the expression of α7 nAChR mRNA and receptor binding sites within the rat cortex was shown to peak during the first postnatal week and then decreased to adult levels.

However, this maturation theory may not be sufficient to explain the inconsistencies with the results in this thesis for several reasons. For one, additional experiments using primary cultures of embryonic cortical neurons in the same study by Laudenbach *et al* (2002) provide evidence that α7 receptor stimulation is neuroprotective, although the authors suggest differences in neuron maturation and density of α7 nAChR-mediated calcium influxes due to a lack of astroglial cells in neuron cultures as a potential explanation for this inconsistency in their own study.

Similar to what is observed in the cortex *in vivo* (Broide *et al*, 1996), α7 nAChRs expression increases with time in OHSCs, reaching the peak at DIV14 and decreasing thereafter (Mielke and Mealing, 2009). However, the majority of α7 subunits were located internally, with only about 11% being present at the surface. Furthermore, an ultrastructural study revealed an abundance and near-ubiquitous expression of α7

receptors at hippocampal synapses in adult rats (Fabian-Fine *et al*, 2001). These reports suggest that differences in receptor expression between neonatal and adult neurons may not be the reason for the opposing effects of α7 nAChR activation.

The theory of developmental differences in receptor expression also seems unsatisfactory as several other studies with similar experimental design to this thesis have reported neuroprotective effects of stimulation of α7 nicotinic receptors (Egea *et al*, 2007; Mulholland *et al*, 2004; Prendergast *et al*, 2001a). These studies provide evidence that both nicotine and choline can enhance neuroprotection against NMDA-mediated excitotoxicity as well as oxygen-glucose deprivation in acute and organotypic hippocampal slice cultures prepared from Sprague-Dawley rats of different ages (PND8 and adults) at different times in culture (DIV8 and DIV25). The involvement of α7 nicotinic receptors was demonstrated in two of these studies by application of the specific α7 nAChR antagonist methyllycaconitine (Mulholland *et al*, 2004) or by the use of α7 nicotinic receptor knockout mice (Egea *et al*, 2007). Due to the use of the non-selective nicotinic receptor antagonist mecamylamine in the study by Prendergast *et al* (2001a), the possible involvement of other nicotinic receptor subtypes, such as the α4β2, cannot be dismissed.

The experimental protocol in the studies mentioned above encompassed a period of pre-treatment of the cultures with the respective nicotinic receptor agonist followed by exposure to the stressor in combination with the same nAChR agonist. The pre-treatment period ranged from 30 minutes (Egea *et al*, 2007) up to 3 days (Mulholland *et al*, 2004) and even 5 days (Prendergast *et al*, 2001a). It is possible that the pre-exposure to nicotinic agonists induces transcriptional and translational intracellular processes, such as

activation of JAK2/STAT3 pathway or the PI3K/Akt pathway (Kawamata and Shimohama, 2011), to increase neuronal survival. With regards to a direct interaction between NMDA receptors and α7 nicotinic receptors, Li *et al* (2013) hypothesize that the α7 nAchR-dependent calcium influx may trigger intracellular signaling pathways that lead to changes in NMDAR function via altered phosphorylation, conformational changes, or altered surface expression.

Nevertheless, several studies indicate that the neuroprotective effects of α7 nicotinic receptors are not dependent on pre-exposure to specific agonists. Indeed, the presence of galantamine during oxygen-glucose deprivation and reoxygenation was able to increase cell viability (Egea *et al*, 2012). Additional experiments in the same study indicated that this neuroprotective effect was not mediated by AChE inhibition, but rather due to activation of α7 nAChRs. The selective α7 nAChR agonist PNU282987 also elicited neuroprotection against subchronic oxidative stress in OHSCs, when applied concurrently to the insult (Navarro *et al*, 2015). In the human neuroblastoma cell line SH-SY5Y, PNU282987 can protect against apoptotic cell death, even if added after an 8 hour stress period (Parada *et al*, 2010). Furthermore, using a similar experimental design to this thesis, Prendergast *et al* (2001b) demonstrated that acute nicotine exposure increases neuronal survival after exposure to NMDA. The α7 nAChR was linked to this neuroprotective effect, as the α7 nAChR antagonist methyllycaconitine mitigated the protective action. Therefore, activation of the α7 nAChR appears to be able to promote neuronal survival regardless of whether agonists are applied before, during or after an insult.

Results of this study indicating potential neurotoxic properties of α7 nAChR stimulation are supported by a recent publication demonstrating that positive allosteric modulation of α7 nAChR can induce cytotoxicity in SH-SY5Y cells, but also in OHSCs (Guerra-Álvarez *et al*, 2015). The authors propose that this is due to sustained opening of the α7 receptor channel and thus receptor over-activation in the presence of the type II positive allosteric modulator PNU120596. Uteshev (2016) points out that the concentrations and exposure durations chosen by Guerra-Álvarez *et al* (2015) are not clinically relevant and the study seems to purposely target excessive levels of α7 nAChR activation. Although two previous publications confirm the cytotoxic potential of excessive α7 nAChR activation by PNU120596 (Ng *et al*, 2007; Williams *et al*, 2012), no cytotoxicity was detected at lower ranges, and in fact a trend for increased cell viability was noticeable in these studies.

With regards to this study, it seems unlikely that the neurotoxic effects elicited by the chosen concentrations of choline (10 mM and 50 mM) (see Figure 3-1) are due to excessive activation of α7 nAChRs, as 10 mM choline were shown to be protective against NMDA-induced toxicity in OHSC if applied before the excitotoxic insult (Ferchmin *et al*, 2003; Mulholland *et al*, 2004). However, as some studies suggest that high doses of agonists may induce prolonged desensitization of nicotinic receptors, thus causing inhibition of the receptor (Laudenbach *et al*, 2002), additional experiments with lower choline concentrations may provide further insights into potential mechanisms of cytotoxicity relating to α7 nicotinic receptors. Addition of 10 μM galantamine did not affect cell damage in OHSCs at all and did not seem to potentiate choline-mediated activity. Experiments in the human embryonal kidney cell line HEK-293 indicate

inhibitory actions of galantamine at concentrations higher than 10 µM (Samochocki *et al*, 2003). Therefore, lower concentrations should be tested in future experiments. However, it should be noted that neuroprotective effects of 10 µM galantamine have previously been shown to involve α7 nAChR activation and not AChE inhibition (Egea *et al*, 2012),

In summary, results obtained from the present experiment provide no evidence of a neuroprotective role of α7 nicotinic receptor activation against NMDA-mediated excitotoxicity in organotypic hippocampal slice cultures. In contrast, some trends toward increased cell death after application of the α7 nAChR agonist choline were detected. Nonetheless, given the small sample size per treatment group as well as the variability observed, further investigation – especially with lower concentrations of choline - is required to draw more firm conclusions from the observations described.

CHAPTER 4:

OVERALL CONCLUSIONS AND FUTURE DIRECTIONS

4.1 CONCLUSIONS

The aim of this thesis was threefold: First, to develop a method that allows objective quantification of cell death in organotypic hippocampal slice cultures using propidium iodide. The second aim was to establish a dose-response curve for NMDA toxicity. Based on these two aims, the effects of co-activation of α7 nicotinic receptors on NMDA-induced cell death in OHSCs could be determined

In order to achieve the first two aims, slice cultures were prepared from rats at PND5/6 according to the interface method and exposed to different concentrations of NMDA on day 13 *in vitro*. PI uptake was measured by separation of the hippocampal subfields using simple landmarks and densitometric quantification of fluorescence intensity in 10 template-oriented counting fields. This protocol facilitates the objective and quantitative analysis of cell death in distinct regions of organotypic hippocampal slice cultures in a standardized format, allowing for analysis and comparison of the effects of drug exposure on cell viability in this preparation. The results of these experiments show that exposure to increasing concentrations of NMDA result in a dose-dependent increase in PI uptake and thus cell death in organotypic hippocampal slice cultures; an effect evident in all hippocampal subfields. Similar to previous literature, a region-specific vulnerability to NMDA-mediated insults was demonstrated, with the CA1 region being the most sensitive.

The PI uptake induced by NMDA in this thesis is lower compared to published reports using similar measures of NMDA-mediated PI uptake in OHSCs. As discussed in Chapter 2, this discrepancy is likely due to variations in the method used to induce

maximal cell death. Future experiments could induce maximal cell death by using high concentrations of Glu to provide evidence for this theory.

The α7 nAChR may play multiple roles with regards to the glutamatergic system, as this receptor type can modulate Glu transmission and therefore NMDA receptor activity by different ways depending on the α7 nAChR location. For example, activation of presynaptic α7 nAChR can facilitate the release of GABA (Arnaiz-Cot *et al*, 2008), which may modulate excitatory neurotransmission and potentially even NMDA receptor calcium signals (Chalifoux and Carter, 2010), as well as Glu (Gray *et al*, 1996) from presynaptic terminals,. The experiments of this thesis focused on investigating the interaction of α7 nAChRs and NMDARs at postsynaptic locations, where α7 nAChRs can modulate the activity of NMDA receptors (Fisher and Dani, 2000).

Using the quantification protocol of PI uptake developed in Chapter 2, the effects of co-activation of α7 nicotinic receptors on NMDA-induced cell death in OHSCs were investigated by treating slice cultures with NMDA in combination with choline, a specific α7 nAChR agonist, and the APL galantamine. While co-activation of α7 nAChRs did not significantly alter NMDA-induced PI uptake in any of the hippocampal regions, stimulation of α7 nAChRs alone in the absence of NMDA resulted in increased cell damage in some hippocampal regions. Taken together, these results imply a role for α7 nAChRs on presynaptic neurons and astrocytes rather than postsynaptic α7 nAChRs. In the saline control groups, administration of choline may activate α7 nAChRs on the presynapse or on astrocytes causing the sudden release of Glu and subsequent activation of postsynaptic NMDA receptors, which subsequently causes neurotoxicity. In contrast, slice cultures that are exposed to NMDA already experience an excitotoxic insult, which

results in increased PI uptake. Compared to cell injury induced by NMDA, the effect of α7 nAChR-mediated Glu release is small and may be obscured in OHSCs exposed to a combination of NMDA and choline. Thus, co-activation of α7 nAChRs in these slice cultures does not affect PI uptake and cell viability. To investigate this possibility, it is necessary to assess the effect of NMDAR antagonists on choline-induced neurotoxicity. If the neurotoxic effects are due to α7 nAChRs-mediated Glu release from presynaptic terminals or astrocytes, NMDAR antagonists should prevent the increase of PI uptake.

4.2 FUTURE DIRECTIONS

As highlighted in section 3.4, other authors have seen neuroprotective actions of α7 nAChR stimulation using the same and lower doses of choline. Future investigations should therefore investigate the effect of lower concentrations of choline and galantamine on NMDA-mediated excitotoxic cell death in order to rule out the possibility that neurotoxic effects seen in these experiments are due to excessive activation of α7 nAChRs. Furthermore, the involvement of α7 nAChR should be conclusively assessed using specific antagonists.

Although NMDA receptors and α7 nicotinic receptors in physiological and pathophysiological events are known to functionally interact, the exact mechanisms underlying neuroprotective or neurotoxic effects of α7 nAChR activation in NMDA-mediated excitotoxicity are still unclear. It is possible that co-activation of α7 nAChRs can influence the switch of NMDAR signaling from a pro-death to a pro-survival pathway or vice versa. Thus, the determination of how α7 nAChR stimulation may influence the expression of proteins in this signaling cascade would be of interest.

However, the choline-induced neurotoxic effects seen in the saline control slice cultures may suggest the involvement α7 nAChR-mediated Glu release. This alternative explanation should be investigated in future experiments using specific NMDAR antagonists.

Furthermore, the use of young animals in stroke research is often criticized and the need to prepare organotypic slice cultures from adult donors has been voiced (Humpel, 2015b). With reports showing developmental differences in receptor expression, it would be useful to investigate the interaction of α7 nicotinic receptors and NMDA receptors in slice cultures prepared from older rats. Although there are still various challenges to overcome, including the long-term maintenance of adult organotypic slices, the implementation of this factor is an important step towards an experimental setting that is more representative of an *in vivo* population.

APPENDIX A: DEVELOPMENT OF THE QUANTIFICATION PROTOCOL — EFFECTS OF CULTURE MEDIA

OBJECTIVE

In order to establish a dose-response relationship between NMDA exposure and cell death in OHSCs, an initial set of experiments was modeled after a publication by Kristensen *et al* (2001). In this study, the authors compared the excitotoxic profiles of several GluR agonists, including NMDA, in OHSCs.

In these initial experiments, OHSCs were prepared as described in Chapter 2 and incubated in MEM-based culture medium. As the magnesium concentration in this type of medium is quite high and Mg^{2+} has the ability to block the channel pore of the NMDA receptor (see Chapter 1, Section 1.3), the cultures were switched after four days of incubation to a Neurobasal® based culture medium, which has a lower concentration of Mg^{2+}, to limit any influence the high Mg^{2+} levels may have on the experiments.

METHODS

Similar to the methods described in Chapter 2, the viability of the slice cultures was assessed by PI uptake on DIV13 and OHSCs with low basal levels of PI uptake were exposed to different concentrations of NMDA for 4 hours followed by 24 hours in fresh Neurobasal® culture medium. The PI uptake was measured again, and the slices were exposed to phosphate buffered saline (PBS) at 4°C for another 24 hours to induce maximal cell death. A final set of PI uptake was taken on DIV15 representing the maximal PI uptake.

The digital pictures of PI uptake were analyzed by densitometry with ImageJ inspired by NIH Image. As the hippocampal structure of these slice cultures were generally not visible in light microscope pictures or in OHSCs with lower PI uptake, quantification of PI uptake in the distinct hippocampal subregions was not possible. However, the irregular shape and size of the hippocampal slices renders the analysis of fluorescence intensity over the whole slice and comparison of slice cultures to each other inaccurate. As a compromise of these two methods, a standard template of 50 circles throughout the picture was used, the placement of which was fixed (see Figure A-1). Two background circles were used for subtraction of any background noise. The raw integrated density, the sum of the pixel values, was calculated for every circle of each slice. Density measurements of OHSCs after induction of maximal cell death were used to establish a threshold value for each individual slice, defined as 30% of the maximum raw integrated density measured for this slice. If the density of a circle was higher than the threshold value, it was considered positive and counted as 1, and if it was lower it was considered negative and given a 0. The ratio of the circles over the threshold value after the drug treatment and the amount of circles over the threshold after the low-temperature exposure to PBS was calculated, and in this way the PI uptake could be expressed in percentage of the maximal PI uptake.

RESULTS

Using this method, control slice cultures treated with saline showed an average PI uptake of 4.41% ± 2.17 (n = 6). However, the PI uptake plateaued at 31.91% ± 9.99 after exposure to 500 µM NMDA (n = 6). To validate these results, two additional methods, a

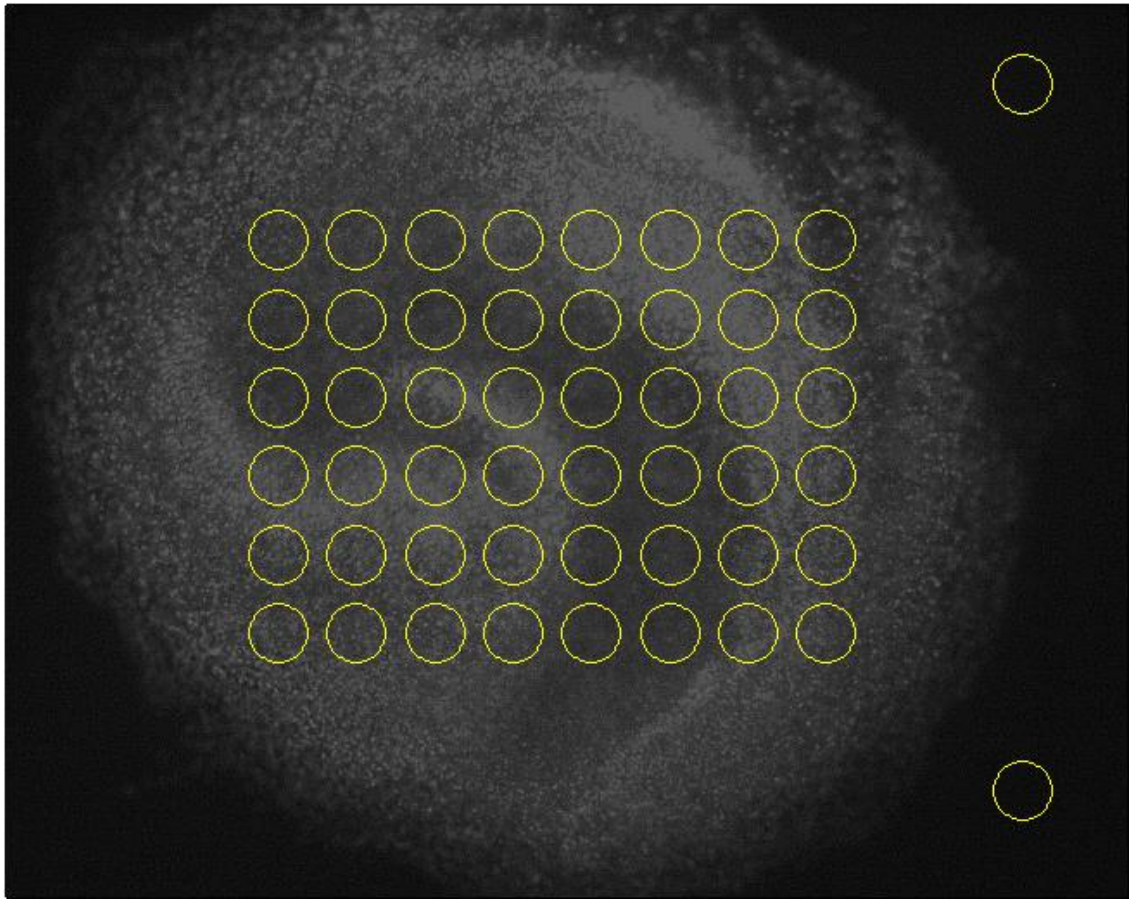

Figure A-1: Standard template to facilitate quantification of propidium iodide. Representative illustration shows placement of measurement windows in the hippocampal areas (dentate gyrus, CA3 and CA1) of propidium iodide-stained organotypic hippocampal slice cultures grown in Neurobasal media®.

lactate dehydrogenase cytotoxicity assay (Abcam, ab65393) and Fluoro-Jade C (FJC) staining (see Appendix B) were tested. The LDH assay was unsuccessful as no LDH could be detected in collected media samples. As preparation for Fluoro-Jade C staining, OHSCs were fixed in 10% formalin, frozen in cryomatrix and sliced using a cryostat following a previously established protocol from our laboratory (Pérez-Gómez and Tasker, 2012).

However, slicing of the cultures was unsuccessful as the tissue was generally undetectable. As the only difference to the methods by Pérez-Gómez and Tasker (2012) was the type of media used (MEM vs Neurobasal®-based), and Neurobasal® culture media has been shown to induce toxicity in hippocampal cell culture (Hogins *et al*, 2011), a small experiment was conducted looking at the effects of different culture media on viability of OHSCs. Slice cultures were prepared as before, but either kept in MEM-based culture medium until DIV13 or switched to the Neurobasal®-based medium at different time points (on DIV4, on DIV11, or on DIV13 2 hours before the exposure). Cultures that were grown in MEM-based medium showed no or only a low basal PI response on DIV13, whereas cultures that were switched to Neurobasal® medium on DIV4 showed a medium to high amount of PI uptake. OHSCs switched to the Neurobasal® medium on DIV11 or two hours before PI exposure showed low to medium PI uptake (data not shown). This suggests that the Neurobasal® medium induces higher rates of spontaneous cell death compared to MEM-based culture medium, potentially mediated by high concentrations of L-cysteine (Hogins *et al*, 2011).

CONCLUSIONS

For further experiments, OHSCs were exclusively grown in MEM-based culture medium. Additionally, omitting the switch to Neurobasal® medium also seemed to have an effect on the growth of the cultures, as the delineation of hippocampal subfields CA1, CA3 and the DG was possible using light microscope pictures in addition to PI images, when cultures were grown in the MEM-based culture medium. This offered the opportunity to develop a method of measuring fluorescence intensity in individual regions (see Section 2.2.5 Image analysis and quantification of PI fluorescence), which provided more accurate results. The higher concentration of Mg^{2+} in this media did not appear to affect NMDA-mediated toxicity, as levels of PI uptake as high as 59.30% ± 3.91 were measured in the CA1 region of the hippocampus after exposure to 1000 µM NMDA.

APPENDIX B: VALIDATION OF THE CELL DEATH QUANTIFICATION METHOD IN ORGANOTYPIC HIPPOCAMPAL SLICE CULTURES

OBJECTIVE

The analysis of cellular uptake of propidium iodide is commonly used in the literature to quantify neuronal cell death in organotypic hippocampal slice cultures and PI has been shown to be a reliable marker, but some doubts about the sole use of PI uptake have been raised (Noraberg *et al*, 1999). Several other markers of neurodegeneration have been tested in OHSCs, including lactate dehydrogenase and Fluoro-Jade staining.

The LDH cytotoxicity assay is a commonly used marker in cytotoxicity studies and has been used in organotypic hippocampal slice cultures in previous literature (Bruce *et al*, 1995; Fotakis and Timbrell, 2006; Noraberg *et al*, 1999). The assay is based on the measurement of LDH activity in the extracellular medium. LDH is a stable enzyme, present in all cell types, and rapidly released into the cell culture medium upon damage of the plasma membrane. LDH can oxidize lactate to generate NADH, which then reacts with the cell proliferation reagent water soluble tetrazolium-1 (WST-1) to produce a yellow color. The intensity of this yellow color correlates directly with the number of lysed cells (Egea *et al*, 2007; Noraberg *et al*, 1999). To investigate this assay for validation of PI uptake, several samples of collected culture media and homogenized OHSC tissue were tested in the current study according to the instructions from the manufacturer (Abcam, ab65393) and previously published protocols (Noraberg *et al*, 1999; Su *et al*, 2011). Samples were collected after exposure to 100 µM NMDA, 500 µM NMDA, or PBS or ethanol at low temperature to serve as a positive control.

Unfortunately, no LDH activity was detected and implementation of this cytotoxicity assay proved unsuccessful. The exact reasons for why this assay may have failed are unclear. However, it is possible that the amount of LDH released through the semiporous membrane insert was too diluted by the 1 ml of media in the culture dish.

Thus, a staining method using the fluorochrome dye Fluoro-Jade C (Millipore) was performed to validate the quantification method described in Chapter 2 using PI uptake. FJC stains all degenerating neurons, regardless of specific insult or mechanism of cell death, and it has a greater signal to background ratio and higher resolution compared to its predecessors, Fluoro-Jade and Fluoro-Jade B (Schmued *et al*, 2005). Additionally, this type of staining has the advantage that double-labeling with other fluorescent markers is possible, such as 4', 6-diamidino-2-phenylindole (DAPI), which labels nuclear DNA. The staining protocol was adapted from previously published protocols (Eyüpoglu *et al*, 2003; Noraberg *et al*, 1999; Schmued *et al*, 2005).

METHODS

Preparation of organotypic hippocampal slice cultures, maintenance, and exposure procedures were as reported in Chapter 2 and Chapter 3 of this thesis. On day 13 *in vitro*, healthy OHSCs, as determined by low PI uptake, were exposed to different concentrations of NMDA (Sigma-Aldrich) (1 µM, 10 µM, 50 µM, 100 µM, 500 µM, and 1 mM) in 0.9% saline, or to 0.9% saline alone as control for 4 hours. Slice cultures were then transferred to fresh culture medium for 24 hours, after which PI uptake was measured. To serve as positive controls, OHSC were exposed to ice cold 70% ethanol for 24 hours at -20°C.

Fluoro-Jade C staining

After slice cultures were exposed to their respective treatments and microscope pictures of PI uptake were taken, slices were prepared for formalin fixation. OHSC were washed 3 times with 1x PBS at room temperature by transferring the inserts with the slices from one dish filled with PBS to the next. The same process was repeated using 10% neutral buffered formalin. After the washes, extra formalin was added to the top of the insert covering the slices. The slices were then left in the final formalin wash for 5 hours at 4°C. The inserts with slices were then washed again with 1x PBS and transferred to a dish containing 1 ml of 1x PBS + 0.1% Triton X solution. This solution acts as a permeabilization buffer to enhance penetration of the dye. The slices were then covered with extra buffer solution, and kept at 4°C overnight. If slices were not used immediately, they were transferred to 1x PBS and kept at 4°C until further processing, but not longer than 2 weeks.

The slice cultures were kept on the inserts for the staining procedure, and solutions were, therefore, always added to the staining dish and on top of the inserts to cover the slices completely. Slices were washed for 3 min in 100% ethanol for 3 min, for 1 min in 75% ethanol and 1 min in ddH_2O, and then incubated in 0.06 potassium permanganate (Sigma) solution for 15 min. Slices were washed again in ddH_2O for 1 min, and then transferred to 0.0001% Fluoro-Jade C (Millipore) in 0.1% acetic acid solution for 60 min. OHSC were washed in ddH_2O 3 times for 3 min each, and then transferred to a 1:500 dilution of DAPI (Sigma), a nuclear counterstain, for 15 min. Slices were rinsed through three changes of ddH_2O for 3 min per change, and then cut out on pieces of membrane and gently placed onto microscope slides coated with 0.5% gelatin, with the membrane

on the bottom. The slides with slice cultures were air dried, cleared in xylene for at least 1 min and then coverslipped with PermaFluor mounting media (Thermo Fisher Scientific).

Image analysis and quantification of FJC staining

The FJC stained sections were examined using a LSM 710 laser scanning confocal microscope (Zeiss, Germany) with a fluorescein isothiocynate (FITC) filter system. To ensure comparability, the following optimal settings for FJC (see Table B-1) were chosen after an initial trial run and always kept the same. DAPI stained cells were visualized using a specific DAPI filter. DAPI staining was not quantified, as it was only auxiliary to determine hippocampal structures. Because of the varying thickness of slice cultures, the focal plane was chosen according to where the highest FJC intensity was detected. Images were taken using the tile scan option.

Table B-1: Laser confocal microscope settings for Fluoro-Jade C quantification.

Dimensions	x: 5120, y: 5120, 8-bit
Objective	Plan-Apochromat 20x/0.8 M27
Pixel dwell	0.64 µs
Average	1
Master gain	764
Digital gain	1.00
Digital offset	-31.79
Pinhole	61 µm
Lasers	488 nm: 0.2559%

RESULTS

Figure B-1 shows a representative picture of a slice culture exposed to 100 µM NMDA and subsequently stained with DAPI and Fluoro-Jade C. FJC intensity was intended to be quantified similarly to the quantification method used for the PI staining (see Chapter 2). Table B-2 summarizes the results of the initial analysis of slice cultures exposed to saline, 50 µM, 100 µM, and 500 µM NMDA obtained using ImageJ, as described in Section 2.2.3 of Chapter 2. The average intensity measured in slice cultures exposed to 70% ethanol at low temperature was set as the maximum (n=5). Figure B-2 shows representative pictures of slice cultures exposed to different concentrations of NMDA.

Table B-2: Comparison of Fluoro-Jade C uptake (as percent of maximum) after exposure to increasing concentrations of NMDA in the dentate gyrus (DG), CA1 and CA3. Data are given as mean ± SEM.

	n	DG	CA1	CA3
saline	5	25.81	14.12	21.65
50 µM NMDA	6	58.08	64.12	58.60
100 µM NMDA	6	43.56	43.78	51.39
500 µM NMDA	6	58.73	57.65	58.25

CONCLUSION

The results show clear differences between saline treated slice cultures, positive control OHSCs and slice cultures exposed to NMDA. However, the FJC staining did not appear to discriminate the effects of increasing NMDA concentrations as well as PI uptake (compare Table B-2 and Figure B-2). The values for FJ intensity are generally

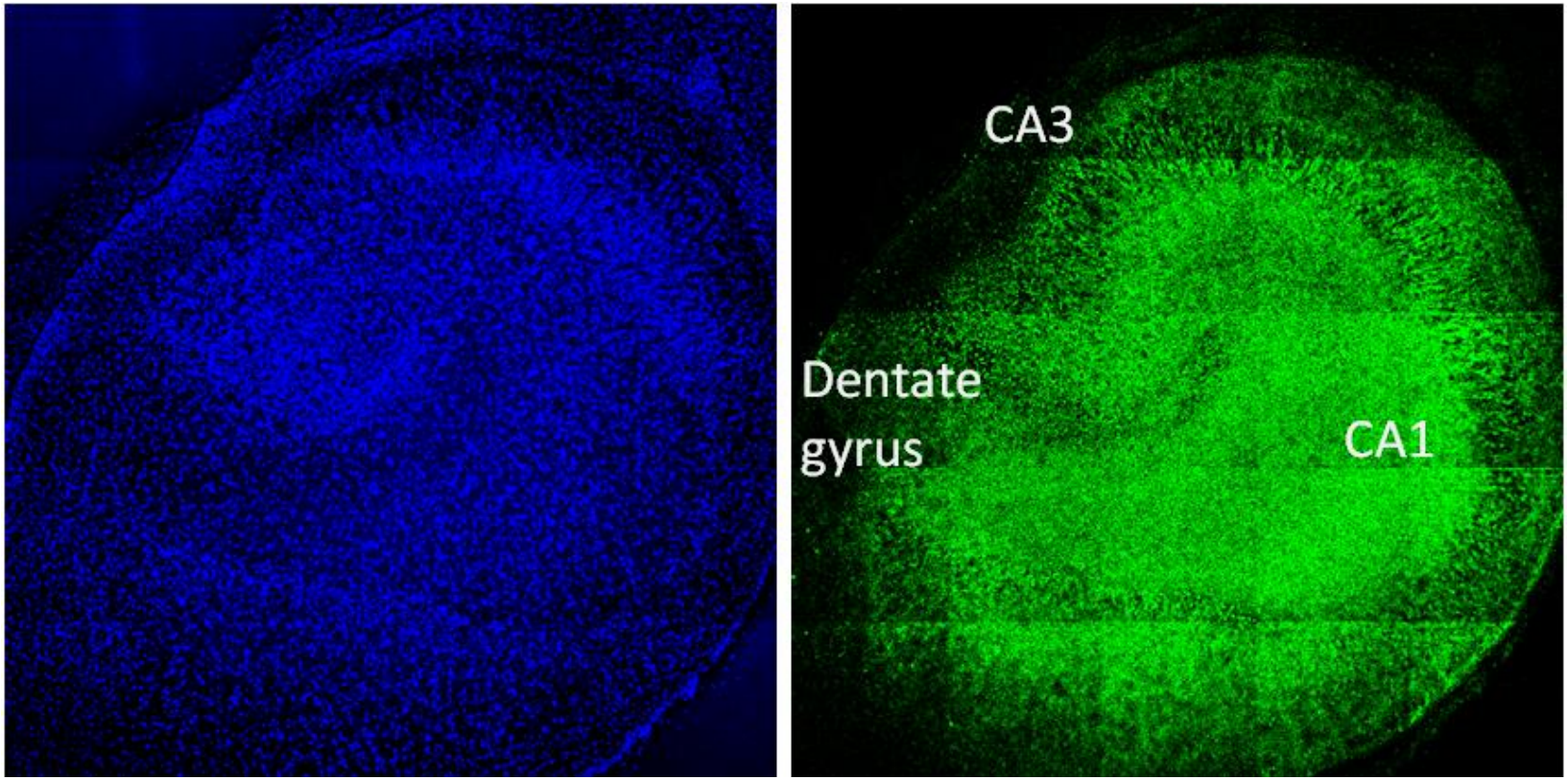

Figure B-1: Representative image of a hippocampal slice culture exposed to 100 µM NMDA and double-labelled with the nuclear stain DAPI (left in blue) and Fluoro-Jade C (green), a marker of neuronal degeneration

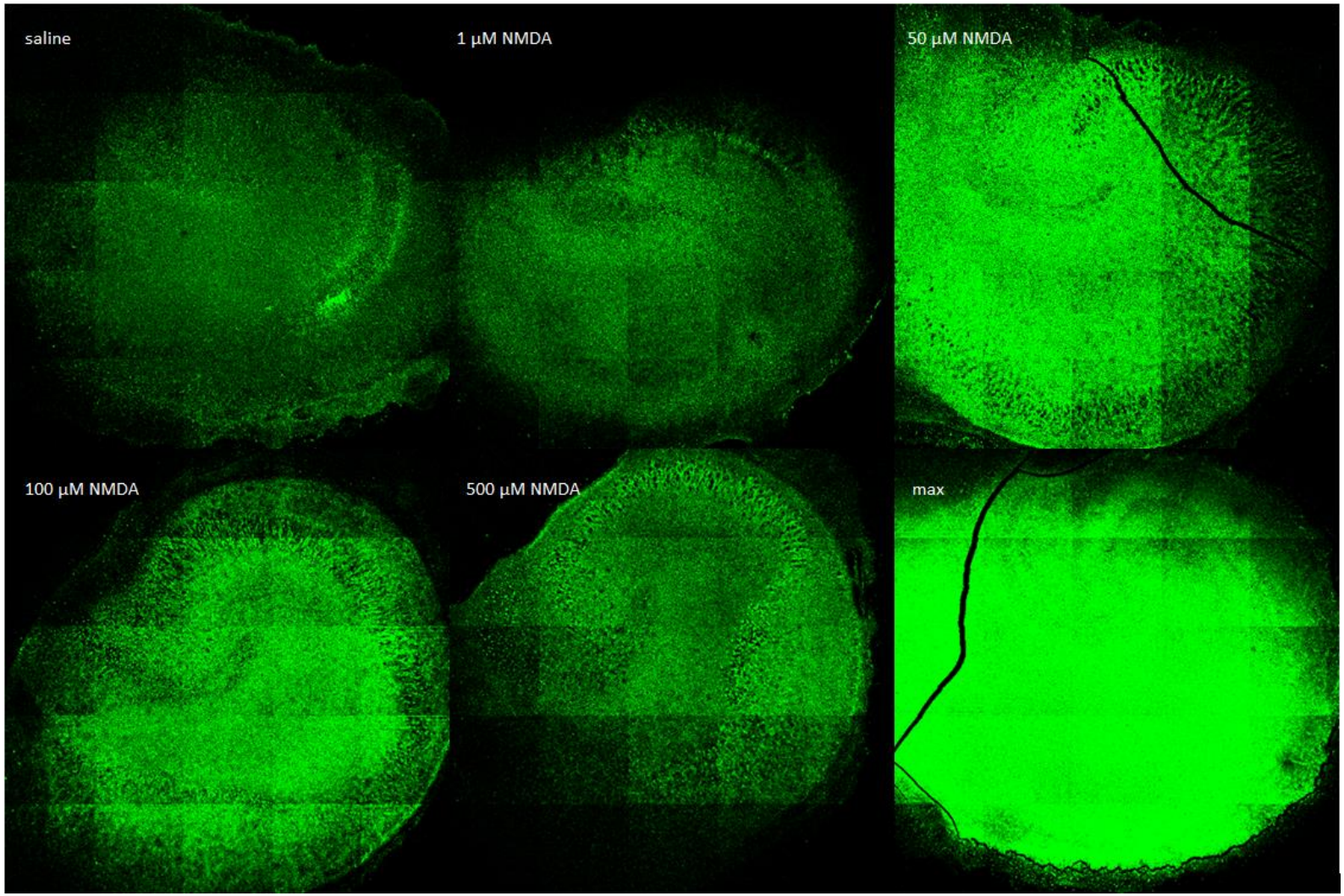

Figure B-2: Representative images of Fluoro-Jade C uptake in organotypic hippocampal slice cultures following 4 h exposure to saline, 1 µM NMDA, 50 µM NMDA, 100 µM NMDA and 500 µM NMDA as measured after 24 h in fresh culture media as well as a slice culture exposed to 70% ethanol at 4°C for 24 h to obtain the maximal possible Fluoro-Jade C uptake.

higher, as even control slice cultures show an uptake of approximately 20%. This is most likely artificially created by the chosen exposure settings.

It is interesting to note that, similar to PI uptake, FJC intensity appears to plateau around 60-65% of the maximum possible value, agreeing with the data obtained using PI.

During these experiments, several problems with this staining method became apparent. Firstly, the staining procedure caused cracks in many slice cultures. This is most likely attributable to the dehydration steps. Additionally, the hippocampal structures were not consistently visible in the DAPI-stained images which made correct placement of the counting fields difficult. The staining procedure and recording of fluorescence imaging using the laser scanning confocal microscope are also very time consuming. As the FJC staining did not provide any additional information, it was decided that analysis of cell death using PI uptake alone would suffice.

APPENDIX C: EFFECT OF DEPOLARIZATION USING DOMOIC ACID ON NMDA RECEPTOR-MEDIATED EXCITOTOXICITY IN ORGANOTYPIC HIPPOCAMPAL SLICE CULTURES

OBJECTIVE

Initial experiments to construct a dose-response curve and quantify cell death using PI revealed less cell death than expected from the literature. For example, data obtained in the experiments described in this thesis show that administration of 100 µM NMDA results in PI uptake of approximately 30% of the maximum possible cell death (as measured after low temperature exposure to 70% ethanol), whereas several publications report PI levels of 80-100% after exposure to 100 µM NMDA (Kristensen *et al*, 2001; Sakaguchi *et al*, 1997). Although differences in methodology of PI quantification account for some of these seemingly contrary results (see Chapter 2 Section 2.4.2 for detailed discussion), additional experiments were performed to test an alternative idea.

As mentioned in Chapter 1, extracellular Mg^{2+} blocks the channel pore of the NMDA receptor at resting potential. Upon membrane depolarization, the Mg^{2+} block is removed and ions can enter the cell through the NMDAR channel. Therefore, the activation of NMDA receptors does not only rely on agonist binding, but also exhibits a voltage-dependence. Moderate local depolarization can be achieved by activation of ionotropic AMPA/kainate receptors, for example, which results in Na^{+} influx.

Domoic acid (DOM) is a naturally occurring Glu analogue found in seaweed and plankton (Costa *et al*, 2010). DOM can elicit a potent excitotoxic response as an agonist

of AMPA and kainate receptors, although some evidence suggests an involvement of NMDA receptors as well (Tasker *et al*, 2005).

Previous studies in our laboratory have shown that low concentrations of DOM can induce mild excitotoxic injury in organotypic hippocampal slice cultures. Concentrations ≥1 µM DOM produced significantly increased PI uptake in the CA1 subfield of the hippocampus, whereas exposure concentrations of ≥5 µM DOM were necessary to induce significant toxicity within the DG and CA3 region (Pérez-Gómez and Tasker, 2012).

The objective of this experiment was to examine whether depolarization using a low dose of DOM can increase cell damage induced by 100 µM NMDA in OHSCs.

METHODS

Preparation of organotypic hippocampal slice cultures, exposure procedures and quantification of PI uptake were as reported in Chapter 2 and Chapter 3 of this thesis.

On day 13 *in vitro*, healthy OHSC, as determined by low PI uptake, were exposed to different combinations of 2 µM DOM, 100 µM NMDA, choline (50 mM or 100 mM) and 10 µM galantamine for 4 hours. Slice cultures were then transferred to fresh culture media for 24 hours, after which PI uptake was measured again to determine the effects of drug exposure on cell viability. The data for the exposure condition of 100 µM NMDA as well as for the positive controls (exposed to ice cold 70% ethanol for 24 hours at -20°C) were used from Chapter 2. PI uptake was quantified by densitometry using the standard template of 10 movable, circular regions of interest, with three in each of the

hippocampal regions as described in Chapter 2, Section 2.2.5. PI uptake induced by the different treatment conditions was expressed as the percentage of the maximal PI uptake.

All densitometric data were expressed as mean ± SEM. Data of the three hippocampal regions, DG, CA1, and CA3, were analyzed separately using one way ANOVA followed by Tukey's post-hoc test or Welch's ANOVA followed by Games-Howell procedure where appropriate. Statistical analyses were performed using SPSS Statistics Version 23 (IBM Corporation, NY, USA) at a level of significance of 0.05.

RESULTS

As shown in Chapter 2, differences in susceptibility to NMDA-induced toxicity exist between the three hippocampal regions. Therefore, results were analyzed for each region individually.

Dentate gyrus

Normality of the data was confirmed using the Kolmogorov-Smirnov test (p>0.05). Levene's test of homogeneity of variances was significant (p=0.026). Thus, Welch's F-ratio was used to assess significance between groups. A significant difference between groups was found using Welch's ANOVA ($F_{8,19.865}$=4.886, p=0.002). The Games-Howell procedure was therefore performed to compare the different treatment groups

Slice cultures exposed to 2 µM DOM alone showed a PI uptake of 27.00% ± 2.87 (n=7) (see Figure C-1). Addition of 50 mM choline did not alter the cell damage in

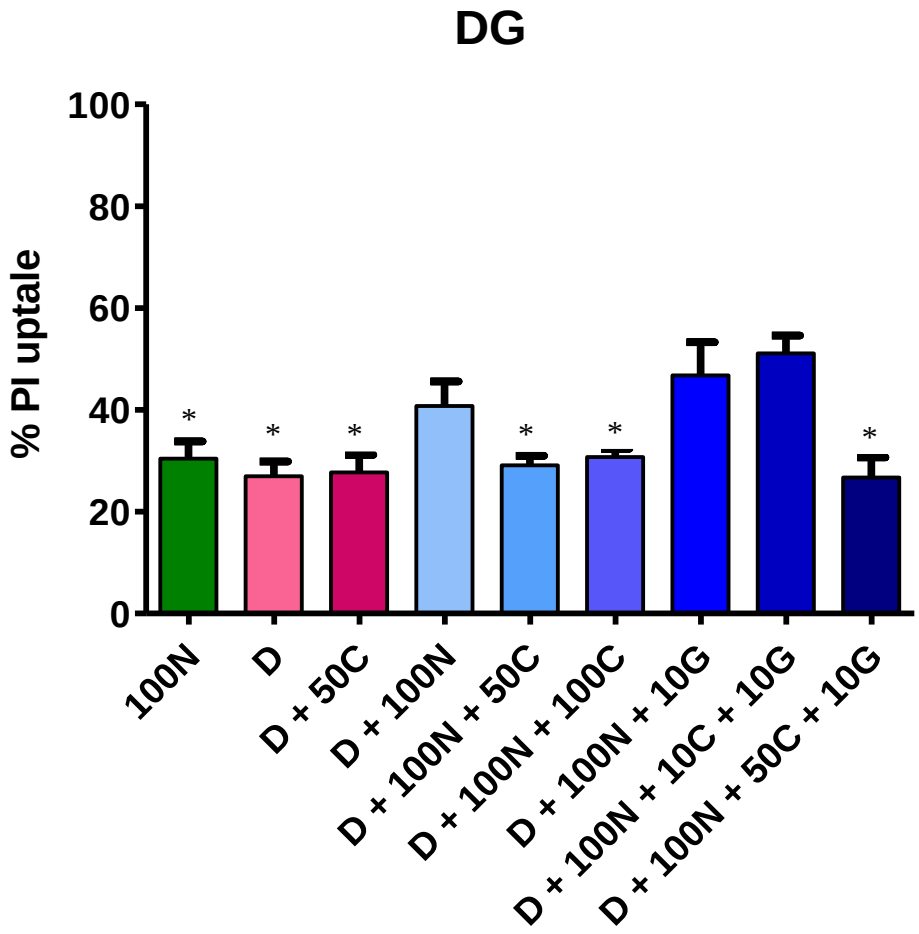

Figure C-1: Histograms show quantification of cell damage using propidium iodide (PI) in the dentate gyrus (DG) of organotypic hippocampal slice cultures. Slice cultures were exposed to different combinations of drugs (100 µM NMDA (100N), 2 µM domoic acid (D), 10 mM choline (10C), 50 mM choline (50C) or 100 mM choline (100C) and 10 µM galantamine (10G)) for 4 hours. PI uptake was measured after 24 hours in fresh media. Data are shown as means ± SEM, with n = 5–9. One way ANOVA using Welch's correction followed by Games-Howell post-hoc test revealed significant differences, *p<0.05 from D + 100N +10C + 10G.

OHSC (27.72% ± 3.46, n=7, p=1.00). In slice cultures exposed to 2 µM DOM in combination with 100 µM NMDA, a PI uptake of 40.76% ± 4.84 (n=9) was measured, which was not significantly different from any other group.

The highest PI levels of 51.12% ± 3.46 were measured in slice cultures treated with 2 µM DOM, 100 µM NMDA, 10 mM choline and 10 µM galantamine (n=5). This value was significantly different from all other treatment conditions, except for OHSCs exposed to 2 µM DOM with 100 µM NMDA (40.76 ± 4.84, n=9, p=0.714) or 2 µM DOM, 100 µM NMDA and 10 µM galantamine (46.76 ± 6.55, n=6, p=0.999). Table C-1 summarizes the values for PI uptake for the other treatment groups.

CA1

Normality of the data was confirmed using the Kolmogorov-Smirnov test (p>0.05). Analysis of the data using Levene's test for homogeneity of variances revealed significance (p<0.0005). Consequently, Welch's ANOVA was used to assess differences between groups and a significant difference was found ($F_{8,19.899}$=5.719, p=0.001). Post-hoc tests were performed using Games-Howell procedure.

Similar to previous experiments (see Chapter 2 and Chapter 3), the highest values in each treatment group were generally measured in the CA1 region, followed by the DG and CA3 (see Table C-1 for a summary of all the values). For example, OHSCs treated with 2 µM DOM showed a PI uptake of 46.73% ± 4.43 in CA1 vs 26.30% ± 2.87 and 23.57% ± 1.85 in DG and CA3 (n=7), respectively.

Table C-1: Propidium iodide uptake in the dentate gyrus (DG) and CA3 and CA1 hippocampal regions in organotypic slice cultures treated with different combinations of 2 µM DOM, 100 µM NMDA, choline (50 mM or 100 mM) and 10 µM galantamine for 4 hours, as recorded after 24 h in fresh media. Data expressed as percentage of positive control exposed to 70% ethanol at low temperature for 24 h (mean ± SEM). *p<0.05 vs D + 100 N + 10 C + 10 G in each region.

Treatment conditions	*n*	DG	CA1	CA3
2 µM DOM (D)	7	26.30 ± 2.87*	46.73 ± 4.43*	23.57 ± 1.85*
D + 50 mM choline (50 C)	7 (6 for CA3)	27.72 ± 3.46*	59.09 ± 5.20	27.54 ± 1.56
D + 100 µM NMDA (100 N)	9	40.76 ± 4.84	62.13 ± 6.06	34.85 ± 1.73
D + 100 N + 10 µM galantamine (10 G)	6	46.76 ± 6.55	73.49 ± 8.45	36.72 ± 3.27
D + 100 N + 50 C	8	29.08 ± 1.93*	43.05 ± 2.19*	26.24 ± 2.30*
D + 100 N + 100 mM choline	8	30.73 ± 1.62*	46.70 ± 3.05*	29.76 ± 3.16
D + 100 N + 10 C + 10 G	5	51.12 ± 3.46	74.03 ± 4.43	41.08 ± 4.45
D + 100 N + 50 C + 10 G	5	26.74 ± 3.93*	49.11 ± 4.39	24.65 ± 1.42*
100 µM NMDA	6	30.40 ± 3.41*	57.33 ± 9.45	27.62 ± 3.36

As in the DG, addition of 50 mM choline did not significantly alter PI incorporation (59.09% ± 5.20, *n*=7, *p*=0.677). When compared to slice cultures treated with 100 µM NMDA alone (57.33% ± 9.45, *n*=6), inducing neuronal depolarization with 2 µM DOM in addition to 100 µM NMDA does not significantly increase cell death (62.13% ± 6.06, *n*=9, *p*=1.000). Furthermore, co-activation of α7 nicotinic receptors using choline does not seem to affect the cell's response to the excitotoxic insult mediated by NMDA exposure for the most part (see Table C-1 and Figure C-2). Resembling the results obtained for the DG, significant differences were found between slice cultures exposed to 2 µM DOM/100 µM NMDA/10 mM choline/10 µM galantamine (74.03% ± 4.43, *n*=5) and OHSCs in the following treatment groups: 2 µM DOM (46.73% ± 4.43, *n*=7, *p*=0.026), 2 µM DOM/100 µM NMDA/50 mM choline (43.05% ± 2.19, *n*=8, *p*=0.010) as well as 2 µM DOM/100 µM NMDA/100 mM choline (46.70% ± 3.05, *n*=8, *p*=0.016). Furthermore, slice cultures exposed to 2 µM DOM/ 100 µM NMDA/ 50 mM choline/ 10 µM galantamine showed 49.11% ± 4.39 PI uptake (*n*=5), which approached significance when compared to OHSCs in the 2 µM DOM/100 µM NMDA/10 mM choline/10 µM galantamine group (*p*=0.056).

CA3

Normality of the data was confirmed using the Kolmogorov-Smirnov test (*p*>0.05), except for the group exposed to 2 µM DOM combined with 50 mM choline (*n*=7, *p*<0.011). Plotting data from this group in a histogram revealed one outlier. After removal of this value, the Kolmogorov-Smirnov test was still significant (*p*=0.047). However, the Shapiro-Wilk test was not significant (*p*=0.100).

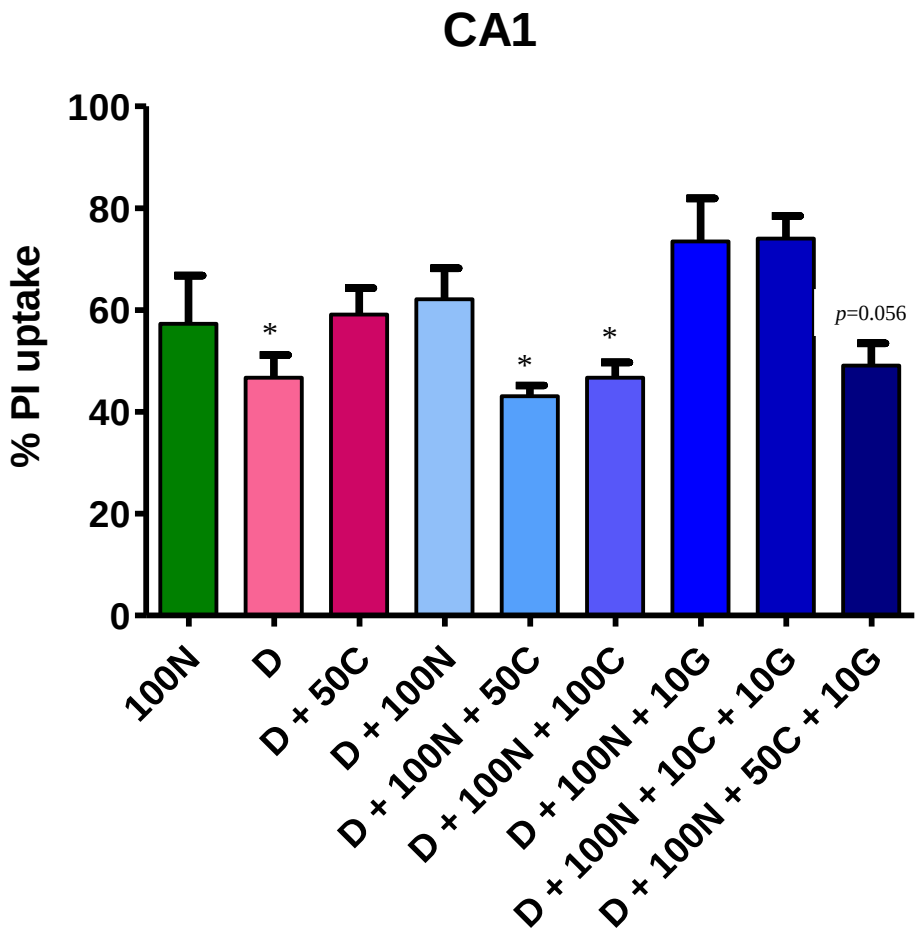

Figure C-2: Histograms show quantification of cell damage using propidium iodide (PI) in the hippocampal region CA1 of organotypic hippocampal slice cultures. Slice cultures were exposed to different combinations of drugs (100 µM NMDA (100N), 2 µM domoic acid (D), 10 mM choline (10C), 50 mM choline (50C) or 100 mM choline (100C) and 10 µM galantamine (10G)) for 4 hours. PI uptake was measured after 24 hours in fresh media. Data are shown as means ± SEM, with n = 5–9. One way ANOVA using Welch's correction followed by Games-Howell post-hoc test revealed significant differences, *p<0.05 from D + 100N +10C + 10G.

Levene's test of homogeneity of variances was not significant for the CA3 hippocampal region (p=0.263). A significant difference between groups was found using one way ANOVA ($F_{8,52}$=3.867, p=0.001). Thus, Games-Howell post-hoc tests were performed.

The general trends seen in the DG and CA1 region were also evident in CA3 (see Figure C-3). A low dose of domoic acid alone was able to induce a PI uptake of 23.57% ± 1.85, which was not significantly altered by administration of 50 mM choline (30.70% ± 3.43, p=0.671). Furthermore, depolarization by stimulation of non-NMDARs could not significantly increase the amount of cell death (34.85% ± 1.73) when compared to activation of NMDARs alone (27.62% ± 3.36, p=0.637). As seen in the other hippocampal regions, OHSCs exposed to 2 µM DOM/100 µM NMDA/10 mM choline/10 µM galantamine (41.08% ± 4.45) showed significantly increased PI levels compared to slice cultures treated with DOM alone (23.57% ± 1.85, p=0.005) or DOM, NMDA and the high dose of choline either alone or in combination with galantamine (26.24% ± 2.30 and 24.65% ± 1.42, respectively, p=0.022). Additionally, slice cultures exposed to 2 µM DOM/100 µM NMDA/10 µM galantamine showed PI uptake of 36.72% ± 3.27, which approached significance when compared to OHSCs treated with 2 µM DOM alone (p=0.052).

CONCLUSION

Compared to administration of 100 µM NMDA alone, addition of a low dose of DOM did not significantly increase PI uptake and thus cell death in any of the three hippocampal regions, suggesting that blockage of the NMDAR channel pore by Mg^{2+} ions does not prevent NMDA-mediated excitotoxicity. This further supports the conclusions drawn in Chapter 2, suggesting the involvement of glial cell death in the

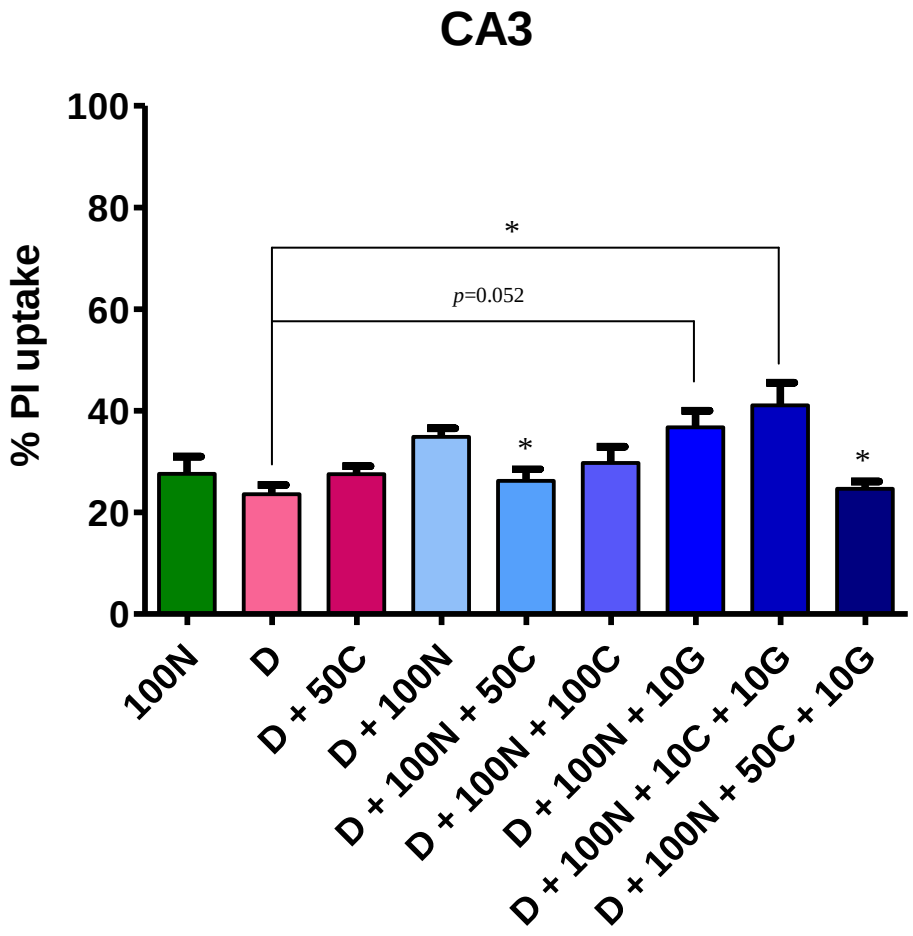

Figure C-3: Histograms show quantification of cell damage using propidium iodide (PI) in the hippocampal region CA3 of organotypic hippocampal slice cultures. Slice cultures were exposed to different combination of drugs (100 µM NMDA (100N), 2 µM domoic acid (D), 10 mM choline (10C), 50 mM choline (50C) or 100 mM choline (100C) and 10 µM galantamine (10G)) for 4 hours. PI uptake was measured after 24 hours in fresh media. Data are shown as means ± SEM, with n = 5–9. One way ANOVA followed by Tukey's post-hoc test revealed significant differences, *p<0.05 from D + 100N +10C + 10G.

maximal PI uptake measured after exposure to 70% ethanol at 4°C for 24 hours. Thus, the cell death of 50% measured after treatment with 1 mM NMDA seems to indicate 100% neuronal cell damage, as exposure to this concentration of NMDA presumably does not affect, or only minimally affects the population of glial cells

Furthermore, the general observations made in Chapter 3 are supported by these data. Despite many reports showing the neuroprotective effect of α7 nicotinic receptors, co-activation of α7 nAChR in this experimental setting using choline and/or galantamine did not seem to prevent or reduce cell damage. Rather, the highest cell death was consistently produced by exposure to 2 µM DOM/100 µM NMDA/10 mM choline/10 µM galantamine in the DG, CA1, and CA3 region. However, one of the lowest PI levels resulted from using either 2 µM DOM/100 µM NMDA/50 mM choline or 2 µM DOM/100 µM NMDA/50 mM choline/10 µM galantamine. Both of these groups exhibited a similar PI uptake to slice cultures exposed to 2 µM DOM alone.

The exact reasons for these lower PI levels are unclear. As no significant alterations were observed using NMDA alone, these observations suggest the involvement of AMPA and kainate receptors. Although interactions between α7 nAChR and AMPA/kainate receptors have not received as much attention compared to NMDARs, there are reports suggesting that α7 nAChRs can modulate the activity of AMPA and kainate receptors. For example, Arias *et al* (2016) have shown that positive allosteric modulation of α7 nAChRs weakly potentiates AMPARs. Furthermore, kainic acid-induced neurotoxicity was attenuated by activation of α7 nAChRs in rats (Shin *et al*, 2007).

However, it is unclear why a lower concentration of choline (10 mM) produces the highest level of PI uptake when combined with 2 µM DOM, 100 µM NMDA, and 10 µM galantamine, while administration of 50 mM choline combined with 2 µM DOM, 100 µM NMDA, and 10 µM galantamine consistently results in one of the lowest levels of PI uptake. Further investigations would be necessary to understand the interactions between AMPA/kainate receptors and α7 nAChRs.

APPENDIX D: IMMUNOHISTOCHEMICAL STAINING WITH NEURONAL AND ASTROCYTIC MARKERS

OBJECTIVE

In our experiments, PI uptake following exposure to NMDA seemed to plateau at about 50% of the maximal PI uptake (see Chapter 2). This observation is similar to results published by Kleczkowska *et al* (2015), whereas other publications suggest higher values of PI uptake (Kristensen *et al*, 2001). As described in Chapter 2, a possible explanation for these differences in the literature could be variations in experimental procedures, such as differences in exposure timing or culture media used. The method chosen to induce maximal cell death, as a way of standardizing the data, can also likely influence the measured PI uptake. For example, Kristensen *et al* (2001) exposed OHSCs to 50 mM Glu following drug treatment to obtain the maximum value of PI uptake, while maximal fluorescence intensity in the experiments described in this thesis was measured after 24 h low-temperature exposure to 70% ethanol. Kleczkowska *et al* (2015) chose yet another method and acquired terminal images after treatment with supramaximal concentrations of NMDA.

Organotypic slice cultures consist of both neuronal cells and glial cells. Glial cells have been shown to generally be more resistant to ischemic cell death (Goldberg and Choi, 1993). However, they are susceptible to cell death induced by ethanol or extremely high doses of NMDA (Holownia *et al*, 1997). This might explain the discrepancy in reported PI uptake after NMDA exposure if the measure of 100% cell death is based on neurons and glia combined vs neurons alone.

To investigate whether glial cell death is in fact implicated in the maximal PI uptake as reported in this thesis, slice cultures were stained with antibodies against NeuN, a neuron specific nuclear protein, and GFAP, a commonly used marker for astrocytes, to differentiate neuronal and glial populations in OHSCs.

METHODS

Preparation of organotypic hippocampal slice cultures, maintenance, and exposure procedures were as reported in Chapter 2 and Chapter 3 of this thesis. On day 13 *in vitro*, three representative OHSCs (on the same dish) were prepared for formalin fixation without any treatment. Immunohistochemical protocols were adapted from methods previously published by our laboratory (Pérez-Gómez and Tasker, 2012, 2013). After washing 3 times with 1x PBS at room temperature, the same process was repeated using 10% neutral buffered formalin. Extra formalin was added after the third wash to the top of the insert covering the slices. The slices were then left in the final formalin wash for 5 hours at 4°C. The slices were then washed again with 1x PBS, transferred to ethylene glycol solution and stored at -20°C.

Slices to be labelled were rinsed in two washes of 1x PBS for 3 minutes each to remove ethylene glycol solution. Slices were then placed in permeabilization buffer (1× PBS + 0.1% Triton X solution) overnight at 4°C, followed by incubation with blocking solution (20% BSA in 1x PBS + 0.1% Triton X) for 6 h at room temperature. They were then incubated with mouse anti-NeuN (1:500, Millipore) and rabbit anti-GFAP (1:500, Sigma) diluted in 5% goat serum in 1x PBS + 0.1% Triton X overnight at 4°C. Following

incubation with primary antibody, sections were washed in 1x PBS (3 x 10 minutes), and incubated with secondary antibody (1:200, Alexa Fluor 594-conjugated goat anti-mouse and 488-conjugated chicken anti-rabbit, Thermo Fisher Scientific) diluted in PBS containing 5% BSA for 4 h in the dark at room temperature. The sections were subsequently washed in PBS (3 × 10 minutes) in the dark, mounted on microscope slides in mounting medium (Thermo Fisher Scientific) and imaged using a LSM 710 laser scanning confocal microscope (Zeiss, Germany).

RESULTS

Figure D-1 shows a representative image of a slice culture double-labelled with the neuronal marker NeuN and the astrocytic marker GFAP.

CONCLUSION

The results suggest that approximately 50% of the cells in OHSC label with the neuronal marker NeuN, whereas the other 50% label with GFAP. In our experiments, after exposure to 1 mM NMDA about 50% cell death was measured (Figure 2-2), and most likely this value reflects 100% neuronal damage.

The ratio of neuronal and glial cells seems to vary, however, between hippocampal sub-fields possibly contributing to regional differences, although further studies to confirm this hypothesis are necessary.

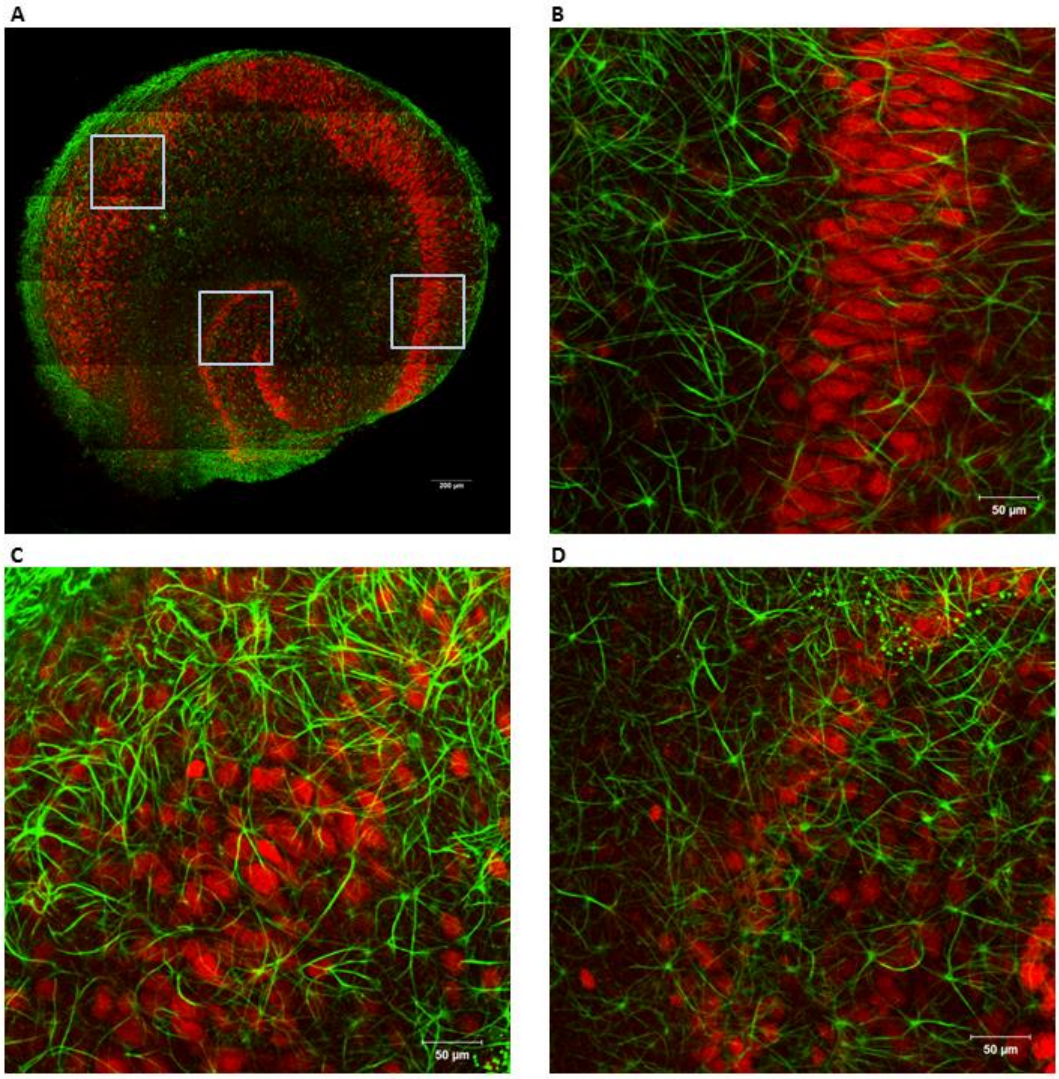

Figure D-1: Confocal images showing double staining for NeuN and GFAP in formalin fixed organotypic hippocampal slice culture at day 13 *in vitro*. (A) Representative image of whole slice with the blue boxes indicating location of magnified images for CA3 (B), CA1 (C), and dentate gyrus (D).

REFERENCES

Aarts M, Liu Y, Liu L, Besshoh S, Arundine M, Gurd JW, *et al* (2002). Treatment of ischemic brain damage by perturbing NMDA receptor- PSD-95 protein interactions. *Science* **298**: 846–50.

Abdel-Hamid KM, Tymianski M (1997). Mechanisms and effects of intracellular calcium buffering on neuronal survival in organotypic hippocampal cultures exposed to anoxia/aglycemia or to excitotoxins. *J Neurosci* **17**: 3538–53.

Adams CE, Broide RS, Chen Y, Winzer-Serhan UH, Henderson TA, Leslie FM, *et al* (2002). Development of the α7 nicotinic cholinergic receptor in rat hippocampal formation. *Dev Brain Res* **139**: 175–187.

Adamson J, Beswick A, Ebrahim S (2004). Is stroke the most common cause of disability? *J Stroke Cerebrovasc Dis* **13**: 171–7.

Adler LE, Olincy A, Waldo M, Harris JG, Griffith J, Stevens K, *et al* (1998). Schizophrenia, sensory gating, and nicotinic receptors. *Schizophr Bull* **24**: 189–202.

Ahlgren H, Henjum K, Ottersen OP, Rundén-Pran E (2011). Validation of organotypical hippocampal slice cultures as an ex vivo model of brain ischemia: different roles of NMDA receptors in cell death signalling after exposure to NMDA or oxygen and glucose deprivation. *Cell Tissue Res* **345**: 329–41.

Albuquerque EX, Pereira EFR, Alkondon M, Rogers SW (2009). Mammalian nicotinic acetylcholine receptors: from structure to function. *Physiol Rev* **89**: 73–120.

Alkondon M, Pereira EF, Barbosa CT, Albuquerque EX (1997a). Neuronal nicotinic acetylcholine receptor activation modulates gamma-aminobutyric acid release from CA1 neurons of rat hippocampal slices. *J Pharmacol Exp Ther* **283**: 1396–411.

Alkondon M, Pereira EFR, Albuquerque EX (1998). α-Bungarotoxin- and methyllycaconitine-sensitive nicotinic receptors mediate fast synaptic transmission in interneurons of rat hippocampal slices. *Brain Res* **810**: 257–263.

Alkondon M, Pereira EFR, Cartes WS, Maelicke A, Albuquerque EX (1997b). Choline is a Selective Agonist of α7 Nicotinic Acetylcholine Receptors in the Rat Brain Neurons. *Eur J Neurosci* **9**: 2734–2742.

Alkondon M, Pereira EFR, Eisenberg HM, Albuquerque EX (1999). Choline and Selective Antagonists Identify Two Subtypes of Nicotinic Acetylcholine Receptors that Modulate GABA Release from CA1 Interneurons in Rat Hippocampal Slices. *J Neurosci* **19**: 2693–2705.

Allard J, Paci P, Elst L Vander, Ris L (2015). Regional and time-dependent neuroprotective effect of hypothermia following oxygen-glucose deprivation. *Hippocampus* **25**: 197–207.

Anand R, Peng X, Lindstrom J (1993). Homomeric and native alpha 7 acetylcholine receptors exhibit remarkably similar but non-identical pharmacological properties, suggesting that the native receptor is a heteromeric protein complex. *FEBS Lett* **327**: 241–6.

Andersen P, Bliss TVP, Skrede KK (1971). Lamellar organization of hippocampal excitatory pathways. *Exp Brain Res* **13**: 222–238.

Aramakis VB, Metherate R (1998). Nicotine selectively enhances NMDA receptor-mediated synaptic transmission during postnatal development in sensory neocortex. *J Neurosci* **18**: 8485–95.

Arias E, Gallego-Sandín S, Villarroya M, García AG, López MG (2005). Unequal Neuroprotection Afforded by the Acetylcholinesterase Inhibitors Galantamine, Donepezil, and Rivastigmine in SH-SY5Y Neuroblastoma Cells: Role of Nicotinic Receptors. *J Pharmacol Exp Ther* **315**: 1346–1353.

Arias HR, Ravazzini F, Targowska-Duda KM, Kaczor AA, Feuerbach D, Boffi JC, *et al* (2016). Positive allosteric modulators of α7 nicotinic acetylcholine receptors affect neither the function of other ligand- and voltage-gated ion channels and acetylcholinesterase, nor β-amyloid content. *Int J Biochem Cell Biol* **76**: 19–30.

Armentero M-T, Fancellu R, Nappi G, Bramanti P, Blandini F (2006). Prolonged blockade of NMDA or mGluR5 glutamate receptors reduces nigrostriatal degeneration while inducing selective metabolic changes in the basal ganglia circuitry in a rodent model of Parkinson's disease. *Neurobiol Dis* **22**: 1–9.

Arnaiz-Cot JJ, González JC, Sobrado M, Baldelli P, Carbone E, Gandía L, *et al* (2008). Allosteric modulation of alpha 7 nicotinic receptors selectively depolarizes hippocampal interneurons, enhancing spontaneous GABAergic transmission. *Eur J Neurosci* **27**: 1097–110.

Arroyo-Jimenez MM, Bourgeois JP, Marubio LM, Sourd AM Le, Ottersen OP, Rinvik E, *et al* (1999). Ultrastructural localization of the alpha4-subunit of the neuronal acetylcholine nicotinic receptor in the rat substantia nigra. *J Neurosci* **19**: 6475–87.

Arundine M, Tymianski M (2003). Molecular mechanisms of calcium-dependent neurodegeneration in excitotoxicity. *Cell Calcium* **34**: 325–37.

Bahr BA, Kessler M, Rivera S, Vanderklish PW, Hall RA, Mutneja MS, *et al* (1995). Stable maintenance of glutamate receptors and other synaptic components in long-term hippocampal slices. *Hippocampus* **5**: 425–39.

Balami JS, Hadley G, Sutherland BA, Karbalai H, Buchan AM, Abou-Chebl A, *et al* (2013). The exact science of stroke thrombolysis and the quiet art of patient selection. *Brain* **136**: 3528–53.

Banerjee C, Nyengaard JR, Wevers A, Vos RAI de, Jansen Steur ENH, Lindstrom J, *et al* (2000). Cellular Expression of α7 Nicotinic Acetylcholine Receptor Protein in the Temporal Cortex in Alzheimer's and Parkinson's Disease— A Stereological Approach. *Neurobiol Dis* **7**: 666–672.

Bano D, Young KW, Guerin CJ, LeFeuvre R, Rothwell NJ, Naldini L, *et al* (2005). Cleavage of the Plasma Membrane Na+/Ca2+ Exchanger in Excitotoxicity. *Cell* **120**: 275–285.

Bartsch T, Döhring J, Reuter S, Finke C, Rohr A, Brauer H, *et al* (2015). Selective neuronal vulnerability of human hippocampal CA1 neurons: lesion evolution, temporal course, and pattern of hippocampal damage in diffusion-weighted MR imaging. *J Cereb Blood Flow Metab* **35**: 1836–45.

Baudry M, Zhu G, Liu Y, Wang Y, Briz V, Bi X (2015). Multiple cellular cascades participate in long-term potentiation and in hippocampus-dependent learning. *Brain Res* **1621**: 73–81.

Bernaudin M, Nouvelot A, MacKenzie ET, Petit E (1998). Selective neuronal vulnerability and specific glial reactions in hippocampal and neocortical organotypic cultures submitted to ischemia. *Exp Neurol* **150**: 30–9.

Bertrand D, Galzi JL, Devillers-Thiéry A, Bertrand S, Changeux JP (1993). Mutations at two distinct sites within the channel domain M2 alter calcium permeability of neuronal alpha 7 nicotinic receptor. *Proc Natl Acad Sci U S A* **90**: 6971–5.

Bhattacharya S, Haertel C, Maelicke A, Montag D (2014). Galantamine slows down plaque formation and behavioral decline in the 5XFAD mouse model of Alzheimer's disease. *PLoS One* **9**: e89454.

Biegon A, Fry PA, Paden CM, Alexandrovich A, Tsenter J, Shohami E (2004). Dynamic changes in N-methyl-D-aspartate receptors after closed head injury in mice: Implications for treatment of neurological and cognitive deficits. *Proc Natl Acad Sci U S A* **101**: 5117–22.

Biton B, Bergis OE, Galli F, Nedelec A, Lochead AW, Jegham S, *et al* (2007). SSR180711, a novel

selective alpha7 nicotinic receptor partial agonist: (1) binding and functional profile. *Neuropsychopharmacology* **32**: 1–16.

Black SM, Bedolli MA, Martinez S, Bristow JD, Ferriero DM, Soifer SJ (1995). Expression of neuronal nitric oxide synthase corresponds to regions of selective vulnerability to hypoxia-ischaemia in the developing rat brain. *Neurobiol Dis* **2**: 145–55.

Bliss T V, Lomo T (1973). Long-lasting potentiation of synaptic transmission in the dentate area of the anaesthetized rabbit following stimulation of the perforant path. *J Physiol* **232**: 331–56.

Boldyrev AA (2000). Functional interaction between various glutamate receptors. *Bull Exp Biol Med* **130**: 823–9.

Bonfoco E, Krainc D, Ankarcrona M, Nicotera P, Lipton SA (1995). Apoptosis and necrosis: two distinct events induced, respectively, by mild and intense insults with N-methyl-D-aspartate or nitric oxide/superoxide in cortical cell cultures. *Proc Natl Acad Sci U S A* **92**: 7162–6.

Bonnekoh P, Barbier A, Oschlies U, Hossmann KA (1990). Selective vulnerability in the gerbil hippocampus: morphological changes after 5-min ischemia and long survival times. *Acta Neuropathol* **80**: 18–25.

Brenneman DE, Forsythe ID, Nicol T, Nelson PG (1990). N-methyl-D-aspartate receptors influence neuronal survival in developing spinal cord cultures. *Brain Res Dev Brain Res* **51**: 63–8.

Broide RS, Robertson RT, Leslie FM (1996). Regulation of alpha7 nicotinic acetylcholine receptors in the developing rat somatosensory cortex by thalamocortical afferents. *J Neurosci* **16**: 2956–71.

Bruce AJ, Sakhi S, Schreiber SS, Baudry M (1995). Development of kainic acid and N-methyl-d-aspartic acid toxicity in organotypic hippocampal cultures. *Exp Neurol* **132**: 209–219.

Bruno V, Goldberg M, Dugan L (1994). Neuroprotective effect of hypothermia in cortical cultures exposed to oxygen- glucose deprivation or excitatory amino acids. *J* at <http://onlinelibrary.wiley.com/doi/10.1046/j.1471-4159.1994.63041398.x/full>.

Bulenger S, Marullo S, Bouvier M (2005). Emerging role of homo- and heterodimerization in G-protein-coupled receptor biosynthesis and maturation. *Trends Pharmacol Sci* **26**: 131–7.

Burghaus L, Schütz U, Krempel U, Vos RA. de, Jansen Steur EN., Wevers A, *et al* (2000). Quantitative assessment of nicotinic acetylcholine receptor proteins in the cerebral cortex of Alzheimer patients. *Mol Brain Res* **76**: 385–388.

Burnashev N, Zhou Z, Neher E, Sakmann B (1995). Fractional calcium currents through recombinant GluR channels of the NMDA, AMPA and kainate receptor subtypes. *J Physiol* 403–18at <http://www.ncbi.nlm.nih.gov/pubmed?term=fractional calcium current through recombinant glur channels of the nmda, ampa and kainate receptor subtypes&cmd=correctspelling>.

Butler TR, Berry JN, Sharrett-Field LJ, Pauly JR, Prendergast MA (2013). Long-term ethanol and corticosterone co-exposure sensitize the hippocampal ca1 region pyramidal cells to insult during ethanol withdrawal in an NMDA GluN2B subunit-dependent manner. *Alcohol Clin Exp Res* **37**: 2066–73.

Butler TR, Self RL, Smith KJ, Sharrett-Field LJ, Berry JN, Littleton JM, *et al* (2010). Selective vulnerability of hippocampal cornu ammonis 1 pyramidal cells to excitotoxic insult is associated with the expression of polyamine-sensitive N-methyl-D-asparate-type glutamate receptors. *Neuroscience* **165**: 525–34.

Campeau JL, Wu G, Bell JR, Rasmussen J, Sim VL (2013). Early increase and late decrease of purkinje cell dendritic spine density in prion-infected organotypic mouse cerebellar cultures. *PLoS One* **8**:

e81776.

Chalifoux JR, Carter AG (2010). GABAB receptors modulate NMDA receptor calcium signals in dendritic spines. *Neuron* **66**: 101–13.

Chen H, Yoshioka H, Kim GS, Jung JE, Okami N, Sakata H, *et al* (2011). Oxidative stress in ischemic brain damage: mechanisms of cell death and potential molecular targets for neuroprotection. *Antioxid Redox Signal* **14**: 1505–17.

Chen L, Huang LY (1992). Protein kinase C reduces Mg2+ block of NMDA-receptor channels as a mechanism of modulation. *Nature* **356**: 521–3.

Chen N, Luo T, Raymond LA (1999). Subtype-dependence of NMDA receptor channel open probability. *J Neurosci* **19**: 6844–54.

Cheng Q, Yakel JL (2014). Presynaptic α7 nicotinic acetylcholine receptors enhance hippocampal mossy fiber glutamatergic transmission via PKA activation. *J Neurosci* **34**: 124–33.

Cheng Q, Yakel JL (2015). The effect of α7 nicotinic receptor activation on glutamatergic transmission in the hippocampus. *Biochem Pharmacol* **97**: 439–44.

Cho C-H, Song W, Leitzell K, Teo E, Meleth AD, Quick MW, *et al* (2005). Rapid Upregulation of 7 Nicotinic Acetylcholine Receptors by Tyrosine Dephosphorylation. *J Neurosci* **25**: 3712–3723.

Cho S, Wood A, Bowlby MR (2007). Brain slices as models for neurodegenerative disease and screening platforms to identify novel therapeutics. *Curr Neuropharmacol* **5**: 19–33.

Choi DW (1985). Glutamate neurotoxicity in cortical cell culture is calcium dependent. *Neurosci Lett* **58**: 293–7.

Choi DW (1987). Ionic dependence of glutamate neurotoxicity. *J Neurosci* **7**: 369–79.

Cincotta SL, Yorek MS, Moschak TM, Lewis SR, Rodefer JS (2008). Selective nicotinic acetylcholine receptor agonists: potential therapies for neuropsychiatric disorders with cognitive dysfunction. *Curr Opin Investig Drugs* **9**: 47–56.

Colović MB, Krstić DZ, Lazarević-Pašti TD, Bondžić AM, Vasić VM (2013). Acetylcholinesterase inhibitors: pharmacology and toxicology. *Curr Neuropharmacol* **11**: 315–35.

Conejero-Goldberg C, Davies P, Ulloa L (2008). Alpha7 nicotinic acetylcholine receptor: a link between inflammation and neurodegeneration. *Neurosci Biobehav Rev* **32**: 693–706.

Cook DJ, Teves L, Tymianski M (2012). Treatment of stroke with a PSD-95 inhibitor in the gyrencephalic primate brain. *Nature* **483**: 213–217.

Corlew R, Brasier DJ, Feldman DE, Philpot BD (2008). Presynaptic NMDA receptors: newly appreciated roles in cortical synaptic function and plasticity. *Neuroscientist* **14**: 609–25.

Cormier A, Morin C, Zini R, Tillement J-P, Lagrue G (2003). Nicotine protects rat brain mitochondria against experimental injuries. *Neuropharmacology* **44**: 642–652.

Costa LG, Giordano G, Faustman EM (2010). Domoic acid as a developmental neurotoxin. *Neurotoxicology* **31**: 409–423.

Cottrell JR, Dubé GR, Egles C, Liu G (2000). Distribution, density, and clustering of functional glutamate receptors before and after synaptogenesis in hippocampal neurons. *J Neurophysiol* **84**: 1573–87.

Coultrap SJ, Nixon KM, Alvestad RM, Valenzuela CF, Browning MD (2005). Differential expression of

NMDA receptor subunits and splice variants among the CA1, CA3 and dentate gyrus of the adult rat. *Brain Res Mol Brain Res* **135**: 104–11.

Couturier S, Bertrand D, Matter JM, Hernandez MC, Bertrand S, Millar N, *et al* (1990). A neuronal nicotinic acetylcholine receptor subunit (alpha 7) is developmentally regulated and forms a homo-oligomeric channel blocked by alpha-BTX. *Neuron* **5**: 847–56.

Cull-Candy S, Brickley S, Farrant M (2001). NMDA receptor subunits: diversity, development and disease. *Curr Opin Neurobiol* **11**: 327–35.

Dajas-Bailador FA, Mogg AJ, Wonnacott S (2002a). Intracellular Ca2+ signals evoked by stimulation of nicotinic acetylcholine receptors in SH-SY5Y cells: contribution of voltage-operated Ca2+ channels and Ca2+ stores. *J Neurochem* **81**: 606–614.

Dajas-Bailador FA, Soliakov L, Wonnacott S (2002b). Nicotine activates the extracellular signal-regulated kinase 1/2 via the alpha7 nicotinic acetylcholine receptor and protein kinase A, in SH-SY5Y cells and hippocampal neurones. *J Neurochem* **80**: 520–530.

Dani JA, Bertrand D (2007). Nicotinic acetylcholine receptors and nicotinic cholinergic mechanisms of the central nervous system. *Annu Rev Pharmacol Toxicol* **47**: 699–729.

Danysz W, Parsons CG (2012). Alzheimer's disease, β-amyloid, glutamate, NMDA receptors and memantine--searching for the connections. *Br J Pharmacol* **167**: 324–52.

Deardorff WJ, Feen E, Grossberg GT (2015). The Use of Cholinesterase Inhibitors Across All Stages of Alzheimer's Disease. *Drugs Aging* **32**: 537–47.

De Simoni, Griesinger CB, Edwards FA (2003). Development of rat CA1 neurones in acute versus organotypic slices: role of experience in synaptic morphology and activity. *J Physiol* **550**: 135–47.

Dirnagl U (2012). Pathobiology of injury after stroke: the neurovascular unit and beyond. *Ann N Y Acad Sci* **1268**: 21–5.

Dirnagl U, Endres M (2014). Found in translation: preclinical stroke research predicts human pathophysiology, clinical phenotypes, and therapeutic outcomes. *Stroke* **45**: 1510–8.

Dirnagl U, Iadecola C, Moskowitz MA (1999). Pathobiology of ischaemic stroke: an integrated view. *Trends Neurosci* **22**: 391–7.

Do KQ, Herrling PL, Streit P, Turski WA, Cuenod M (1986). In vitro release and electrophysiological effects in situ of homocysteic acid, an endogenous N-methyl-(D)-aspartic acid agonist, in the mammalian striatum. *J Neurosci* **6**: 2226–34.

Dong X, Wang Y, Qin Z (2009). Molecular mechanisms of excitotoxicity and their relevance to pathogenesis of neurodegenerative diseases. *Acta Pharmacol Sin* **30**: 379–387.

Doyle KP, Simon RP, Stenzel-Poore MP (2008). Mechanisms of ischemic brain damage. *Neuropharmacology* **55**: 310–318.

Durukan A, Tatlisumak T (2007). Acute ischemic stroke: overview of major experimental rodent models, pathophysiology, and therapy of focal cerebral ischemia. *Pharmacol Biochem Behav* **87**: 179–97.

Egea J, Martín-de-Saavedra MD, Parada E, Romero A, Barrio L del, Rosa AO, *et al* (2012). Galantamine elicits neuroprotection by inhibiting iNOS, NADPH oxidase and ROS in hippocampal slices stressed with anoxia/reoxygenation. *Neuropharmacology* **62**: 1082–1090.

Egea J, Rosa AO, Sobrado M, Gandía L, López MG, García AG (2007). Neuroprotection afforded by nicotine against oxygen and glucose deprivation in hippocampal slices is lost in α7 nicotinic receptor

knockout mice. *Neuroscience* **145**: 866–872.

Erreger K, Dravid SM, Banke TG, Wyllie DJA, Traynelis SF (2005). Subunit-specific gating controls rat NR1/NR2A and NR1/NR2B NMDA channel kinetics and synaptic signalling profiles. *J Physiol* **563**: 345–58.

Eyüpoglu IY, Savaskan NE, Bräuer AU, Nitsch R, Heimrich B (2003). Identification of neuronal cell death in a model of degeneration in the hippocampus. *Brain Res Protoc* **11**: 1–8.

Fabian-Fine R, Skehel P, Errington ML, Davies HA, Sher E, Stewart MG, *et al* (2001). Ultrastructural distribution of the alpha7 nicotinic acetylcholine receptor subunit in rat hippocampus. *J Neurosci* **21**: 7993–8003.

Faden AI, Demediuk P, Panter SS, Vink R (1989). The role of excitatory amino acids and NMDA receptors in traumatic brain injury. *Science* **244**: 798–800.

Fayuk D, Yakel JL (2005). Ca2+ permeability of nicotinic acetylcholine receptors in rat hippocampal CA1 interneurones. *J Physiol* **566**: 759–768.

Ferchmin PA, Perez D, Eterovic VA, Vellis J de (2003). Nicotinic receptors differentially regulate N-methyl-D-aspartate damage in acute hippocampal slices. *J Pharmacol Exp Ther* **305**: 1071–8.

Ferrante RJ, Kowall NW, Cipolloni PB, Storey E, Beal MF (1993). Excitotoxin Lesions in Primates as a Model for Huntington's Disease: Histopathologic and Neurochemical Characterization. *Exp Neurol* **119**: 46–71.

Fisher JL, Dani JA (2000). Nicotinic receptors on hippocampal cultures can increase synaptic glutamate currents while decreasing the NMDA-receptor component. *Neuropharmacology* **39**: 2756–2769.

Fotakis G, Timbrell JA (2006). In vitro cytotoxicity assays: Comparison of LDH, neutral red, MTT and protein assay in hepatoma cell lines following exposure to cadmium chloride. *Toxicol Lett* **160**: 171–177.

Freedman R, Hall M, Adler LE, Leonard S (1995). Evidence in postmortem brain tissue for decreased numbers of hippocampal nicotinic receptors in schizophrenia. *Biol Psychiatry* **38**: 22–33.

Friberg H, Connern C, Halestrap AP, Wieloch T (1999). Differences in the activation of the mitochondrial permeability transition among brain regions in the rat correlate with selective vulnerability. *J Neurochem* **72**: 2488–97.

Fujii S, Ji Z, Morita N, Sumikawa K (1999). Acute and chronic nicotine exposure differentially facilitate the induction of LTP. *Brain Res* **846**: 137–143.

Gähwiler BH (1981). Organotypic monolayer cultures of nervous tissue. *J Neurosci Methods* **4**: 329–42.

Gähwiler BH, Capogna M, Debanne D, McKinney RA, Thompson SM (1997). Organotypic slice cultures: a technique has come of age. *Trends Neurosci* **20**: 471–7.

Gambrill AC, Barria A (2011). NMDA receptor subunit composition controls synaptogenesis and synapse stabilization. *Proc Natl Acad Sci U S A* **108**: 5855–60.

Garcia de Arriba S, Wegner F, Grüner K, Verdaguer E, Pallas M, Camins A, *et al* (2006). Different capacities of various NMDA receptor antagonists to prevent ischemia-induced neurodegeneration in human cultured NT2 neurons. *Neurochem Int* **49**: 466–474.

Ge S, Dani JA (2005). Nicotinic Acetylcholine Receptors at Glutamate Synapses Facilitate Long-Term Depression or Potentiation. *J Neurosci* **25**: 6084–6091.

Gee CE, Benquet P, Raineteau O, Rietschin L, Kirbach SW, Gerber U (2006). NMDA receptors and the differential ischemic vulnerability of hippocampal neurons. *Eur J Neurosci* **23**: 2595–603.

Gerace E, Landucci E, Scartabelli T, Moroni F, Pellegrini-Giampietro DE (2012). Rat hippocampal slice culture models for the evaluation of neuroprotective agents. *Methods Mol Biol* **846**: 343–54.

Ginsberg MD (2008). Neuroprotection for ischemic stroke: past, present and future. *Neuropharmacology* **55**: 363–89.

Girod R, Barazangi N, McGehee D, Role LW (2000). Facilitation of glutamatergic neurotransmission by presynaptic nicotinic acetylcholine receptors. *Neuropharmacology* **39**: 2715–2725.

Gladding CM, Raymond LA (2011). Mechanisms underlying NMDA receptor synaptic/extrasynaptic distribution and function. *Mol Cell Neurosci* **48**: 308–20.

Go AS, Mozaffarian D, Roger VL, Benjamin EJ, Berry JD, Borden WB, *et al* (2013). Heart disease and stroke statistics--2013 update: a report from the American Heart Association. *Circulation* **127**: e6–e245.

Goldberg MP, Choi DW (1993). Combined oxygen and glucose deprivation in cortical cell culture: calcium-dependent and calcium-independent mechanisms of neuronal injury. *J Neurosci* **13**: 3510–24.

Gotoh O, Asano T, Koide T, Takakura K (1985). Ischemic brain edema following occlusion of the middle cerebral artery in the rat. I: The time courses of the brain water, sodium and potassium contents and blood-brain barrier permeability to 125I-albumin. *Stroke* **16**: 101–109.

Graulich J, Hoffmann U, Maier RF, Ruscher K, Pomper JK, Ko H-K, *et al* (2002). Acute neuronal injury after hypoxia is influenced by the reoxygenation mode in juvenile hippocampal slice cultures. *Brain Res Dev Brain Res* **137**: 35–42.

Gray R, Rajan AS, Radcliffe KA, Yakehiro M, Dani JA (1996). Hippocampal synaptic transmission enhanced by low concentrations of nicotine. *Nature* **383**: 713–6.

Gregersen M, Lee DH, Gabatto P, Bickler PE (2013). Limitations of Mild, Moderate, and Profound Hypothermia in Protecting Developing Hippocampal Neurons After Simulated Ischemia. *Ther Hypothermia Temp Manag* **3**: 178–188.

Guerra-Álvarez M, Moreno-Ortega AJ, Navarro E, Fernández-Morales JC, Egea J, López MG, *et al* (2015). Positive allosteric modulation of alpha-7 nicotinic receptors promotes cell death by inducing Ca(2+) release from the endoplasmic reticulum. *J Neurochem* **133**: 309–19.

Guo JZ, Tredway TL, Chiappinelli VA (1998). Glutamate and GABA release are enhanced by different subtypes of presynaptic nicotinic receptors in the lateral geniculate nucleus. *J Neurosci* **18**: 1963–9.

Guthrie KM, Tran A, Baratta J, Yu J, Robertson RT (2005). Patterns of afferent projections to the dentate gyrus studied in organotypic co-cultures. *Dev Brain Res* **157**: 162–171.

Gutiérrez R, Heinemann U (1999). Synaptic reorganization in explanted cultures of rat hippocampus. *Brain Res* **815**: 304–16.

Guy Y, Rupert AE, Sandberg M, Weber SG (2011). A simple method for measuring organotypic tissue slice culture thickness. *J Neurosci Methods* **199**: 78–81.

Hardingham GE, Bading H (2003). The Yin and Yang of NMDA receptor signalling. *Trends Neurosci* **26**: 81–9.

Hardingham GE, Bading H (2010). Synaptic versus extrasynaptic NMDA receptor signalling: implications

for neurodegenerative disorders. *Nat Rev Neurosci* **11**: 682–96.

Hardingham GE, Fukunaga Y, Bading H (2002). Extrasynaptic NMDARs oppose synaptic NMDARs by triggering CREB shut-off and cell death pathways. *Nat Neurosci* **5**: 405–14.

Hatanpaa K, Raisanen J, Herndon E, Burns D, Foong C, Habib A, *et al* (2014). Hippocampal sclerosis in dementia, epilepsy, and ischemic injury: differential vulnerability of hippocampal subfields. *J Neuropathol Exp Neurol* **73**: 136–42.

Hazell AS (2007). Excitotoxic mechanisms in stroke: An update of concepts and treatment strategies. *Neurochem Int* **50**: 941–953.

Hellström-Lindahl E, Mousavi M, Zhang X, Ravid R, Nordberg A (1999). Regional distribution of nicotinic receptor subunit mRNAs in human brain: comparison between Alzheimer and normal brain. *Brain Res Mol Brain Res* **66**: 94–103.

Hermans E, Challiss RAJ (2001). Structural, signaling and regulatory properties of the group I metabotropic glutamate receptors: prototypic family C G-protein-coupled receptors. *Biochem J* **359**: 465–484.

Hertz L (2008). Bioenergetics of cerebral ischemia: A cellular perspective. *Neuropharmacology* **55**: 289–309.

Hezel M, Ebrahimi F, Koch M, Dehghani F (2012). Propidium iodide staining: a new application in fluorescence microscopy for analysis of cytoarchitecture in adult and developing rodent brain. *Micron* **43**: 1031–8.

Hill JA, Zoli M, Bourgeois JP, Changeux JP (1993). Immunocytochemical localization of a neuronal nicotinic receptor: the beta 2-subunit. *J Neurosci* **13**: 1551–68.

Hill MD, Martin RH, Mikulis D, Wong JH, Silver FL, terBrugge KG, *et al* (2012). Safety and efficacy of NA-1 in patients with iatrogenic stroke after endovascular aneurysm repair (ENACT): a phase 2, randomised, double-blind, placebo-controlled trial. *Lancet Neurol* **11**: 942–950.

Hogins J, Crawford DC, Zorumski CF, Mennerick S (2011). Excitotoxicity triggered by Neurobasal culture medium. *PLoS One* **6**: e25633.

Holownia A, Ledig M, Ménez J-F (1997). Ethanol-induced cell death in cultured rat astroglia. *Neurotoxicol Teratol* **19**: 141–146.

Humpel C (2015a). Organotypic vibrosections from whole brain adult Alzheimer mice (overexpressing amyloid-precursor-protein with the Swedish-Dutch-Iowa mutations) as a model to study clearance of beta-amyloid plaques. *Front Aging Neurosci* **7**: 47.

Humpel C (2015b). Organotypic brain slice cultures: A review. *Neuroscience* **305**: 86–98.

Hunter BE, Fiebre CM de, Papke RL, Kem WR, Meyer EM (1994). A novel nicotinic agonist facilitates induction of long-term potentiation in the rat hippocampus. *Neurosci Lett* **168**: 130–134.

Hurst R, Rollema H, Bertrand D (2013). Nicotinic acetylcholine receptors: from basic science to therapeutics. *Pharmacol Ther* **137**: 22–54.

Ikegaya Y, Matsuki N (2002). Regionally selective neurotoxicity of NMDA and colchicine is independent of hippocampal neural circuitry. *Neuroscience* **113**: 253–6.

Ikonomidou C, Turski L (2002). Why did NMDA receptor antagonists fail clinical trials for stroke and traumatic brain injury? *Lancet Neurol* **1**: 383–386.

Ivanov A, Pellegrino C, Rama S, Dumalska I, Salyha Y, Ben-Ari Y, *et al* (2006). Opposing role of synaptic and extrasynaptic NMDA receptors in regulation of the extracellular signal-regulated kinases (ERK) activity in cultured rat hippocampal neurons. *J Physiol* **572**: 789–98.

Jäderstad LM, Jäderstad J, Herlenius E (2010). Graft and host interactions following transplantation of neural stem cells to organotypic striatal cultures. *Regen Med* **5**: 901–17.

Jantas D, Szymanska M, Budziszewska B, Lason W (2009). An involvement of BDNF and PI3-K/Akt in the anti-apoptotic effect of memantine on staurosporine-evoked cell death in primary cortical neurons. *Apoptosis* **14**: 900–912.

Jarrard LE, Meldrum BS (1993). Selective excitotoxic pathology in the rat hippocampus. *Neuropathol Appl Neurobiol* **19**: 381–9.

Julio-Pieper M, Flor PJ, Dinan TG, Cryan JF (2011). Exciting Times beyond the Brain: Metabotropic Glutamate Receptors in Peripheral and Non-Neural Tissues. *Pharmacol Rev* **63**: 35–58.

Kalia L V, Kalia SK, Salter MW (2008). NMDA receptors in clinical neurology: excitatory times ahead. *Lancet Neurol* **7**: 742–55.

Kang WH, Morrison B (2015). Predicting changes in cortical electrophysiological function after in vitro traumatic brain injury. *Biomech Model Mechanobiol* **14**: 1033–1044.

Kasof GM, Mahanty NK, Pozzo Miller LD, Curran T, Connor JA, Morgan JI (1995). Spontaneous and evoked glutamate signalling influences Fos-lacZ expression and pyramidal cell death in hippocampal slice cultures from transgenic rats. *Brain Res Mol Brain Res* **34**: 197–208.

Katayama T, Kobayashi H, Okamura T, Yamasaki-Katayama Y, Kibayashi T, Kimura H, *et al* (2012). Accumulating microglia phagocytose injured neurons in hippocampal slice cultures: involvement of p38 MAP kinase. *PLoS One* **7**: e40813.

Kawai H, Lazar R, Metherate R (2007). Nicotinic control of axon excitability regulates thalamocortical transmission. *Nat Neurosci* **10**: 1168–75.

Kawamata J, Shimohama S (2011). Stimulating nicotinic receptors trigger multiple pathways attenuating cytotoxicity in models of Alzheimer's and Parkinson's diseases. *J Alzheimer's Dis* **24 Suppl 2**: 95–109.

Kihara T, Shimohama S, Sawada H, Honda K, Nakamizo T, Shibasaki H, *et al* (2001). alpha 7 nicotinic receptor transduces signals to phosphatidylinositol 3-kinase to block A beta-amyloid-induced neurotoxicity. *J Biol Chem* **276**: 13541–6.

Kihara T, Shimohama S, Sawada H, Kimura J, Kume T, Kochiyama H, *et al* (1997). Nicotinic receptor stimulation protects neurons against beta-amyloid toxicity. *Ann Neurol* **42**: 159–163.

Kim E, Sheng M (2004). PDZ domain proteins of synapses. *Nat Rev Neurosci* **5**: 771–81.

Kim UJ, Won R, Lee KH (2015). Neuroprotective effects of okadaic acid following oxidative injury in organotypic hippocampal slice culture. *Brain Res* **1618**: 241–8.

Kleczkowska P, Kawalec M, Bujalska-Zadrozny M, Filip M, Zablocka B, Lipkowski AW (2015). Effects of the Hybridization of Opioid and Neurotensin Pharmacophores on Cell Survival in Rat Organotypic Hippocampal Slice Cultures. *Neurotox Res* **28**: 352–360.

Klein J, Köppen A, Löffelholz K (1998). Regulation of free choline in rat brain: dietary and pharmacological manipulations. *Neurochem Int* **32**: 479–485.

Kosuge Y, Imai T, Kawaguchi M, Kihara T, Ishige K, Ito Y (2008). Subregion-specific vulnerability to

endoplasmic reticulum stress-induced neurotoxicity in rat hippocampal neurons. *Neurochem Int* **52**: 1204–11.

Koukouli F, Maskos U (2015). The multiple roles of the α7 nicotinic acetylcholine receptor in modulating glutamatergic systems in the normal and diseased nervous system. *Biochem Pharmacol* **97**: 378–387.

Kreutz F, Frozza RL, Breier AC, Oliveira VA de, Horn AP, Pettenuzzo LF, *et al* (2011). Amyloid-β induced toxicity involves ganglioside expression and is sensitive to GM1 neuroprotective action. *Neurochem Int* **59**: 648–55.

Kristensen BW, Noraberg J, Zimmer J (2001). Comparison of excitotoxic profiles of ATPA, AMPA, KA and NMDA in organotypic hippocampal slice cultures. *Brain Res* **917**: 21–44.

Laake JH, Haug F-M, Wieloch T, Ottersen OP (1999). A simple in vitro model of ischemia based on hippocampal slice cultures and propidium iodide fluorescence. *Brain Res Protoc* **4**: 173–184.

Lai TW, Zhang S, Wang YT (2014). Excitotoxicity and stroke: Identifying novel targets for neuroprotection. *Prog Neurobiol* **115C**: 157–188.

Laube B, Hirai H, Sturgess M, Betz H, Kuhse J (1997). Molecular determinants of agonist discrimination by NMDA receptor subunits: analysis of the glutamate binding site on the NR2B subunit. *Neuron* **18**: 493–503.

Laudenbach V, Medja F, Zoli M, Rossi FM, Evrard P, Changeux J-P, *et al* (2002). Selective activation of central subtypes of the nicotinic acetylcholine receptor has opposite effects on neonatal excitotoxic brain injuries. *FASEB J* **16**: 423–5.

Lavenex P, Sugden SG, Davis RR, Gregg JP, Lavenex PB (2011). Developmental regulation of gene expression and astrocytic processes may explain selective hippocampal vulnerability. *Hippocampus* **21**: 142–9.

Lee FJS, Xue S, Pei L, Vukusic B, Chéry N, Wang Y, *et al* (2002). Dual regulation of NMDA receptor functions by direct protein-protein interactions with the dopamine D1 receptor. *Cell* **111**: 219–30.

Lee JM, Grabb MC, Zipfel GJ, Choi DW (2000). Brain tissue responses to ischemia. *J Clin Invest* **106**: 723–31.

Levin E., Bradley A, Addy N, Sigurani N (2002). Hippocampal α7 and α4β2 nicotinic receptors and working memory. *Neuroscience* **109**: 757–765.

Li S, Li Z, Pei L, Le AD, Liu F (2012). The α7nACh-NMDA receptor complex is involved in cue-induced reinstatement of nicotine seeking. *J Exp Med* **209**: 2141–7.

Li S, Nai Q, Lipina T V, Roder JC, Liu F (2013). α7nAchR/NMDAR coupling affects NMDAR function and object recognition. *Mol Brain* **6**: 58.

Li S, Wong AHC, Liu F (2014). Ligand-gated ion channel interacting proteins and their role in neuroprotection. *Front Cell Neurosci* **8**: 125.

Li Y, Papke RL, He Y-J, Millard WJ, Meyer EM (1999). Characterization of the neuroprotective and toxic effects of α7 nicotinic receptor activation in PC12 cells. *Brain Res* **830**: 218–225.

Lin H, Vicini S, Hsu F-C, Doshi S, Takano H, Coulter DA, *et al* (2010). Axonal 7 nicotinic ACh receptors modulate presynaptic NMDA receptor expression and structural plasticity of glutamatergic presynaptic boutons. *Proc Natl Acad Sci* **107**: 16661–16666.

Lipton P (1999). Ischemic cell death in brain neurons. *Physiol Rev* **79**: 1431–568.

Lipton SA, Nakanishi N (1999). Shakespeare in love--with NMDA receptors? *Nat Med* **5**: 270–1.

Liu Q, Huang Y, Xue F, Simard A, DeChon J, Li G, *et al* (2009). A Novel Nicotinic Acetylcholine Receptor Subtype in Basal Forebrain Cholinergic Neurons with High Sensitivity to Amyloid Peptides. *J Neurosci* **29**: 918–929.

Liu R, Liu W, Doctrow SR, Baudry M (2003). Iron toxicity in organotypic cultures of hippocampal slices: role of reactive oxygen species. *J Neurochem* **85**: 492–502.

Liu Y, Wong TP, Aarts M, Rooyakkers A, Liu L, Lai TW, *et al* (2007). NMDA receptor subunits have differential roles in mediating excitotoxic neuronal death both in vitro and in vivo. *J Neurosci* **27**: 2846–57.

Lossi L, Alasia S, Salio C, Merighi A (2009). Cell death and proliferation in acute slices and organotypic cultures of mammalian CNS. *Prog Neurobiol* **88**: 221–45.

Lutz JA, Carter M, Fields L, Barron S, Littleton JM (2015). The Dietary Flavonoid Rhamnetin Inhibits Both Inflammation and Excitotoxicity During Ethanol Withdrawal in Rat Organotypic Hippocampal Slice Cultures. *Alcohol Clin Exp Res* **39**: 2345–53.

Maelicke A, Albuquerque E (1996). New approach to drug therapy in Alzheimer's dementia Alfred Maelicke and Edson X. Albuquerque. *Drug Discov Today* **1**: 53–59.

Mandelzys A, Koninck P De, Cooper E (1995). Agonist and toxin sensitivities of ACh-evoked currents on neurons expressing multiple nicotinic ACh receptor subunits. *J Neurophysiol* **74**: 1212–21.

Margaill I, Parmentier S, Callebert J, Allix M, Boulu RG, Plotkine M (1996). Short therapeutic window for MK-801 in transient focal cerebral ischemia in normotensive rats. *J Cereb Blood Flow Metab* **16**: 107–13.

Martin EJ, Panickar KS, King MA, Deyrup M, Hunter BE, Wang G, *et al* (1994). Cytoprotective actions of 2,4-dimethoxybenzylidene anabaseine in differentiated PC12 cells and septal cholinergic neurons. *Drug Dev Res* **31**: 135–141.

Massey P V, Johnson BE, Moult PR, Auberson YP, Brown MW, Molnar E, *et al* (2004). Differential roles of NR2A and NR2B-containing NMDA receptors in cortical long-term potentiation and long-term depression. *J Neurosci* **24**: 7821–8.

Mayer S, Harris BR, Gibson DA, Blanchard JA, Prendergast MA, Holley RC, *et al* (2002). Acamprosate, MK-801, and ifenprodil inhibit neurotoxicity and calcium entry induced by ethanol withdrawal in organotypic slice cultures from neonatal rat hippocampus. *Alcohol Clin Exp Res* **26**: 1468–78.

Mazzone GL, Mladinic M, Nistri A (2013). Excitotoxic cell death induces delayed proliferation of endogenous neuroprogenitor cells in organotypic slice cultures of the rat spinal cord. *Cell Death Dis* **4**: e902.

McGehee DS, Heath MJ, Gelber S, Devay P, Role LW (1995). Nicotine enhancement of fast excitatory synaptic transmission in CNS by presynaptic receptors. *Science* **269**: 1692–6.

Medeiros R, Castello NA, Cheng D, Kitazawa M, Baglietto-Vargas D, Green KN, *et al* (2014). α7 Nicotinic Receptor Agonist Enhances Cognition in Aged 3xTg-AD Mice with Robust Plaques and Tangles. *Am J Pathol* **184**: 520–529.

Mehta A, Prabhakar M, Kumar P, Deshmukh R, Sharma PL (2013). Excitotoxicity: bridge to various triggers in neurodegenerative disorders. *Eur J Pharmacol* **698**: 6–18.

Meldrum BS (2000). Glutamate as a neurotransmitter in the brain: review of physiology and pathology. *J Nutr* **130**: 1007S–15S.

Mielke JG, Mealing GAR (2009). Cellular distribution of the nicotinic acetylcholine receptor α7 subunit in rat hippocampus. *Neurosci Res* **65**: 296–306.

Miguel-Hidalgo J., Alvarez X., Cacabelos R, Quack G (2002). Neuroprotection by memantine against neurodegeneration induced by β-amyloid(1–40). *Brain Res* **958**: 210–221.

Mike A, Castro NG, Albuquerque EX (2000). Choline and acetylcholine have similar kinetic properties of activation and desensitization on the α7 nicotinic receptors in rat hippocampal neurons. *Brain Res* **882**: 155–168.

Minnerup J, Sutherland BA, Buchan AM, Kleinschnitz C (2012). Neuroprotection for stroke: current status and future perspectives. *Int J Mol Sci* **13**: 11753–72.

Monaghan DT, Cotman CW (1985). Distribution of N-methyl-D-aspartate-sensitive L-[3H]glutamate-binding sites in rat brain. *J Neurosci* **5**: 2909–19.

Monyer H, Burnashev N, Laurie DJ, Sakmann B, Seeburg PH (1994). Developmental and regional expression in the rat brain and functional properties of four NMDA receptors. *Neuron* **12**: 529–40.

Moretti A, Ferrari F, Villa RF (2015). Neuroprotection for ischaemic stroke: current status and challenges. *Pharmacol Ther* **146**: 23–34.

Moriyoshi K, Masu M, Ishii T, Shigemoto R, Mizuno N, Nakanishi S (1991). Molecular cloning and characterization of the rat NMDA receptor. *Nature* **354**: 31–7.

Morris RG (1989). Synaptic plasticity and learning: selective impairment of learning rats and blockade of long-term potentiation in vivo by the N-methyl-D-aspartate receptor antagonist AP5. *J Neurosci* **9**: 3040–57.

Mowrey DD, Liu Q, Bondarenko V, Chen Q, Seyoum E, Xu Y, *et al* (2013). Insights into distinct modulation of α7 and α7β2 nicotinic acetylcholine receptors by the volatile anesthetic isoflurane. *J Biol Chem* **288**: 35793–800.

Mozaffarian D, Benjamin EJ, Go AS, Arnett DK, Blaha MJ, Cushman M, *et al* (2016). Heart Disease and Stroke Statistics-2016 Update: A Report From the American Heart Association. *Circulation* **133**: e38–60.

Mulholland PJ, Self RL, Harris BR, Littleton JM, Prendergast MA (2004). Choline exposure reduces potentiation of N-methyl-D-aspartate toxicity by corticosterone in the developing hippocampus. *Brain Res Dev Brain Res* **153**: 203–11.

Murray TA, Bertrand D, Papke RL, George AA, Pantoja R, Srinivasan R, *et al* (2012). α7β2 nicotinic acetylcholine receptors assemble, function, and are activated primarily via their α7-α7 interfaces. *Mol Pharmacol* **81**: 175–88.

Navarro E, Buendia I, Parada E, León R, Jansen-Duerr P, Pircher H, *et al* (2015). Alpha7 nicotinic receptor activation protects against oxidative stress via heme-oxygenase I induction. *Biochem Pharmacol* **97**: 473–481.

Neumar RW (2000). Molecular mechanisms of ischemic neuronal injury. *Ann Emerg Med* **36**: 483–506.

Newell DW, Barth A, Papermaster V, Malouf AT (1995). Glutamate and non-glutamate receptor mediated toxicity caused by oxygen and glucose deprivation in organotypic hippocampal cultures. *J Neurosci* **15**: 7702–11.

Newell DW, Malouf AT, Franck JE (1990). Glutamate-mediated selective vulnerability to ischemia is present in organotypic cultures of hippocampus. *Neurosci Lett* **116**: 325–30.

Ng HJ, Whittemore ER, Tran MB, Hogenkamp DJ, Broide RS, Johnstone TB, *et al* (2007). Nootropic alpha7 nicotinic receptor allosteric modulator derived from GABAA receptor modulators. *Proc Natl Acad Sci U S A* **104**: 8059–64.

Noraberg J, Kristensen BW, Zimmer J (1999). Markers for neuronal degeneration in organotypic slice cultures. *Brain Res Protoc* **3**: 278–290.

Noraberg J, Poulsen FR, Blaabjerg M, Kristensen BW, Bonde C, Montero M, *et al* (2005). Organotypic hippocampal slice cultures for studies of brain damage, neuroprotection and neurorepair. *Curr Drug Targets CNS Neurol Disord* **4**: 435–52.

Norenberg MD, Rao KVR (2007). The mitochondrial permeability transition in neurologic disease. *Neurochem Int* **50**: 983–997.

O'Collins VE, Macleod MR, Donnan GA, Horky LL, Worp BH van der, Howells DW (2006). 1,026 experimental treatments in acute stroke. *Ann Neurol* **59**: 467–77.

Olincy A, Harris J, Johnson L, Pender V, Kongs S, Allensworth D, *et al* (2006). Proof-of-concept trial of an alpha7 nicotinic agonist in schizophrenia. *Arch Gen Psychiatry* **63**: 630–8.

Olney JW (1969). Brain lesions, obesity, and other disturbances in mice treated with monosodium glutamate. *Science* **164**: 719–21.

Ouyang Y-B, Voloboueva LA, Xu L-J, Giffard RG (2007). Selective dysfunction of hippocampal CA1 astrocytes contributes to delayed neuronal damage after transient forebrain ischemia. *J Neurosci* **27**: 4253–60.

Pandya RS, Mao L, Zhou H, Zhou S, Zeng J, Popp AJ, *et al* (2011). Central nervous system agents for ischemic stroke: neuroprotection mechanisms. *Cent Nerv Syst Agents Med Chem* **11**: 81–97.

Paoletti P (2011). Molecular basis of NMDA receptor functional diversity. *Eur J Neurosci* **33**: 1351–65.

Paoletti P, Neyton J (2007). NMDA receptor subunits: function and pharmacology. *Curr Opin Pharmacol* **7**: 39–47.

Papadia S, Hardingham GE (2007). The dichotomy of NMDA receptor signaling. *Neuroscientist* **13**: 572–9.

Papadia S, Soriano FX, Léveillé F, Martel M-A, Dakin KA, Hansen HH, *et al* (2008). Synaptic NMDA receptor activity boosts intrinsic antioxidant defenses. *Nat Neurosci* **11**: 476–87.

Papke RL (2014). Merging old and new perspectives on nicotinic acetylcholine receptors. *Biochem Pharmacol* doi:10.1016/j.bcp.2014.01.029.

Papke RL, Bencherif M, Lippiello P (1996). An evaluation of neuronal nicotinic acetylcholine receptor activation by quaternary nitrogen compounds indicates that choline is selective for the α7 subtype. *Neurosci Lett* **213**: 201–204.

Parada E, Egea J, Romero A, Barrio L del, García AG, López MG (2010). Poststress treatment with PNU282987 can rescue SH-SY5Y cells undergoing apoptosis via α7 nicotinic receptors linked to a Jak2/Akt/HO-1 signaling pathway. *Free Radic Biol Med* **49**: 1815–1821.

Parkin AJ (1996). Human memory: the hippocampus is the key. *Curr Biol* **6**: 1583–5.

Paschen W, Doutheil J (1999). Disturbances of the Functioning of Endoplasmic Reticulum: A Key Mechanism Underlying Neuronal Cell Injury? *J Cereb Blood Flow Metab* **19**: 1–18.

Pereira EFR, Hilmas C, Santos MD, Alkondon M, Maelicke A, Albuquerque EX (2002). Unconventional ligands and modulators of nicotinic receptors. *J Neurobiol* **53**: 479–500.

Pérez-Gómez A, Tasker RA (2012). Enhanced neurogenesis in organotypic cultures of rat hippocampus after transient subfield-selective excitotoxic insult induced by domoic acid. *Neuroscience* **208**: 97–108.

Pérez-Gómez A, Tasker RA (2013). Transient domoic acid excitotoxicity increases BDNF expression and activates both MEK- and PKA-dependent neurogenesis in organotypic hippocampal slices. *BMC Neurosci* **14**: 72.

Petralia RS, Wang YX, Hua F, Yi Z, Zhou A, Ge L, *et al* (2010). Organization of NMDA receptors at extrasynaptic locations. *Neuroscience* **167**: 68–87.

Picciotto MR, Higley MJ, Mineur YS (2012). Acetylcholine as a Neuromodulator: Cholinergic Signaling Shapes Nervous System Function and Behavior. *Neuron* **76**: 116–129.

Pisani A, Bonsi P, Centonze D, Giacomini P, Calabresi P (2000). Involvement of Intracellular Calcium Stores During Oxygen/Glucose Deprivation in Striatal Large Aspiny Interneurons. *J Cereb Blood Flow Metab* **20**: 839–846.

Pohanka M (2012). Alpha7 nicotinic acetylcholine receptor is a target in pharmacology and toxicology. *Int J Mol Sci* **13**: 2219–38.

Prendergast M., Harris B., Mayer S, Holley R., Hauser K., Littleton J. (2001a). Chronic nicotine exposure reduces N-methyl-d-aspartate receptor-mediated damage in the hippocampus without altering calcium accumulation or extrusion: evidence of calbindin-D28K overexpression. *Neuroscience* **102**: 75–85.

Prendergast MA, Harris BR, Mayer S, Holley RC, Pauly JR, Littleton JM (2001b). Nicotine exposure reduces N-methyl-D-aspartate toxicity in the hippocampus: relation to distribution of the alpha7 nicotinic acetylcholine receptor subunit. *Med Sci Monit Int Med J Exp Clin Res* **7**: 1153–60.

Prickaerts J, Goethem NP van, Chesworth R, Shapiro G, Boess FG, Methfessel C, *et al* (2012). EVP-6124, a novel and selective α7 nicotinic acetylcholine receptor partial agonist, improves memory performance by potentiating the acetylcholine response of α7 nicotinic acetylcholine receptors. *Neuropharmacology* **62**: 1099–1110.

Radley E, Akram A, Grubb BD, Gibson CL (2012). Investigation of the mechanisms of progesterone protection following oxygen-glucose deprivation in organotypic hippocampal slice cultures. *Neurosci Lett* **506**: 131–5.

Resende RR, Adhikari A (2009). Cholinergic receptor pathways involved in apoptosis, cell proliferation and neuronal differentiation. *Cell Commun Signal* **7**: 20.

Ring A, Tanso R, Noraberg J (2010). The use of organotypic hippocampal slice cultures to evaluate protection by non-competitive NMDA receptor antagonists against excitotoxicity. *Altern Lab Anim* **38**: 71–82.

Robinson MB, Jackson JG (2016). Astroglial Glutamate Transporters Coordinate Excitatory Signaling and Brain Energetics. *Neurochem Int* doi:10.1016/j.neuint.2016.03.014.

Roerig B, Nelson DA, Katz LC (1997). Fast synaptic signaling by nicotinic acetylcholine and serotonin 5-HT3 receptors in developing visual cortex. *J Neurosci* **17**: 8353–62.

Rosa AO, Egea J, Gandía L, López MG, García AG (2006). Neuroprotection by nicotine in hippocampal slices subjected to oxygen-glucose deprivation: involvement of the alpha7 nAChR subtype. *J Mol Neurosci* **30**: 61–2.

Rothman SM, Olney JW (1987). Excitotoxity and the NMDA receptor. *Trends Neurosci* **10**: 299–302.

Sacco RL, DeRosa JT, Haley EC, Levin B, Ordronneau P, Phillips SJ, *et al* (2001). Glycine antagonist in neuroprotection for patients with acute stroke: GAIN Americas: a randomized controlled trial. *JAMA* **285**: 1719–28.

Sakaguchi T, Okada M, Kuno M, Kawasaki K (1997). Dual mode of N-methyl-d-aspartate-induced neuronal death in hippocampal slice cultures in relation to N-methyl-d-aspartate receptor properties. *Neuroscience* **76**: 411–423.

Salamone A, Mura E, Zappettini S, Grilli M, Olivero G, Preda S, *et al* (2014). Inhibitory effects of beta-amyloid on the nicotinic receptors which stimulate glutamate release in rat hippocampus: the glial contribution. *Eur J Pharmacol* **723**: 314–321.

Samochocki M, Höffle A, Fehrenbacher A, Jostock R, Ludwig J, Christner C, *et al* (2003). Galantamine is an allosterically potentiating ligand of neuronal nicotinic but not of muscarinic acetylcholine receptors. *J Pharmacol Exp Ther* **305**: 1024–36.

Samochocki M, Zerlin M, Jostock R, Groot Kormelink PJ, Luyten WHML, Albuquerque EX, *et al* (2000). Galantamine is an allosterically potentiating ligand of the human alpha4/beta2 nAChR. *Acta Neurol Scand* **102**: 68–73.

Santos MD, Alkondon M, Pereira EFR, Aracava Y, Eisenberg HM, Maelicke A, *et al* (2002). The nicotinic allosteric potentiating ligand galantamine facilitates synaptic transmission in the mammalian central nervous system. *Mol Pharmacol* **61**: 1222–34.

Sanz-Clemente A, Nicoll RA, Roche KW (2013). Diversity in NMDA receptor composition: many regulators, many consequences. *Neuroscientist* **19**: 62–75.

Sato K, Matsuki N (2002). A 72 kDa heat shock protein is protective against the selective vulnerability of CA1 neurons and is essential for the tolerance exhibited by CA3 neurons in the hippocampus. *Neuroscience* **109**: 745–56.

Sattler R, Charlton MP, Hafner M, Tymianski M (1998). Distinct influx pathways, not calcium load, determine neuronal vulnerability to calcium neurotoxicity. *J Neurochem* **71**: 2349–64.

Sattler R, Tymianski M (2001). Molecular mechanisms of glutamate receptor-mediated excitotoxic neuronal cell death. *Mol Neurobiol* **24**: 107–29.

Sattler R, Xiong Z, Lu WY, Hafner M, MacDonald JF, Tymianski M (1999). Specific coupling of NMDA receptor activation to nitric oxide neurotoxicity by PSD-95 protein. *Science* **284**: 1845–8.

Sattler R, Xiong Z, Lu WY, MacDonald JF, Tymianski M (2000). Distinct roles of synaptic and extrasynaptic NMDA receptors in excitotoxicity. *J Neurosci* **20**: 22–33.

Schmidt-Kastner R, Ophoff BG, Hossmann KA (1990). Pattern of neuronal vulnerability in the cat hippocampus after one hour of global cerebral ischemia. *Acta Neuropathol* **79**: 444–55.

Schmued LC, Stowers CC, Scallet AC, Xu L (2005). Fluoro-Jade C results in ultra high resolution and contrast labeling of degenerating neurons. *Brain Res* **1035**: 24–31.

Schousboe A, Waagepetersen HS (2005). Role of astrocytes in glutamate homeostasis: implications for excitotoxicity. *Neurotox Res* **8**: 221–5.

Schrattenholz A, Pereira EF, Roth U, Weber KH, Albuquerque EX, Maelicke A (1996). Agonist responses of neuronal nicotinic acetylcholine receptors are potentiated by a novel class of allosterically acting ligands. *Mol Pharmacol* **49**: 1–6.

Séguéla P, Wadiche J, Dineley-Miller K, Dani JA, Patrick JW (1993). Molecular cloning, functional properties, and distribution of rat brain alpha 7: a nicotinic cation channel highly permeable to

calcium. *J Neurosci* **13**: 596–604.

Shapiro ML, Eichenbaum H (1999). Hippocampus as a memory map: synaptic plasticity and memory encoding by hippocampal neurons. *Hippocampus* **9**: 365–84.

Shen J, Yakel JL (2012). Functional α7 nicotinic ACh receptors on astrocytes in rat hippocampal CA1 slices. *J Mol Neurosci* **48**: 14–21.

Shimohama S, Greenwald D., Shafron D., Akaika A, Maeda T, Kaneko S, *et al* (1998). Nicotinic α7 receptors protect against glutamate neurotoxicity and neuronal ischemic damage. *Brain Res* **779**: 359–363.

Shin E-J, Chae JS, Jung M-E, Bing G, Ko KH, Kim W-K, *et al* (2007). *Repeated intracerebroventricular infusion of nicotine prevents kainate-induced neurotoxicity by activating the α7 nicotinic acetylcholine receptor*. *Epilepsy Res* **73**: .

Simantov R, Liu W, Broutman G, Baudry M (1999). Antisense knockdown of glutamate transporters alters the subfield selectivity of kainate-induced cell death in rat hippocampal slice cultures. *J Neurochem* **73**: 1828–35.

Simon RP, Griffiths T, Evans MC, Swan JH, Meldrum BS (1984). Calcium overload in selectively vulnerable neurons of the hippocampus during and after ischemia: an electron microscopy study in the rat. *J Cereb Blood Flow Metab* **4**: 350–61.

Smart TG (1997). Regulation of excitatory and inhibitory neurotransmitter-gated ion channels by protein phosphorylation. *Curr Opin Neurobiol* **7**: 358–367.

Smith KJ, Butler TR, Prendergast MA (2010). Inhibition of sigma-1 receptor reduces N-methyl-D-aspartate induced neuronal injury in methamphetamine-exposed and -naive hippocampi. *Neurosci Lett* **481**: 144–8.

Sommer W (1880). Erkrankung des Ammonshorns als aetiologisches Moment der Epilepsie. *Eur Arch Psychiatry Clin …* at <http://www.springerlink.com/index/Y225087T72102802.pdf>.

Soriano FX, Papadia S, Hofmann F, Hardingham NR, Bading H, Hardingham GE (2006). Preconditioning doses of NMDA promote neuroprotection by enhancing neuronal excitability. *J Neurosci* **26**: 4509–18.

Spielmeyer W (1927). Die pathogenese des epileptischen krampfes. *Zeitschrift für die gesamte Neurol und Psychiatr* at <http://link.springer.com/article/10.1007/BF02870249>.

Stanika RI, Winters CA, Pivovarova NB, Andrews SB (2010). Differential NMDA receptor-dependent calcium loading and mitochondrial dysfunction in CA1 vs. CA3 hippocampal neurons. *Neurobiol Dis* **37**: 403–11.

Starkov AA, Chinopoulos C, Fiskum G (2004). Mitochondrial calcium and oxidative stress as mediators of ischemic brain injury. *Cell Calcium* **36**: 257–264.

Stoppini L, Buchs PA, Muller D (1991). A simple method for organotypic cultures of nervous tissue. *J Neurosci Methods* **37**: 173–182.

Storch A, Schrattenholz A, Cooper JC, Ghani EMA, Gutbrod O, Weber K-H, *et al* (1995). Physostigmine, galanthamine and codeine act as “noncompetitive nicotinic receptor agonists” on clonal rat pheochromocytoma cells. *Eur J Pharmacol Mol Pharmacol* **290**: 207–219.

Su T, Paradiso B, Long Y-S, Liao W-P, Simonato M (2011). Evaluation of cell damage in organotypic hippocampal slice culture from adult mouse: A potential model system to study neuroprotection. *Brain Res* **1385**: 68–76.

Sudweeks SN, Yakel JL (2000). Functional and molecular characterization of neuronal nicotinic ACh receptors in rat CA1 hippocampal neurons. *J Physiol* **527 Pt 3**: 515–28.

Sugawara T, Fujimura M, Noshita N, Kim GW, Saito A, Hayashi T, *et al* (2004). Neuronal death/survival signaling pathways in cerebral ischemia. *NeuroRX* **1**: 17–25.

Sun H-S, Doucette TA, Liu Y, Fang Y, Teves L, Aarts M, *et al* (2008). Effectiveness of PSD95 Inhibitors in Permanent and Transient Focal Ischemia in the Rat. *Stroke* **39**: 2544–2553.

Szydlowska K, Tymianski M (2010). Calcium, ischemia and excitotoxicity. *Cell Calcium* **47**: 122–9.

Takahashi M, Billups B, Rossi D, Sarantis M, Hamann M, Attwell D (1997). The role of glutamate transporters in glutamate homeostasis in the brain. *J Exp Biol* **200**: 401–9.

Tasker RAR, Perry MA, Doucette TA, Ryan CL (2005). NMDA receptor involvement in the effects of low dose domoic acid in neonatal rats. *Amino Acids* **28**: 193–6.

Thomsen MS, Hansen HH, Timmerman DB, Mikkelsen JD (2010). Cognitive improvement by activation of alpha7 nicotinic acetylcholine receptors: from animal models to human pathophysiology. *Curr Pharm Des* **16**: 323–43.

Tomarken A, Serlin R (1986). Comparison of ANOVA alternatives under variance heterogeneity and specific noncentrality structures. *Psychol Bull* **99**: 90–99.

Traynelis SF, Wollmuth LP, McBain CJ, Menniti FS, Vance KM, Ogden KK, *et al* (2010). Glutamate receptor ion channels: structure, regulation, and function. *Pharmacol Rev* **62**: 405–96.

Treinin M, Chalfie M (1995). A mutated acetylcholine receptor subunit causes neuronal degeneration in C. elegans. *Neuron* **14**: 871–7.

Turner RC, Dodson SC, Rosen CL, Huber JD (2013). The science of cerebral ischemia and the quest for neuroprotection: navigating past failure to future success. *J Neurosurg* **118**: 1072–85.

Tymianski M, Charlton MP, Carlen PL, Tator CH (1993a). Source specificity of early calcium neurotoxicity in cultured embryonic spinal neurons. *J Neurosci* **13**: 2085–104.

Tymianski M, Charlton MP, Carlen PL, Tator CH (1993b). Secondary Ca2+ overload indicates early neuronal injury which precedes staining with viability indicators. *Brain Res* **607**: 319–23.

Uteshev V (2016). Are positive allosteric modulators of α7 nAChRs clinically safe? *J Neurochem* **136**: 217–9.

Verbitsky M, Rothlin C V, Katz E, Belén Elgoyhen A (2000). Mixed nicotinic–muscarinic properties of the α9 nicotinic cholinergic receptor. *Neuropharmacology* **39**: 2515–2524.

Vicini S, Wang JF, Li JH, Zhu WJ, Wang YH, Luo JH, *et al* (1998). Functional and pharmacological differences between recombinant N-methyl-D-aspartate receptors. *J Neurophysiol* **79**: 555–66.

Vogt C, Vogt O (1937). Sitz und Wesen der Krankheiten im Lichte der topistischen Hirnforschung und des Variierens der Tiere. *J Psychol Neurol* **47**: 237–457.

Wallace TL, Porter RHP (2011). Targeting the nicotinic alpha7 acetylcholine receptor to enhance cognition in disease. *Biochem Pharmacol* **82**: 891–903.

Wang HY, Lee DH, D'Andrea MR, Peterson PA, Shank RP, Reitz AB (2000a). beta-Amyloid(1-42) binds to alpha7 nicotinic acetylcholine receptor with high affinity. Implications for Alzheimer's disease pathology. *J Biol Chem* **275**: 5626–32.

Wang HY, Lee DH, Davis CB, Shank RP (2000b). Amyloid peptide Abeta(1-42) binds selectively and with picomolar affinity to alpha7 nicotinic acetylcholine receptors. *J Neurochem* **75**: 1155–61.

Wang JQ, Guo M-L, Jin D-Z, Xue B, Fibuch EE, Mao L-M (2014). Roles of subunit phosphorylation in regulating glutamate receptor function. *Eur J Pharmacol* **728**: 183–187.

Wang Q, Andreasson K (2010). The organotypic hippocampal slice culture model for examining neuronal injury. *J Vis Exp* doi:10.3791/2106.

Wang Y -b., Wang J -j., Wang S -h., Liu S-S, Cao J -y., Li X -m., *et al* (2012). Adaptor Protein APPL1 Couples Synaptic NMDA Receptor with Neuronal Prosurvival Phosphatidylinositol 3-Kinase/Akt Pathway. *J Neurosci* **32**: 11919–11929.

Webster KA (2012). Mitochondrial membrane permeabilization and cell death during myocardial infarction: roles of calcium and reactive oxygen species. *Future Cardiol* **8**: 863–84.

Wei G, Yin Y, Li W, Bito H, She H, Mao Z (2012). Calpain-mediated degradation of myocyte enhancer factor 2D contributes to excitotoxicity by activation of extrasynaptic N-methyl-D-aspartate receptors. *J Biol Chem* **287**: 5797–805.

Wiesner A, Fuhrer C (2006). Regulation of nicotinic acetylcholine receptors by tyrosine kinases in the peripheral and central nervous system: same players, different roles. *Cell Mol Life Sci* **63**: 2818–2828.

Williams DK, Peng C, Kimbrell MR, Papke RL (2012). Intrinsically Low Open Probability of 7 Nicotinic Acetylcholine Receptors Can Be Overcome by Positive Allosteric Modulation and Serum Factors Leading to the Generation of Excitotoxic Currents at Physiological Temperatures. *Mol Pharmacol* **82**: 746–759.

Williams DK, Wang J, Papke RL (2011). Positive allosteric modulators as an approach to nicotinic acetylcholine receptor-targeted therapeutics: Advantages and limitations. *Biochem Pharmacol* **82**: 915–930.

Wise-Faberowski L, Robinson PN, Rich S, Warner DS (2009a). Oxygen and glucose deprivation in an organotypic hippocampal slice model of the developing rat brain: the effects on N-methyl-D-aspartate subunit composition. *Anesth Analg* **109**: 205–10.

Wise-Faberowski L, Warner DS, Spasojevic I, Batinic-Haberle I (2009b). Effect of lipophilicity of Mn (III) ortho N-alkylpyridyl- and diortho N, N'-diethylimidazolylporphyrins in two in-vitro models of oxygen and glucose deprivation-induced neuronal death. *Free Radic Res* **43**: 329–39.

Xing C, Arai K, Lo EH, Hommel M (2012). Pathophysiologic cascades in ischemic stroke. *Int J Stroke* **7**: 378–85.

Xu G, Perez-Pinzon MA, Sick TJ (2003). Mitochondrial complex I inhibition produces selective damage to hippocampal subfield CA1 in organotypic slice cultures. *Neurotox Res* **5**: 529–38.

Yamakura T, Shimoji K (1999). Subunit- and site-specific pharmacology of the NMDA receptor channel. *Prog Neurobiol* **59**: 279–98.

Yu G, Wu F, Wang E-S (2015). BQ-869, a novel NMDA receptor antagonist, protects against excitotoxicity and attenuates cerebral ischemic injury in stroke. *Int J Clin Exp Pathol* **8**: 1213–25.

Yu W-F, Guan Z-Z, Bogdanovic N, Nordberg A (2005). High selective expression of α7 nicotinic receptors on astrocytes in the brains of patients with sporadic Alzheimer's disease and patients carrying Swedish APP 670/671 mutation: a possible association with neuritic plaques. *Exp Neurol* **192**: 215–225.

Zappettini S, Grilli M, Olivero G, Chen J, Padolecchia C, Pittaluga A, *et al* (2014). Nicotinic α7 receptor activation selectively potentiates the function of NMDA receptors in glutamatergic terminals of the nucleus accumbens. *Front Cell Neurosci* **8**: 332.

Zhou C, Li C, Yu H, Zhang F, Han D (2008). Neuroprotection of γ-aminobutyric acid receptor agonists via enhancing neuronal nitric oxide synthase (Ser847) phosphorylation through increased neuronal nitric. *J* **86**: 2973–2983.

Zhou Q, Sheng M (2013). NMDA receptors in nervous system diseases. *Neuropharmacology* **74**: 69–75.

Zimmer J, Kristensen BW, Jakobsen B, Noraberg J (2000). Excitatory amino acid neurotoxicity and modulation of glutamate receptor expression in organotypic brain slice cultures. *Amino Acids* **19**: 7–21.

Zoppo GJ del, Saver JL, Jauch EC, Adams HP, Council on behalf of the AHAS (2009). Expansion of the Time Window for Treatment of Acute Ischemic Stroke With Intravenous Tissue Plasminogen Activator: A Science Advisory From the American Heart Association/American Stroke Association. *Stroke* **40**: 2945–2948.

Zwart R, Vijverberg HP. (2000). Potentiation and inhibition of neuronal α4β4 nicotinic acetylcholine receptors by choline. *Eur J Pharmacol* **393**: 209–214.